POSTPROCESSING OF DCT CODED IMAGES

A Thesis Submitted

in Partial Fulfillment of the Requirements

for the Degree of

DOCTOR OF PHILOSOPHY

By

Vinay Kumar Srivastava

to the

DEPARTMENT OF ELECTRICAL ENGINEERING

INDIAN INSTITUTE OF TECHNOLOGY KANPUR

JANUARY, 2001

dedicated to

my family

dedicated to

my family

Certificate

It is certified that the work contained in the thesis entitled **POSTPROCESSING OF DCT CODED IMAGES** by *Vinay Kumar Srivastava* has been carried out under my supervision and that this work has not been submitted elsewhere for a degree.

GRay 22.1.2001

(Dr.G.C.Ray)
Professor
Department of Electrical Engineering
Indian Institute of Technology
Kanpur–208016 India

January, 2001.

Synopsis

Name of Student: Vinay Kumar Srivastava Roll no.: 9710463

Degree for which submitted: Ph.D. Department: Electrical Engineering

Thesis Title: **Postprocessing of DCT coded images**

Name of thesis supervisor: Prof. G. C. Ray

Month and year of thesis submission: January 2001.

Discrete Cosine Transform (DCT) based image compression with its well known advantages is being used in various applications. Especially, most of the international standards for image and video compression such as JPEG, H.261, H.263 and MPEG have recommended the use of block DCT as a main compression technique. The DCT scheme has potential to be used as a compression scheme because of its desirable energy compactness property and relative ease of implementation. The performance of such a system at high compression ratio is limited by *blocking artifacts.*

In DCT based compression schemes, the high compression ratios are obtained by discarding information about DCT coefficients that are considered to be less important. This results in visible discontinuities along the block boundaries, commonly known as blocking artifacts. These artifacts often limit the maximum compression ratios that could be achieved. One main reason of blocking artifacts is that the blocks are encoded and quantized independently without considering the correlation between adjacent blocks. These blocking artifacts cause three types of noise: grid noise in monotone area, staircase noise near the edges and corner outliers at the cross point of $M \times M$ blocks. Noise in block coding is correlated with the *local characteristics* of signal. Grid noise in monotone area, causing visually annoying artifacts, manifests itself as an artificial boundary among the pixels of adjacent blocks. An edge usually partitions an image into two monotone regions. Block coder can maintain continuity of edges within the blocks but cannot assure this across them. Furthermore, if the coder is not able to adequately represent the part of an edge within a block, then the degradation of an entire edge is increased. Therefore, edges tend to unsmooth in block boundaries and each side of an edge is no longer a monotone region. This is known as staircase noise. The ringing further increases the problems in edge area. Ringing is well known *Gibbs phenomenon* due to the truncation of high frequency components by quantization.

Postprocessing of the DCT coded the images can reduce the coding artifacts and therefore it is a very promising research area. The main objective of postprocessing is to remove the coding artifacts with lowest computational complexity. As discussed above, the noise in block-coded images is correlated with the local characteristics of the signal; so space-invariant filters are unable to exploit the correlation to reduce the noise. These filters are not suitable because they will blur the edge and degrade the visual quality of image. This is because most of the grid noise is out-of-band, while staircase noise is in the direction parallel to the edge. Signal bandwidth in monotone area is much lower than the bandwidth of the average spectrum of the edge blocks. Thus, this filter cannot remove the locally out-of-band noise in monotone area without blurring the edges. It is also found that the Human Visual System (HVS) is more sensitive to blocking artifacts in monotone regions than the edge regions. Thus, effect of noise in edge area reduces due to masking effect. A strong smoothing filter is required in monotone area but this smoothing operation in edge region tends to introduce undesirable blur. For edge regions, smoothing of a few pixels around block boundaries by directional lowpass filter is sufficient. Hence, space-variant or adaptive filtering depending on local image characteristics is preferable. The information about local image characteristics can be obtained from the image by edge detection or measuring the flatness of the region. Thus, one of the best approach for postprocessing is to classify the image blocks into various categories and then each is processed by one or two-dimensional (2D) filter.

Several postprocessing algorithms based on space-variant/ adaptive filtering have been proposed to reduce the blocking effect of block coding system [1–4]. As discussed, linear space-invariant filtering is inadequate to remove these artifacts. Iterative methods such as Projection Onto Convex Set (POCS) and Constrained Least Square (CLS) are not suitable for real-time applications because of their greater computational complexity. Space-variant/ adaptive filtering schemes require the edge information extracted from the received blocky images which contain false edges due to the blocking artifacts. Recovery of loss of accuracy of DCT coefficient by discontinuity criterion is another method [5] to reduce the artifacts. But this method provides good results only in the monotone area. Thus, the algorithms proposed in the literature are not able to reduce the coding artifacts in various regions of image simultaneously with low computational complexity. Therefore, they are not suitable for real time applications. The performance of DCT based image compression scheme degrades at high compression ratios and most of the existing postprocessing algorithms are not able to give good results in this situation. Therefore,. postprocessing algorithms with good performance at high compression ratios are much needed.

This thesis addresses various postprocessing issues that may arise in practice: (i) reduction of coding artifacts; and (ii) computationally efficient methods to make it suitable for real time applications such as video and still image decoding. The coding artifacts are more visible at higher compression ratios but they can be reduced more efficiently than the existing postprocessing techniques. Various aspects of DCT based image compression and postprocessing methods are studied with a state-of-art survey on the subject. A number of postprocessing algorithms for reducing the coding artifacts are being proposed in this work.

The first contribution of the thesis is the development of a hybrid scheme for postprocessing by clubbing the merits of several existing algorithms. Smoothing of artificial discontinuities due to blocking artifacts improves the image quality whereas smoothing of actual image edges degrades it. Thus, there is a need to satisfy these two conflicting requirements as simply as possible. The proposed algorithm includes the advantage of adaptive filtering in edge area and block-boundary discontinuity minimization in monotone area along with the corner outliers reduction.

The second contribution of the thesis is the design of a 2D multiple-notch (Both FIR and IIR) filter and its applications in reducing the blocking artifacts. These filters are designed with the goal of reducing blocking artifacts from DCT coded images.

The third contribution of the thesis is to provide four computationally efficient algorithms for postprocessing of DCT coded images. In literature several powerful postprocessing algorithms have been developed to reduce blocking artifacts. However, from application point of view, these are complex for real time applications such as video and still image decoding. These proposed algorithms can improve visual quality with improvement in peak signal-to-noise ratio (PSNR) with a very low computational complexity. The performance analysis and the simulation results show that the proposed algorithms are very competitive compared with those available in the literature.

Summary of algorithms proposed in this work

In the present work, a number of algorithms for postprocessing of DCT coded images have been proposed. These algorithms can be summarized as:

A hybrid scheme for the postprocessing of DCT coded images is proposed. The scheme is named as hybrid as the processing is done in both DCT as well as in spatial domain by two different algorithms. The scheme makes use of adaptive filtering in edge area and block-boundary discontinuity minimization in monotone area. The use of a lower order signal adaptive filter and the block-boundary discontinuity minimization algorithm reduces the processing time. Corner outliers reduction scheme further improves the performance. In this scheme, the compensating DCT coefficients for monotone block are calculated and added to corresponding DCT coefficients to achieve minimum block-boundary discontinuity. These compensating DCT coefficients for monotone blocks are calculated from the DCT of the block-boundary pixel differences. In this calculation, some of the block-boundary pixel differences are made zero if the neighboring block is an edge block. In the proposed scheme, the edge information is extracted and used for the classification of image blocks. For edge blocks, a signal adaptive filter performs the filtering along the edge to reduce the staircase noise. This filter also uses the same edge information (edge-map). It has been observed that the performance of this algorithm is better than the space variant filtering as well as the two individual algorithms used in the hybrid scheme.

We have developed the design method for 2D IIR multiple-notch filter and some of its applications are being proposed here. A simple algebraic method [6] is used for the design of this filter. In this design approach, first two 1D multiple-tone filters are designed as per the specifications of 2D multiple-notch filter and then these two filters are used to obtain 2D multiple-vertical line filter and 2D multiple-horizontal line filter. Finally, cascade of these two filters gives the desired 2D multiple-notch filter. The design of 1D multiple-tone filter is based on the design of allpass filter as discussed in [7]. Then two new applications of 2D multiple-notch filter is being suggested. The possibility of using 2D multiple-notch filter for reducing blocking artifact is fully examined. It has been shown that 2D multiple-notch filter can eliminate the square grid. It can also reduce the blocking artifacts from DCT coded images. The concept of reducing blocking artifacts by 2D multiple-notch filter is based on the fact that the discontinuities due to block artifacts in block decoded image have periodic structure which ultimately results in some peaks in the DCT domain. These discontinuities are highlighted in the gradient of the image and thus dominant peaks can be observed in the DCT of this gradient-image. A 2D multiple-notch filter can kill these peaks to remove the false edges from the edge-map of blocky image. In addition to this, as the discontinuities due to blocking artifacts are more visible in the monotone area, the filter can be applied directly in these areas. Thus, improvement in the performances of space-variant/adaptive filter by the removal of false edges from the edge-map and the reduction of blocking artifacts directly in the monotone area, are the new possible applications of 2D multiple-notch filter.

We have extended the design approach of 2D multiple-notch filter to FIR type. FIR filters are suitable for image processing applications as they cause less distortion due to their linear phase property. The drawback of FIR filter is that they cause more delay. The design procedure for the 2D FIR multiple-tone filter is similar to IIR type of this filter but the desired 2D multiple-notch filter is obtained as a complementary filter [9] of the 2D multiple-tone filter. In this case, two 1D FIR multiple-tone filters are designed by windowed Fourier series method with Kaiser window. Various plots show that all 1D and 2D filters are obtained as per the design approach. This filter is also applied for the reduction of blocking artifacts and removal of false edges from edge of blocky decompressed image. The results obtained in case of FIR filter are better than IIR filter, as expected.

At the end of this work, four simple and effective algorithms for the postprocessing of DCT coded images are being proposed. Although these algorithms look simple but they are able to reduce blocking artifacts significantly without much computational complexity. The performance of these computationally efficient algorithms is better at high compression ratios; therefore these are suitable for low bit rate video and image decoding applications.

First algorithm proposed in this part of the work reduces the blocking artifacts by exploiting the residual inter-block correlation that exists in the received blocky image. For this purpose a signal adaptive filter is used to smoothen out a sub-image of DC coefficients of all the blocks. The algorithm reduces the blocking artifacts with a very low computational complexity. The second algorithm reduces the blocking artifacts significantly by capturing the discontinuities due to blocking artifacts in the new blocks (made by the re-division of the image) and removing them in the DCT domain by selective attenuation of AC components corresponding to these discontinuities. These two algorithms together reduce the blocking artifacts considerably with slight improvement in PSNR. It has been verified by calculating the various discontinuity measures. In the third algorithm, the discontinuities are captured in the same way but the singular value decomposition (SVD) based filtering scheme is used for their reduction. This algorithm is very effective for reducing blocking artifacts but its computational complexity is slightly more because SVD algorithm is applied to each monotone block. Fourth algorithm proposed here is again a DCT domain algorithm. It reduces the blocking artifacts by eliminating some selected DCT coefficients of concatenated block of two adjacent blocks. The algorithm has low computational complexity, because no filtering is required. The availability of fast algorithm for DCT computation makes this algorithm suitable for low bit rate video and image decoding applications. In this algorithm, only the first row and first column of concatenated block are selected for elimination, which further reduces the computation time. The results show that this algorithm provides very good performance with minimum computational complexity.

Motivations

Therefore the motivations behind the work presented in this thesis are:

- Uncompressed video and audio data are huge and there is a big problem for their storage and network communication. Therefore data compression is required. As the compression ratio of lossless methods (e.g., Huffman, Arithmetic) is not high enough for image and video compression, a lossy compression scheme that can provide higher compression ratio is needed.
- Very good energy compaction and decorrelation properties of DCT motivated to work on the DCT based image compression scheme. The performance of DCT based compression scheme is limited by blocking artifacts. So, the main objective was to find a DCT based scheme that can minimize these blocking artifacts.
- Most of the existing popular standards for image compression also use DCT based image compression schemes. This was also one of the main reasons for taking up this problem. Although at the beginning a number of possibilities of modified coding schemes are studied but looking at these existing standards the work is centered around the postprocessing of DCT coded images.
- DCT-based image compression is very popular and finds various applications. Improvement in quantization, encoding and postprocessing can increase the capabilities of DCT-based image compression scheme over other schemes in many applications.
- Low bit rate coding applications motivate to find computationally efficient algorithms for postprocessing of such images.

Organization of Thesis

Chapter 1 introduces various aspects of data compression with an overview of DCT based image compression scheme. Various methods of postprocessing of DCT coded images are discussed and a state-of-the-art survey on the subject is presented.

In *Chapter 2*, a hybrid scheme is presented which takes advantages of adaptive filtering in edge area and block boundary discontinuity algorithm in monotone area.

Chapter 3 presents an approach based on space-variant/ adaptive filtering. In this approach, a 2D IIR multiple-notch filter is designed from 1D multiple-notch filter. This filter is applied to reduce the blocking artifacts from DCT coded images either by improving the classification scheme or by directly filtering the blocking artifacts in monotone areas.

In *Chapter 4*, the design approach presented in *Chapter 3* of 2D multiple-notch filter is extended to FIR type filter. This filter is also applied to reduce the blocking artifacts from DCT coded images as in *Chapter 3*.

Chapter 5 is devoted to some new computationally efficient algorithms. Four algorithms to reduce the artifacts in DCT domain are presented.

Chapter 6 concludes the major contributions of this thesis and suggests the scope for future research work in this area.

References

[1] **Ramamurthi**, B. and **Gersho**, A., "Non-linear space-variant post processing of block coded image," *IEEE Trans. Acoustics, Speech and Signal Processing*, vol. ASSP-34, pp. 1258–1268, Oct. 1986.

[2] **Hsia**, S. C., **Yang**, J. F., and **Liu**, B. D., "Efficient postprocessor for blocky effect removal based on transform characteristics," *IEEE Trans. Circuits Syst. Video Technol.*, vol. 7, pp. 924–929, Dec. 1997.

[3] **Park**, Hyun Wook and **Lee**, Yung Lyul, "A postprocessing method for reducing quantization effects in low bit-rate moving picture coding," *IEEE Trans. Circuits Syst. Video Technol.*, vol. 9, pp. 161–171, Feb. 1999.

[4] **Paek**, Hoon, **Kim**, Rin-Chul, and **Lee**, Sang-Uk, "A DCT-based spatially adaptive postprocessing technique to reduce the blocking artifacts in transform coded images," *IEEE Trans. Circuits Syst. Video Technol.*, vol. 10, pp. 36–41, Feb. 2000.

[5] **Jeon**, B. and **Jeong**, J., "Blocking artifacts reduction in image compression with block boundary discontinuity criterion," *IEEE Trans. Circuits Syst. Video Technol.*, vol. 8, pp. 345–357, June 1998.

[6] **Pei**, Soo-Chang and **Tseng**, Chien-Cheng, "Two dimensional IIR digital notch filter design," *IEEE Trans. on circuits and systems-II: Analog and digital signal processing*, vol. 41, pp. 227–231, March 1994.

[7] **Pei**, Soo-Chang and **Tseng**, Chien-Cheng, "IIR multiple notch filter design based on all pass filter," *IEEE Trans. on circuits and systems-II: Analog and digital signal processing*, vol. 44, pp. 133–136, Feb. 1997.

[8] **Huang**, J., **Shi**, Y. Q., and **Dai**, X., "Blocking artifact removal based on frequency analysis," *Electronics letters*, vol. 34, pp. 2323–2325, Nov. 1998.

[9] **Yu**, T. H., **Mitra**, S. K., and **Babic**, H., "Design of linear phase FIR filters," *Sadhana*, vol. 15, pp. 133–155, Nov. 1990.

Acknowledgements

On the completion of this work, it is my privilege to express my deep sense of gratitude and indebtedness to my supervisor Dr. G.C. Ray for his invaluable guidance, unfailing support and constant encouragement during this work. I can offer my most humble and profound indebtedness only to him for deep concern both for my academics and for personal welfare.

I am extremely grateful to Professors Dr. P. Sirkar, Dr. S. Umesh, Dr. (Mrs) Sumanna Gupta, and Dr. S. K. Mullik, Dr. (Mrs) Preeti Rao who taught me various courses during my academic program to build the foundation for this work.

I thank the college authorities of my parent institute, Motilal Nehru Regional Engineering College, Allahabad for sponsoring me to pursue Ph. D. degree under Quality Improvement Programme.

I am greatly indebted to my colleagues Mr. R. K. Singh, Mr. N. K. Sharma, Mr. Manoranjan Sinha, Mr. Shafi Ullah Khan, Mr. R. K. Tripathi, Mr. Mukul Shukla and Mr. Vinod Yadav for their useful discussion in connection with this work.

I gratefully acknowledge the help and encouragement given by Mr. B. N. Singh at the time of thesis preparation and always ready to help me.

During my years at I.I.T. Kanpur, I had the pleasure to work with a number of friends including Mr. S. R. Das and Mr. Arindbm Banerjee. I would like to thank all of them for the enjoyable collaborations we had.

My thanks also goes to those friends who have directly or indirectly helped me during the stay at I.I.T. Kanpur.

I don't have adequate words to express my indebtedness to my parents, brothers, brother-in-laws and sister-in-law for all their pains and sufferings. I express sincere feelings to all of them for their patience, co-operation and understanding during the course of this thesis.

Finally, I appreciate my wife Mrs. Anju for her sincere co-operation and loving daughter Ayushi for providing me entertainment.

Vinay Kumar Srivastava

Contents

List of Figures

List of Tables

Chapter 1

Introduction

1.1 Data Compression

Digital images have become an important source of information in the modern world of communication systems. In their raw form, digital images require a huge amount of memory. Many research efforts have been made in solving the problem of image compression in the last two decades. Image compression is an extremely important part of modern computing. Due to the ability to compress images to a fraction of their original size, valuable and expensive disk space can be saved. In addition, transportation of images from one computer to another becomes easier and less time consuming. Therefore, image compression has played such an important role in the development of the Internet.

Image, video, and audio signals can be compressed because there is considerable statistical redundancy in the signal due to the existence of spatial and temporal correlation. There is also considerable information in the signal that is irrelevant from a perceptual point of view. Compression scheme may use these factors to achieve the desired data rate.

The compression algorithms can be divided into two categories: lossless and lossy. Lossless compression is achieved if no distortion is introduced in the coded image. Predictive methods are suited to lossless and low-compression applications. A lossless compression means that the restored data file is identical to the original. This is absolutely necessary for many types of data, for example: executable code, word processing files, tabulated numbers, etc. In this type of information we cannot afford to misplace even a single bit. In comparison, data files that represent images and other acquired signals do not need to be kept in perfect condition for storage or transmission. All real world measurements inherently contain a certain amount of noise. If the changes made to these signals resemble a small amount of additional noise, no harm is done. Compression techniques that allow this type of degradation are called lossy. The lossy techniques are much more effective for compression than lossless methods.

At higher compression ratio the noise added to the data is more. Images transmitted over the World Wide Web are an excellent example of why data compression is important, and the effectiveness of lossless versus lossy compression. Suppose we need to download a detailed color image over a computer's 33.6 kbps modem. If the image has not been compressed, it will contain about 504 Kbytes of data. If it has been compressed using a lossless technique, it will be about one-half this size, or 252 Kbytes. If lossy compression has been used (a JPEG file), it will be about 42 Kbytes. The inference is that the download times for these three equivalent files are 120 seconds, 60 seconds, and 10 seconds, respectively.

A number of lossy compression methods have been developed in which the transform compression has proven to be the most valuable. The best example of transform compression is embodied in the popular JPEG standard of image encoding. JPEG is named after its origin, the Joint Photographers Experts Group. Transform compression is based on the fact that when the signal is transformed, the resulting data values will be no longer equal to their information carrying roles. In particular, the low frequency components of a signal are more important than the high frequency components. Thus, removal of large number of bits from the high frequency components causes very small loss of the encoded information.

Transform-based coding schemes achieve higher compression ratios for lossy compression but suffer from blocking artifacts at high-compression ratios. Multiresolution approaches are suited for lossy as well as for lossless compression. At lossy high-compression ratios, the typical artifact visible in the reconstructed images is the ringing effect. A comparative study of DCT and wavelet based image coding technique is available in [10]. New applications in a multimedia environment need some new functionalities of the image coding schemes. For that purpose, second-generation coding techniques segment the images into semantically meaningful pairs. Therefore, parts of these methods have been adopted to work for arbitrarily shaped regions. In order to add another functionality, such as progressive transmission of the information, specific quantization algorithms must be defined.

Comparison of transform-based image compression methods with the prediction methods

- Transform-based methods can better preserve the subjective image quality, and are less sensitive to statistical image property changes both inside a single image and between images.

- Prediction methods, on the other hand, can achieve larger compression ratios in a much less expensive way, tend to be much faster than transform-based or vector quantization compression schemes, and can easily be realized in hardware.

- If compressed images are transmitted, an important property is insensitivity to transmission channel noise. Transform-based techniques are significantly less sensitive to the channel noise - if a transform coefficient is corrupted during transmission, the resulting image distortion is homogeneously spread throughout the image or image part and is not too disturbing.

- Erroneous transmission of a difference value in prediction compression methods causes not only an error in a particular pixel but it also influences values in the neighborhood and it causes a considerable visual effect in a reconstructed image.

This work is related to the Discrete Cosine Transform (DCT) based image compression so various aspects of this scheme will be discussed in this Chapter. To point out the advantages and problems with this scheme, the block DCT and coding artifacts are discussed in the next section.

1.2 Block Discrete Cosine Transform (BDCT) and Blocking Artifacts

Discrete Cosine Transform (DCT) [11–18] has been widely used as a standard method for the compression and coding of image and video pictures. The standards specified by JPEG, MPEG and H.263 apply DCT for encoding the images before the compressed data is transmitted or stored. BDCT is the most widely used transform for the compression of both still and sequence of images. In DCT-based image compression, image is first divided into blocks of suitable size and then each block is transformed into DCT domain. In this scheme, high compression ratio is usually achieved by discarding information about the BDCT coefficients that are considered unimportant and yields image that exhibit the visually annoying blocking artifact.

1.2.1 Block Discrete Cosine Transform

Many transforms have been investigated for data compression; some of them have been invented specifically for this purpose. For instance, the Karhunen-Loeve transform (KLT) provides the best possible compression ratio, but is difficult to implement. The Basis functions of KLT are image dependent where as other transforms like Discrete Fourier Transform (DFT), Discrete Cosine Transform (DCT), Discrete Sine Transform (DST), and Discrete Hartley Transform (DHT) are image independent. The DFT is easy to use, but does not provide adequate compression. After much competition DCT, the relative of the Fourier transform, has been found to be the best. Just as the Fourier transform uses sine and cosine waves to represent a signal, the DCT only uses cosine waves. The 64 basis functions of DCT are shown in Fig. 1.1. DCT is a lossless, reversible

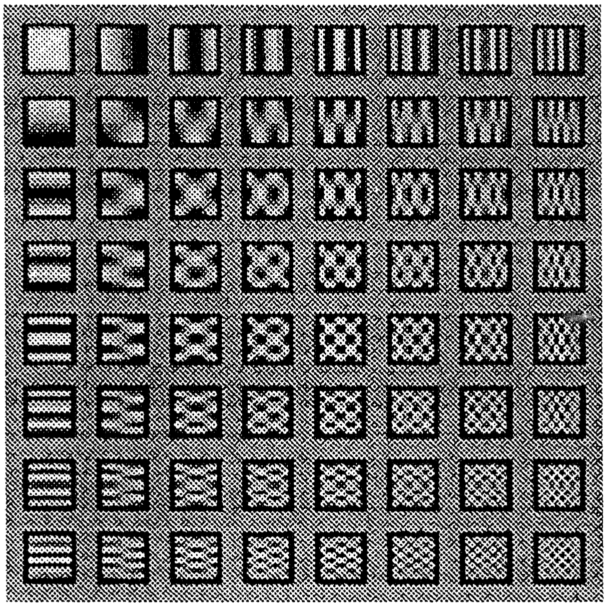

Figure 1.1: 64 basis functions of DCT.

process, which can de-correlate the image signal and achieve energy concentration. It can therefore reduce the redundancy in the image signal before transmitting through a band-limited channel, or storing it in a memory-limited media. DCT is best suited for natural images. The mathematical definition of 2D DCT and IDCT for N×N block are given by:

$$F(u,v) = \frac{2}{N}c(u)c(v)[\sum_{m=0}^{N-1}\sum_{n=0}^{N-1} f(m,n) * cos(\frac{\pi(2m+1)u}{2N})cos(\frac{\pi(2n+1)v}{2N})] \tag{1.1}$$

$$f(x,y) = \frac{2}{N}[\sum_{u=0}^{N-1}\sum_{v=0}^{N-1} c(u)c(v)F(m,n) * cos(\frac{\pi(2m+1)u}{2N})cos(\frac{\pi(2n+1)v}{2N})] \tag{1.2}$$

where $c(w) = 2^{-1/2}$ for $w = 0; c(w) = 1$ for $w = 1, 2, ...N-1$. Several desirable properties of DCT made it so popular for data compression:

1. It exhibits very good energy compaction and de-correlation properties. DCT is real and orthogonal transform. Linear transform like DCT and KLT perform a de-correlation of incoming signal resulting in a compaction of the energy into small number of AC coefficients of lower order. These transform play an important

role when signal de-correlation is the major property required. KLT is optimum transform but difficult to compute efficiently. BDCT takes advantages of local spatial correlation properties of image.

2. DCT is asymptotic approximation to the optimal KLT when the statistical properties of image can be described by a first order Markov model.

3. DCT can be computed very efficiently using fast algorithm similar to Fast Fourier Transform (FFT) algorithm.

1.2.2 Blocking Artifacts

In DCT based image compression scheme, the reconstructed image from highly compressed data has noticeable degradation due to blocking artifacts. In BDCT based image compression schemes, some high frequency DCT coefficients are transmitted with less accuracy. In this scheme, high compression ratios are usually achieved by discarding information about the BDCT coefficients that are considered to be unimportant. It is done by the quantization of DCT coefficients. This process is irreversible process that results in noticeable degradation near the block boundaries of decoded image. This visually annoying effect is called "blocking artifact". The blocking artifact manifests itself as an artificial boundary among the pixels of adjacent blocks and constitutes a serious bottleneck for many important visual communication applications where the pleasing image is required at very high compression ratios. In case of very low bit rate coding (8 kbps to 64 kbps) compression ratio is also very high. Thus, the main objective of image compression is to get necessary bit rate with sufficient image quality and reasonable hardware cost.

Blocking artifacts causes major degradation in block-based image coding techniques, especially at higher compression ratio. One main reason of blocking artifacts is that blocks are encoded and quantized independently without considering the correlation between adjacent blocks. Apart from blocking artifacts, ringing is another annoying artifact that appears frequently in transform based compressed image. The ringing artifacts appear as sharp oscillations along the edges in compressed image. Ringing is the *Gibb's phenomenon* due to truncation of high frequency components by quantization. Effect of noise in edge area is less due to masking effect. These coding artifacts cause three types of noise: grid noise in monotone area, staircase noise near the edges and corner outliers at the cross point of $M \times M$ block. Noise in block coding is correlated with the *local characteristics* of signal. Grid noise in monotone area causing visually annoying artifacts manifests itself as an artificial boundary among the pixels of adjacent blocks. Staircase noise in edge area causes ringing which blurs the edges.

In monotone areas where intensity changes gradually, there is tendency for intensity to change abruptly from one block to another. The abrupt changes in intensity are often visible since they occur along the block boundaries. An edge usually partitions the image into two monotone areas. Block coder can maintain continuity of edges within the block but cannot assure this across the blocks. Therefore, edges tend to be unsmooth in block boundaries.

In BDCT based image compression, the image degradation becomes visible when compression ratio exceeds certain level. These degradations manifest themselves as blocking artifacts due to the rigid block partitioning of the image and ringing noise around edges due to the course quantization. These blocks are processed independently but the DCT basis functions do not generally decay smoothly to zero. Thus, they exhibit discontinuities when thought of as being padded by zero beyond the boundaries. Therefore independent processing of spectra of adjacent blocks generates the well-known blocking artifacts.

1.3 DCT Based Image Compression and Coding

The DCT based image compression is discussed in detail in [19–21]. A typical DCT operates on blocks of image or video sequences of size 8×8. Although DCT is a lossless process by itself, quantization of the DCT coefficients is a lossy process. The quantized DCT coefficients are scanned in a zigzag order, before the run-level coding is performed.

Through zigzag scanning and run-level coding, the numbers of zero coefficients preceding a non-zero DCT coefficient, except for the DC coefficient, are grouped together to form a RUN-LEVEL code. The run-level code can be encoded by fixed or variable-length codes (VLC), such as Huffman code. A replica of the original image can be reconstructed at the receiver by reversing the processes at the transmitter, i.e., VLC decoding, run-level decoding, inverse zigzag scan, scaling and inverse DCT. Simplified block diagram of DCT based image compression scheme is shown in Fig. 1.2. The DCT coefficients have an important property that their values usually decay rapidly as one scans through the block of image in a zigzag order. Most of the AC coefficients have relatively small values as compared to the DC coefficient, i.e., the first coefficient. Therefore, a considerable number of these small coefficients can become zero after quantization. The zigzag scan and run-level coding makes use of this property in order to lower the bit rate required to transmit the relevant information. In trade-off, the reconstructed image will be distorted in accordance with the characteristics of the quantizer. The main steps of DCT based compression scheme are:

- Division of image into blocks
- Block Discrete Cosine Transformation (BDCT)
- Quantization
- Zigzag Scan
- DPCM on DC coefficient
- RLE on AC coefficient
- Entropy Coding

These are also the major steps of the most popular JPEG image compression algorithm. The JPEG image compression algorithm provides a very effective way to compress images with minimal loss in quality. JPEG is a good example of how several data compression

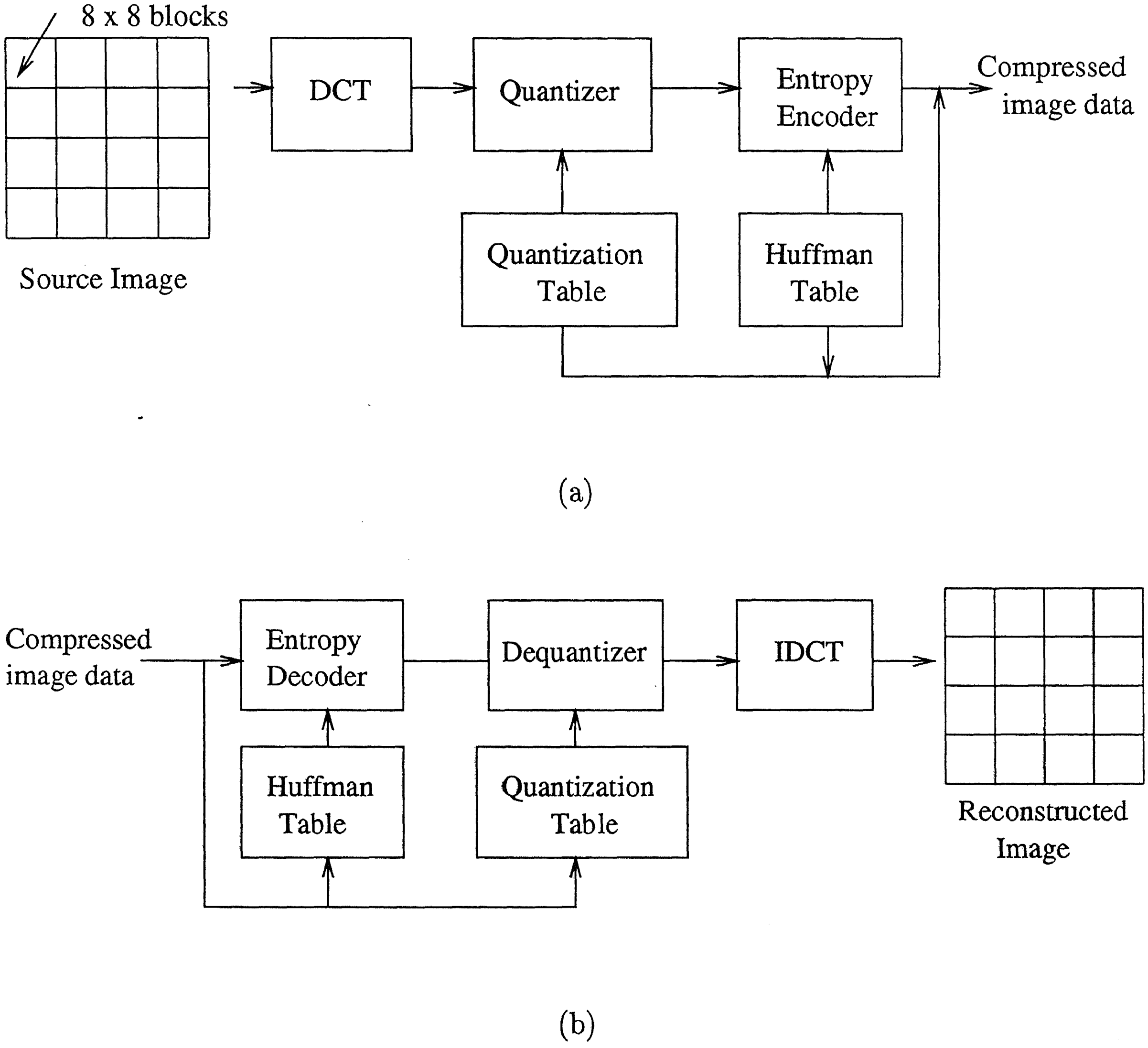

Figure 1.2: Block Diagram of DCT Based Image Compression scheme. (a) Encoder (b) Decoder

schemes can be combined for greater effectiveness. This standard is discussed in detail in Appendix A. Now, the remaining steps will be discussed in brief in the following subsections.

1.3.1 Quantization

In BDCT based image compression, high compression ratios are usually achieved by discarding information about the BDCT coefficients by quantization process. In any real coding system, the representation of coefficients using finite number of bits requires the presence of quantizers. Even a non-orthogonal or sub optimal transform can achieve smaller mean square error compared to optimal KLT, in noisy case. There is a tradeoff between image quality and degree of quantization. A large quantization step size can produce unacceptably larger image distortion. Unfortunately, finer quantization leads to lower compression ratios. The question is how to quantize the DCT coefficients most efficiently. Because of human eyesight's natural high frequency roll-off, these frequencies play a less important role than low frequencies. Thus, DCT based schemes uses a much higher step size for the high frequency coefficients, with little noticeable image deterioration.

Quantization Table

The quantization strategy in DCT based coding is expressed in the form of quantization table Q, which specifies the step size for mid-tread uniform scalar quantization of each coefficient. The quantization matrix is the 8×8 matrix of step sizes (one element for each DCT coefficient). Step sizes will be smaller in the upper left (low frequencies), and larger in the upper right (high frequencies); a step size of 1 is the most precise. The quantizer divides the DCT coefficient by its corresponding element in quantization matrix, and then rounds it to the nearest integer. Division by large value drives small coefficients down to zero. This results in many high frequency coefficients becoming zero, and therefore easier to code. The low frequency coefficients undergo only minor adjustment.

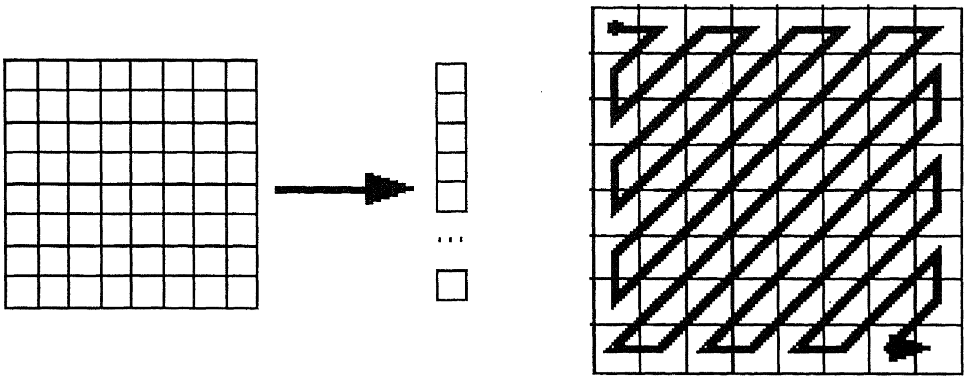

Figure 1.3: Zigzag Scanning.

The most common approach for finding a quantization table for a desired rate/distortion target is to use default quantization table and scale it by a scalar multiplier (called the quality factor) until the target is achieved. Thus, multiplying the default quantization table by quality factor controls the quantization step size for desired compressed file size.

1.3.2 Zigzag Scan

After quantization, it is not unusual for more than half of the DCT coefficients to be equal to zero. JPEG incorporates run-length coding to take advantage of this. For each non-zero DCT coefficient, JPEG records the number of zeros that preceded the number, the number of bits needed to represent the numbers amplitude, and the amplitude itself. To consolidate the runs of zeros, JPEG processes DCT coefficients in the zigzag pattern as shown in Fig. 1.3.

1.3.3 Differential Pulse Code Modulation (DPCM) on DC coefficient

Since the blocking artifact mainly from the DC coefficient is sensitive to spatial frequency response by human visual system, the DC coefficient is treated separately from the 63 AC coefficients. DC coefficient is large and varied, but often close to previous value (like lossless JPEG). Therefore difference from previous 8×8 blocks is encoded using DPCM.

1.3.4 Run Length Encode (RLE) on AC coefficients

After zigzag scan, the 1×64 vector has lots of zeros in it. The run length coding is used to encode it as (skip, value) pairs, where skip is the number of zeros and value is the next non-zero coefficient.

1.3.5 Encoding

The number of previous zeros and the bits needed for the current numbers amplitude form a pair. Each pair has its own code word, assigned through a variable length code (for example Huffman, Shannon-Fano or Arithmetic coding). JPEG outputs the code word of the pair, and then the codeword for the coefficient's amplitude (also from a variable length code). After each block, JPEG writes a unique end-of-block sequence to the output stream, and moves to the next block. When finished with all blocks, JPEG writes the end-of-file marker.

1.4 Postprocessing of DCT coded images: State-of-the-Art

Currently, transform-based image compression is very popular and finds various applications. Especially, most of the international standards for image and video compression, such as JPEG, H.261, H.263 and MPEG recommend the use of block Discrete Cosine Transform (BDCT) as a main compression technique. The DCT scheme has potential to be used as a compression scheme because of the desirable energy compactness property and low computational complexity.

In DCT based compression schemes, as discussed earlier, the high compression ratios are obtained by discarding information about DCT coefficients that is considered to be less important. The major drawback is visible discontinuities along block boundaries, commonly referred to as blocking artifacts. These often limit the maximum compression ratios that can be achieved. A number of techniques have been studied to reduce the visual effects of coding artifacts. Coding artifact reduction method can be classified into two categories: First is variation in transform structure such as the interleaved block transform, the lapped transform and the combined transform and the second is postprocessing techniques. The postprocessing techniques are attractive because they keep codec itself unchanged. Thus one can use commercial products while implementing hardware systems. If we consider the coded images to be distorted by a codec system, we can apply image restoration techniques for the coding noise reduction.

Postprocessing of DCT coded image is a very promising area for research. The performance of such system at high compression ratio is limited by blocking artifacts. The reconstructed image from highly compressed JPEG data has noticeable degradation due to blocking artifacts. Therefore the main objective of postprocessing is to remove this with lowest computational complexity. Linear, space-invariant filtering is inadequate to remove these artifacts. Iterative method such as Projection on to Convex Set (POCS) and Constrained Least Square (CLS), are not suitable for real time applications because of their greater computational complexity. So, space-variant or adaptive filtering is required. These schemes are based on edge information extracted from the received blocky image, which contains false edges due to blocking artifacts. Recovery of accuracy loss in DCT coefficient by discontinuity criterion is another method that can reduce these artifacts. It has low computational complexity and gives good results in monotone area.

1.5 Literature Survey

This work is focused on the postprocessing of image so literature survey on variation of transform structure is not being presented. Various postprocessing techniques have been published that reduce these blocking effects, but most of them introduce unnecessary blurring, ringing, or other artifacts. In this section, a literature survey with brief description of various existing postprocessing techniques is presented. For this purpose, various postprocessing method can be divided into following categories:

(i) Low Pass Filtering

(ii) Space-variant/Adaptive Filtering

(iii) Regularized Image Recovery

(iv) Block Boundary Discontinuity criterion

(v) Prediction of Boundary Pixels

(vi) Wavelet Transform

1.5.1 Low Pass Filtering

Considering the fact that artifacts are visible due to spatially high frequency components produced by the block discontinuity. Several kinds of lowpass filters are applied and it is observed that the Gaussian Low Pass Filter (LPF) gives the best performance. The main draw back of lowpass filtering is that it smoothen out the image details such as edges. Therefore, in lowpass filtering, special care should be taken not to smoothen out the image details. Since block and ringing effects resulting from block DCT coding are high frequency artifacts, a straightforward solution is to apply LPF to the region where they occur. In this respect Reeves and Lim [22] in 1984 applied 3 × 3 Gaussian LPF only to those pixels along block boundary.

1.5.2 Space-variant/Adaptive Filtering

The noise in block-coded images is correlated with the local characteristics of the signal; so space-invariant filters are unable to exploit the correlation to reduce the noise. These filters are not suitable because they will blur the edges and degrade the image visual quality. This is because most of the grid noise is out-of-band, while staircase noise is in the direction parallel to the edge. Signal bandwidth in monotone area is much lower than the bandwidth of the average spectrum of the edge blocks. Thus, this filter cannot remove locally out-of-band noise in monotone area. It is also found that the human visual system (HVS) is more sensitive to blocking artifacts in monotone regions than edge regions. Thus, effect of noise is less visible in edge area than monotone area due to this masking effect of HVS. Therefore, a strong smoothing filter is required in monotone area whereas in edge regions the smoothing operation tend to introduce undesirable blur, so smoothing of a few pixels around block boundaries by directional lowpass filter is sufficient. Hence, space-variant or adaptive filtering depending on local image characteristics is preferable. Thus classification of image regions is used in these schemes to capture the non-stationary behavior of images. The goal of classification is to classify the image into different regions based on their statistical properties such that an optimum filters can be applied in each of the region. The information about local image characteristics can be extracted from image by edge detection or measuring flatness of the region. Thus, one of the best approach of reducing blocking artifact is to classify the image blocks into various categories and each is processed by one or two-dimensional filter. Several postprocessing algorithms based on space-variant/ adaptive filtering have been proposed to reduce blocking effect of block coding system [1–3, 23–28].

In adaptive filtering, the coefficients of 2D filter are chosen by edge information of the image. Generally, no filtering is done at edge pixels but weighted or unweighted filtering is performed at the pixels in the monotone area or near the edge.

Both non-linear space-variant filtering and adaptive filtering requires the classification of image, which is based on available edge information extracted from the received blocky image.

Ramamurthi and Gersho [1] in 1986, proposed a non-linear space-variant filtering to reduce both so-called "staircase noise" and "grid noise". In this algorithm, the image is divided into monotone area and edge area using edge information obtained from detecting edge by gradient operator. Here two-dimensional lowpass filter is used to reduce grid noise in monotone area, whereas a directional one-dimensional filter is used to reduce staircase noise along the edges. The main features of their approach are:

- Space-variant filter reduces *locally out of band noise.* It is found that most of the grid noise is out of band while staircase noise is out of band only in the direction parallel to the edge. Therefore, in this algorithm, they used separable 2D 3 × 3 FIR filter to reduce blocking artifacts in monotone area and 1D FIR filter was applied in the direction parallel to the edges to reduce the staircase noise in the area containing the edges.

- Signal bandwidth in monotone regions is much lower than the bandwidth of average spectrum of edge block.

- All 1D filters are designed using Parks-McClellan algorithm. Bandwidth of the monotone area is computed from average spectrum of 8 × 8 block in the monotone area.

- Edge orientation is found by gradient thresholding algorithm. Here the ratio of change in intensity to the average intensity is compared with a threshold. Two counter K and L are set to zero. For horizontal adjacent pixel counter K is incremented for positive gradient above preselected threshold and it is decremented for negative gradient above threshold. Similarly counter L computed for vertical adjacent pixels.

  Monotone : if $\mid K \mid< m$ and $\mid L \mid< m$

  Edge, 0^o : if $\mid K \mid< m$ and $\mid L \mid> m$

  Edge, 45^o : if $\mid K \mid> m$ and $\mid L \mid> m,$ and sgn(K)=sgn(L)

  Edge, 90^o : if $\mid K \mid> m$ and $\mid L \mid< m$

  Edge, 135^o : if $\mid K \mid> m$ and $\mid L \mid> m,$ and $sgn(K) = -sgn(L)$

  where m is some predetermined threshold, and $sgn(.)$ is the usual signum function.

Hsu and Chen: 1993 [23] in 1993, reported an adaptive scheme transforming the median filter progressively to the LPF as the filter approached the block boundary. Post-filtering (spatial or temporal) has advantage of a low computational complexity and adaptation to local statistics relies on good classification scheme.

Kuo and Hsieh [24] in 1995, proposed an adaptive postprocessor for reducing blocking artifacts in which the adaptation is achieved by changing filter coefficient according to the local characteristics of image and the blocking effects. Here a space-variant LPF is used to smooth the pixel at block boundaries where the blocking artifacts are highly visible. In addition, the pixels that are close to an edge are adaptively filtered by directional lowpass filter. The edge pixels are left untouched by the postprocessor. Therefore, blocking artifacts can be removed without blurring the edges. The positions of edges are detected and a 2D regional or directional LPF is specially designed to remove blocking artifacts without blurring edges.

Hsia *et al.* [2] in 1997, proposed transform domain classification and algorithm for blocky strength (sum of absolute value of A.C. components) estimation. This transform domain algorithm has low computational complexity. Adaptive FIR filter is used to remove blocking artifacts. Stronger filter is used for greater blocky strength (results in larger energy spread) where as narrow filter is used for smaller blocky effect.

Castagno *et al.* [25] in 1998, applied rational filter for reducing blocking artifacts. The basic concept of the rational filter, which was devised to perform edge-preserving noise smoothing, is to modulate the coefficients of linear lowpass filter in order to limit its action in presence of image details. Its input/output relation is the ratio of two polynomials. Roughly speaking, the numerator has lowpass behavior, while the denominator is a function of difference between couples of pixels within the filtering mask. For large difference, it is assumed that the mask is located across a signal transition, and frequency response of the lowpass filter is automatically made less selective in the direction of the signal transition itself.

Lee *et al.* [26] in 1998, proposed a algorithm for removing coding artifacts in JPEG compressed image. In this algorithm the blocks are classified according to type of noise: grid noise, staircase noise, and corner outliers. It makes use of signal adaptive filter based on edge information as well as corner outliers detection and replacement scheme. Here Sobel's operator is used to find edge map which has advantage of differentiating and smoothing along the orthogonal directions. A signal adaptive filter performs weighted or unweighted filtering depending on whether edge points are included or not included in 5 × 5 filter window.

Park and Lee [3] in 1999, proposed a method for reducing quantization effects in highly compressed MPEG data. The reconstructed image have degradations, like blocking artifacts near the block boundaries, corner outliers at cross points of blocks, and ringing noise near the edges. It reduces these artifacts adaptively by using both spatial and temporal information extracted from the compressed data. The blocking artifacts are reduced by 1D horizontal and vertical LPF whereas the ringing noise is reduced by 2D signal adaptive filter (SAF). The blocking and ringing semaphores of each block greatly contribute to reducing computational complexity. In this method, the corner outliers are detected and compensated. This algorithm has low computational complexity.

Kim *et al.* [27] in 1999, proposed a de-blocking filter with two separate modes in low bit rate block based video coding. The first mode corresponds to flat regions where a strong 1D filter is applied because flat regions are more sensitive to the human visual system (HVS). In the second mode corresponding to other regions, a sophisticated smoothing filter based on the frequency information around block boundaries is used to reduce blocking artifacts adaptively without introducing blur.

Apostolopoulos and Jayant [28] in 1999, proposed a algorithm in which pixel by pixel processing is used to identify and reduce blocking artifacts while preserving sharpness and naturalness. In this algorithm artifacts are detected just by counting number of coefficients used to represent the block. The advantages of this simple scheme are the robustness and the low computational complexity. The algorithm is based on the assumption that surrounding pixels are less distorted and can improve estimate of distorted pixels. Therefore the filter is applied along the boundaries but updating the pixels within the distorted block. To reduce mosquito noise, the edge pixels are carefully identified and preserved while remaining non-edge pixels are smoothened. They have used a pixel based edge detection algorithm. To avoid false edge detection due to mosquito noise it is essential to distinguish between true and false edges. To counteract this problem, their approach is based on idea that a true edge has a string of connected pixels, while false edges are isolated points.

Comes *at el.* [29] in 1999, proposed a scheme for the restoration of the visual quality of image affected by coding noise. It is based on the tuned channels model of human perception. It uses the phenomenon of masking as criterion for the processing of the noise. Their aim of postprocessing was to improve the image quality by processing the perceptual channels of the noisy image where the noise is above visibility threshold. This operation is called filtering of unmasked noise. Postprocessing is based on a model of the human visual system that considers the relationship between visual stimuli and their visibility. This phenomenon is known as masking which is used as a criterion for the locally adaptive filter design. An image transformation that yields visual stimuli tuned to frequency and orientation according to the perceptual model is proposed. It allows a local measure of the masking of each perceptual stimulus considering the contrast between signal and estimated noise. This measure is obtained by analytic filtering. Processing schemes are presented with applications to discrete cosine transform (DCT) and subband coded images.

Paek *at el.* [4] in 2000, proposed a DCT based postprocessing method to alleviate blocking artifacts in transform coded images. The high frequency components are mainly caused by edge components. In this approach, two adjacent blocks are considered as homogeneous if no adjacent pixel difference is greater than the difference of block-boundary. Then a local frequency characteristic in homogeneous block is examined through DCT. They also derived the relationship between the DCT coefficients of two homogeneous blocks of different sizes. By considering the information about the original edge and using this relationship, they detected the high frequency components due to blocking artifacts. By forcing their high frequency components to zero, they reduced the blocking artifacts in two homogeneous blocks.

1.5.3 Regularized Image Recovery

Basic idea is to *impose a number of constraints on the coded image in such a way as to restore it to its original artifact free form.* One such constraint can be derived by exploiting the fact that the transform coded image suffering blocking effects contains high frequency vertical and horizontal artifacts corresponding to vertical and horizontal discontinuities across boundaries of neighboring blocks. Since these components are missing in the original uncoded image, one step of iterative procedure consists of projecting the coded image onto the set of signals that are band limited in the horizontal or vertical directions. This constraint is referred as filtering constraint. Two similar approaches based on regularized image recovery are Projection onto Convex Set (POCS) and Constrained Least Square (CLS). Both the approaches are almost free from blocking artifacts but main drawback is their computational complexity. These methods need significant increase of processing time due to iterative procedure. So they are not suitable for real time video processing. These schemes will be discussed in brief in the following subsections:

Projection onto Convex Set (POCS)

The restoration algorithm based on POCS has advantage that it enables a large number of *a priori* (desirable) known constraints to be incorporated in the algorithm through the mechanism of POCS, if the constraints can be associated with convex set. If the convex sets have common intersection, the sequence of iteration converges to a restored image that satisfies all of the constraints. For POCS method, a new constrained set is defined that captures the smoothness between the blocks. The convexity of the set shown and projection on to it is computed. Thus, the reconstructed image is obtained by altering projection onto the smoothness set and the set defined by the available partial information about the BDCT coefficients.

Zakhor [30] in 1992, first tried to apply the Theory of POCS to the reduction of blocking artifacts of block coded images and suggested an iterative algorithm. Alternating projection onto two sets, starting from blocky image, reduces the blocking artifacts. The quantization constraint defines a set containing all images that are mapped by the video coder onto the same blocky image. This is accomplished by the set of bandlimited images obtained by lowpass filtering. While first set enforces the restored image to be close to the received blocky image, the projection on to second one carries out the actual enhancement. Blocking artifacts are reduced but at the cost of some blurring. **Reeves and Eddins** pointed out in [31] that the theory of POCS is inadequate as a basis for justifying the algorithm with the lowpass filter employed. This is mainly because non-ideal lowpass filter is not a projection operator onto a convex set.

Yang-*et al.* [32] in 1993, proposed three constraint sets based on the theory of POCS. The first is the quantization constraint set (QCS) whereas other two sets are smoothness constraint sets (SCS), contains information that is lost. The main features of POCS based approach are:

- Every known property of the original image (available data and prior knowledge) is represented by closed convex set.
- A vector common to all the sets can be found by alternating the projection onto each one of them, starting from any initial guess vector.
- *Filtering constraint:* available transform coded image contains high frequency vertical and horizontal artifacts corresponding to vertical and horizontal discontinuities.
- *Quantization constraint:* captures the between block smoothness

Constrained Least Square (CLS)

In CLS method, an objective function is introduced that incorporates into the recovery process both requirements that is fidelity to the available information about the BDCT coefficients and smoothness. Objective function which consists of two terms, is iteratively minimized. The first term measures the blockiness of an image by applying a high pass operator and is minimized for smooth images. The second term calculates the deviation from received blocky image. The regularization operator captures the smoothness properties of the image. The tradeoff between the conflicting requirements of the fidelity to the available data and smoothness is controlled by regularization parameters. Thus, minimization of objective functions reflects the smoothness properties. To incorporate quantization constraint, the solution after every iteration is projected onto the corresponding set of images.

Yang *at el.* [32] in 1993, used this method for reducing blocking artifacts, which is similar to POCS method. The recovered image is obtained by minimizing an objective function that imposes conflicting requirements on the reconstructed image. In this approach, if one of these function penalizes deviation from the available data, the other must penalize the undesired effects if the image is reconstructed only from the available data or, constraints the behavior of the reconstructed image. Reconstructed image is almost free from blocking artifacts butt computational complexity of this method is more due to its *iterative nature*

Minami and Zakhor [33] in 1995, proposed an optimization approach for removing blocking effects in transform coding. This technique exploits the correlation between the intensity values of boundary pixels of two neighboring blocks. It is based on the theoretical and empirical observation that under mild assumption, quantization of the DCT coefficients of two neighboring blocks increases the expected value of mean squared difference of slope (MSDS) between the slope across two adjacent blocks, and the average between the boundary slops of each of the two blocks. The amount of this increase is dependent upon the width of the quantization intervals of the transform coefficients. Therefore, among all permissible inverse quantized coefficients, the set which reduces the expected value of this MSDS by appropriate amount, is most likely to decease the blocking artifacts. To estimate the set of unquantized coefficients, they solved constrained programming problem in which the quantization decision intervals provide upper and lower bound constraints on the coefficients. The approach is based on gradient projection method.

Morkov random field (MRF) have been successfully used to model images. Their generality for modeling and capacity to incorporate different constraint and characteristics e.g. smooth region, edges etc., have made them popular. They have been used to develop algorithm to deconvolve blur and remove white noise. **O'Rourke and Stevenson** [34] in 1995, proposed a method for producing higher quality reconstructed image based on a stochastic model for the image data. Quantization partitions the transform coefficient space and maps all points in partition cell to representative reconstruction point, usually taken as the centroid of the cell. The proposed image restoration technique selects the reconstruction point within the quantization partition cell which results in a reconstructed image that best fits a non-Gaussian Morkov random field (MRF) image model. This approach results in a convex constraint optimization problem that can be solved iteratively.

Ozcelik *et al.* [35] proposed an iterative technique to reduce the unwanted degradation such as blocking and mosquito artifacts while keeping the necessary detail present in the original image. The proposed technique makes use of *a priori* information about the original image through a non-stationary Gauss-Markov model. Utilizing this model, *a maximum a posteriori* (MAP) estimate is obtained iteratively using mean filed annealing (MFA), which is an optimization technique. At each iteration, projecting the image onto constraint set defined by the quantization preserves the fidelity to the data. The maximization of the *posterior* function is carried out using man field annealing. Image models based on MRF have advantage that the field of interest (i.e. the intensity or motion) can be considered as consists of two fields: one representing the function that is to be estimated, and the other representing discontinuities. Furthermore, the probability distribution of the fields is characterized by a Gibbs distribution. The model containing the *a priori* information is specified through the "energy function" of the Gibbs distribution. The interaction of the variables characterizing image processing system is highly localized and the probability distribution of the fields is characterized tribution. In such type of systems, the optimization using MFA closely he optimal solution.

al. [36] in 1999, proposed the application of hierarchical Bayesian paradigm estoration problem. In 2000, they also used the same Bayesian approach ion and transmission of regularization parameters for reducing blocking In this paper they proposed the application of Bayesian paradigm to BDCT compressed image and the estimation of the required parameters.

estoration based on Adaptive Constrained Optimization.

[38] in 1998 have proposed a fast adaptive image restoration filter using ge classification for reducing artifacts. This scheme can be summarized steps:

e degradation operator $H = C^{-1}D^{-1}QC$ where [C] and $[C]^{-1}$ are the nd inverse DCT matrices respectively and $[Q]$ and $[D]^{-1}$ are the quanti- d inverse quantization matrices respectively, then $y = Hx$. Degradation H results in both discontinuities at block boundaries and loss of high details inside blocks. Based on image restoration theory, the original s best estimated by applying the inverse of H to the blocky image y, if e of H exists and well defined.

ive Constrained least square (CLS) filter along the direction of edge is ltering corresponding block. It incorporates a priori constraints into the n process without significant computational overhead. The frequency of CLS restoration filter is given by

$$G(k,l) = \frac{H^*(k,l)}{\mid H(k,l) \mid^2 + \lambda \mid A(k,l) \mid^2}$$

$k,l)$ and $A(k,l)$ are the 2D DFT of degradation operator and a high pass denominator of $G(k,l)$, $\mid H(k,l) \mid^2$ tries to reduce the degradation due $(k,l) \mid^2$ suppresses excess amplification of high frequency components, and the Lagrange multiplier λ is determines such that the solution satisfies the $||Ax||^2 = e^2$ subjected to above equation.

- Find x such that $||y - Hx|| = 0$ subjected to $||Ax|| \leq e^2$ where A is high pass filter (HPF).
- Hence the solution is such that which minimizes the variance across block boundary less than specified.
- Two DCT coefficients C(0,1) and C(1,0) is used for edge classification.
- Real time restoration filter is implemented as truncated FIR filter.

Paek *at el.* [39] in 1998, proposed a scheme based on POCS to reduce the blocking artifacts. They assumed the original image is highly correlated so the global frequency characteristics of two adjacent blocks are similar to local ones in each block. They considered the high frequency components in the global characteristics of a decoded image, which are not found in the local ones, as the result of blocking artifacts. They employed N-point DCT to obtain local characteristics, and 2N-point DCT to obtain global ones, and derived the relation between N-point and 2N-point DCT coefficients. A careful comparison of N-point and 2N-point DCT coefficients makes possible to detect the undesirable high frequency components due to blocking artifacts. They have also proposed novel convex set and their projection operators in DCT domain.

1.5.4 Block Boundary Discontinuity Criterion

Tien and Hung [40] in 1993, proposed a method of adjusting the quantized transform coefficients of the decoded image. It first decides whether the block is over edges or in a monotone area. In monotone area, the DC and first order horizontal and vertical DCT coefficients are adjusted to reduce the discontinuity over block boundary.

Error concealment problems in ATM network environment was handled by **Wang** *at el.* [41] to recover DCT coefficients lost during network transmission by maximally smoothing the transition of pixel values over block boundary. Blocking artifacts reduction can similarly be considered as an attempt to recover the accuracy loss of quantization coefficients.

Jeon and Jeong [5] in 1998, proposed a postprocessing approach, which can achieve minimum discontinuity of pixel value over block boundaries by compensating the loss of coefficient accuracy in transform domain. To quantify blocking artifacts, the block boundary discontinuity measure is obtained as the sum of squared pixel differences over the four block boundaries. The blocking artifacts are caused by loss of accuracy of transform coefficients in the processes of independent quantization of each block. Since quantization takes place in transform domain, the effect of quantization error is spread over all of the spatial locations within the block. The Artifacts are more noticeable in plain or slowing varying areas. This method finds the compensating transform coefficient whose inverse transform can minimize the block discontinuity when added to the quantized received image.

1.5.5 Prediction of Boundary Pixels

Choy *at el.* [42] in 1997, proposed a technique based on the weighted least squares estimation of transform coefficients from their quantized version and the available information about the quantizers used.

Chan *at el.* [43] in 1998, proposed a real time, non-iterative method to restore the block encoded images. This method is based on concept of linear prediction and vector quantization. Since the blocking artifact is a consequence of ignoring the inter-block correlation during compression therefore one of the best way to restore the original image is to make use of residual inter-block correlation to recover the block boundary pixels. Here the relation between two are investigated and then make use of the statistics obtain to predict the original pixel intensity. As considerable amount of residual inter-block correlation exists, the linear predication can provide a good prediction. In this approach, the selection of prediction filter coefficients is based on the least squares minimization criterion.

1.5.6 Wavelet Transform

In [44–47] the blocking artifacts are reduced by using a wavelet transform. **Xiong** *at el.* [44] in 1997, proposed a algorithm to reduce blocking artifacts using wavelet transform. By exploiting cross-scale correlation among wavelet coefficients, edge information in JPEG image is extracted and protected, while blocky noise in smooth background regions is smooth out in wavelet domain. This scheme has much lower computational complexity and able to achieve same PSNR as the best iterative method. In over complete wavelet representation signal is characterized by local maxima of wavelet transform modulus and finding these local maxima is equivalent to canny edge detector. Here, instead of finding the exact local maxima of wavelet transform modulus, cross-scale correlation is exploited for edge detection by directly multiplying the over complete representations of JPEG compressed image at different scales. Locations with cross-scale correlation above certain threshold are identified as edges, while low cross correlation regions are treated as background. So, by this method edges are extracted and protected across block boundaries. It is found that quantization noise is structured and blockiness has strong showings in first scale high-pass wavelet image. With edge information, high-pass wavelet image is thresholded to smooth out blocky discontinuities in background regions.

Kim *at el.* [45] in 1998, proposed a method the blocking components for the signal are removed because they causes the stepwise discontinuities in the spatial domain and which appears as impulse at each block boundary in the first scale of the wavelet transform. For multiscale analysis, they used the wavelet transform for the characterization of edges and singularities in multiscales by Mallat and Zhong. Each discontinuity is classified into three classes, and the removal of discontinuities in multiscales is applied to each class in a different way.

Choi and Kim [47] in 2000, proposed a scheme for postprocessing in wavelet transform domain in which they divided the blocking artifacts into two categories. One is blocky noise which exhibits a block pattern, and the other is granular noise which can be assumed white Gaussian. Subband decomposition makes the blocky noise more noticeable as vertical and horizontal false edges periodically appearing at block boundaries in high frequency subbands. By identifying such high frequency components, they reduced the blocky noise with linear minimum mean square error filter. The granular noise can be reduced by the wavelet based thresholding method.

1.6 Introduction to Digital Notch Filter

The notch filter highly attenuates a particular frequency component in the input signal while leaving nearby frequency components relatively unchanged. One application of notch filter is in the elimination of sinusoidal interferences corrupting signal, such as power line interferences in the design of digital instrumentation systems.

1.6.1 1D Digital Notch Filter

Hirano *et al.* [48], have given the systematic design approach for designing the 1D digital notch filter. Second order digital notch filter is characterized by two parameters, *notch frequency and 3 dB rejection bandwidth.* In the approach, they suggested the realization of notch filter by minimum number (two) of multipliers. The transfer function of analog notch filter is:

$$H(s) = \frac{s^2 + c^2}{s^2 + bs + c^2} \tag{1.3}$$

Here $\omega = c$ is the notch frequency at which no signal is transmitted through the filter. Within the frequency band centered at $\omega = c$ and of width b, all signal components are attenuated by more than 3 dB. Hence 3 dB rejection bandwidth is b. Digital notch filter can be developed by applying *bilinear transformation*$(s = (z-1)/(z+1))$ to analog notch filter. Using this transformation, the transfer function of digital notch filter can be obtained as:

$$G(z) = 1 + \frac{z^{-2} - a_1 z^{-1} + a_2}{1 - a_1 z^{-1} + a_2 z^{-2}} \tag{1.4}$$

where a_1 and a_2 in terms of notch frequency ω_o and 3 dB rejection bandwidth BW are given by:

$$a_1 = \frac{2\cos\omega_o}{1+\tan(BW/2)} \qquad and \qquad a_2 = \frac{1-\tan(BW/2)}{1+\tan(BW/2)}$$

1.6.2 1D IIR Multiple-notch Filter

Pei and Tseng [7] in 1997, have given a method for designing 1D IIR multiple-notch filter from allpass filter. In this method the specifications of notch filter is first transformed into that of allpass filter. Therefore, the notch filter design problem becomes an allpass filter design problem. The specifications of multiple-notch filter is given by:

$$H(e^{j\omega}) = \begin{cases} 0 & for\ \omega = \omega_{Nk} \quad k = 1,2,...M \\ 1 & otherwise \end{cases} \tag{1.5}$$

The transfer function of 2M-order allpass filter is given by:

$$A(z) = \frac{a_{2M} + ... + a_1 z^{-2M+1} + z^{-2M}}{1 + a_1 z^{-1} + ... + a_{2M} z^{-2M}} \tag{1.6}$$

where $A(e^{j\omega})$=$e^{j\theta_A(\omega)}$ and $H(e^{j\omega})$=$\frac{1}{2}[1+e^{j\theta_A(\omega)}]$. To design allpass filter, a set of linear equation in the filter coefficient is generated from its phase characteristics and solved. The set of linear equation is given by

$$\mathbf{Q.a} = \mathbf{p} \tag{1.7}$$

where

$$a = [a_1, a_2, ...a_{2M}]^T$$

$$p = [tan\beta_1, tan\beta_2, ...tan\beta_{2M}]^T$$

$$q_{ik} = sin(k\omega_1) - tan\beta_i cos(k\omega_i)$$

Thus the realization of notch filter H(z) is equivalent to realization of APF A(z). The H(z) is expressed as

$$H(z) = [1 + A(z))]/2 \tag{1.8}$$

Due to mirror image symmetry relation between the numerator and denominator polynomials of allpass filter, the notch filter can be realized by computationally efficient lattice structure.

Joshi and Dutta Roy [49] in 1999, have modified the method for designing 1D IIR-multiple notch filter. They realized all-pass filter is by cascade of N *second order allpass filter.* This method ensures those 3 dB rejection bandwidths are lower than those specified.

1.6.3 Linear-phase FIR notch Filter

To provide the linear phase, the digital notch filter must be a finite-duration impulse-response filter with a symmetric impulse response. Design of FIR digital notch filter has been discussed in [9, 50]. **Yu** *et al.* [9] investigated some approaches for designing 1D linear-phase FIR notch filters, which are based on the modification of several established design techniques of linear phase FIR band selective filters. In addition, the design of 2D linear-phase FIR single notch filter is briefly considered. They exploited the three commonly used design techniques for designing linear phase FIR notch (LPFN) filter: (i) windowed Fourier series approach (ii) frequency sampling approach and, (iii) optimal filter design approach, based on Remez exchange algorithm. They also considered the use of some special techniques for the linear phase FIR filter design, such as the frequency response sharpening approach and interpolated FIR filter technique. In windowed Fourier series approach for designing LPFN filter Kaiser window is used, which is also the most frequently used window for designing the FIR filter.

1.6.4 2D Single Notch Filter

Pei and Tseng [6, 51] in 1994, developed a simple algebraic method for 2D IIR filter design to yield not only closed form transfer function but also to satisfy bounded-input/bounded-output (BIBO) stability condition. They have applied this filter to eliminate sinusoidal/narrowband interferences superimposed on an image. The frequency specifications of a 2D ideal notch filter is given by

$$H_d(e^{j\omega_1}, e^{j\omega_2}) = \begin{cases} 0 & for \quad (\omega_1, \omega_2) = (\omega_{1N}, \omega_{2N}) \\ 1 & otherwise \end{cases} \tag{1.9}$$

If $H_p(z_1, z_2)$ is 2D-parallel line filter and $H_s(z_1, z_2)$ is 2D-straight line filter, then desired notch filter is given by

$$H_N(z_1, z_2) = 1 - H_p(z_1, z_2)H_s(z_1, z_2) \tag{1.10}$$

To design these two filter they started with the frequency specifications of a 2D parallel line filter which is given by

$$H_d(e^{j\omega_1}, e^{j\omega_2}) = \begin{cases} 1 & for \quad \omega_2 = \pm\omega_{2N} \\ 0 & otherwise \end{cases} \tag{1.11}$$

The 2D parallel line filters can be designed by choosing $H_p(z_1, z_2)$ as:

$$H_p(z_1, z_2) = H_{bp}(z)|_{z=z_2} \qquad for \quad i = 1, 2 \tag{1.12}$$

where $H_{bp}(z)$ is 1D-bandpass filter and given as:

$$H_{bp}(z) = 1 - \frac{z^{-2} - a_1 z^{-1} + a_2}{1 - a_1 z^{-1} + a_2 z^{-2}} \tag{1.13}$$

In above expression a_1 and a_2 are given by:

$$a_1 = \frac{2\cos\omega_o T}{1 + \tan(BW/2)} \qquad and \qquad a_2 = \frac{1 - \tan(BW/2)}{1 + \tan(BW/2)}$$

where ω_o is the center frequency and BW is the 3 dB bandwidth of $H_{bp}(z)$. 2D straight-line filter is designed by frequency transformation of 2D analog protype filter.

Pei and Tseng in 1997 [52] and in 1998 [53] reduced the 2D notch filter design problem into two pairs of 1D filter design problem. In [52], they designed 2D IIR notch filter by writing outer product expansion of sampled frequency response matrix of ideal 2D notch filter using singular value decomposition. They also proposed similar approach to design 2D FIR notch filter by singular value decomposition in [53].

Huang *et al.* [8] have used notch filter in Fourier domain to remove the artificial edges due to blocking artifacts. In this scheme, the edge image is notch filtered and used for a neighborhood analysis. Then, a space-variant filter is applied to the coded image adaptively, dependent on frequency analysis. Blocking artifacts are expected to have periodic texture. According to signal processing theory, the periodic textures will results in some peak in the Fourier transform domain. This means the periodic texture can be detected more efficiently in frequency domain. In this approach, based on an analysis in frequency domain, the edge image is notch filtered and then used for a neighborhood analysis. A space-variant filter is applied to the coded image adaptively, dependent on frequency analysis.

1.7 Summary of few algorithms proposed in this work

A number of algorithms for reducing blocking artifacts are proposed in present work. First the hybrid scheme is proposed which takes advantages of adaptive filtering and the recovery method for the loss of accuracy of DCT coefficients. Then both IIR and FIR 2D multiple-notch filters are designed and applied to improve the performance of the space-variant/adaptive filtering method. At the end of this work few computationally efficient algorithms are also proposed.

1.7.1 Hybrid Scheme

From the available literature, it has been seen that the filtering of decoded image without considering the local image statistics often cause the loss of high frequency detail such as edges. Any single algorithm proposed in literature is not able to perform best in different types of regions of an image. Thus, a hybrid scheme is developed for postprocessing of DCT coded images by clubbing the merits of several existing algorithms. This scheme is named as hybrid scheme as the processing is done in both DCT as well as spatial domain by two different algorithms. Smoothing artificial discontinuities due to blocking artifacts improves the image quality whereas smoothing actual image edges degrades it. Thus, objective was to satisfy these two conflicting requirements as simply as possible.

Classification is essential in postprocessing which attempts to exploit local statistics of image regions and the sensitivity of human eyes. In this approach, the edges of BDCT coded image is detected and used for the classification of regions into monotone area and edge area. The scheme makes use of adaptive filtering in edge area and block-boundary discontinuity minimization algorithm in monotone area. For monotone area, the minimum discontinuity of pixel values over block boundaries is achieved by compensating for the loss of accuracy of transform coefficients by the algorithm suggested by Jeon and Jeong in [5] with some modification. For edge area, a signal adaptive filter is proposed which perform the filtering approximately parallel to the edge to avoid blurring. The use of a lower order signal adaptive filter and the block-boundary discontinuity minimization algorithm reduces the processing time. Corner outliers reduction scheme further improves the performance.

It has been observed that the performance of this algorithm is better than space-variant filtering as well as the two individual algorithms used in hybrid scheme. It has been found that the performance of the proposed algorithm improves as compression ratio increases. The reduction of discontinuity signifies that the blocking artifacts are reduced. The improvement in PSNR for block-boundary pixels is more as compared to over all PSNR which also indicates the same.

1.7.2 Design and applications of 2D IIR multiple-notch filter

In present work, the design and some new applications of 2D IIR multiple-notch filter have also been proposed. In proposed design approach, a simple algebraic method [6] is used to design the 2D IIR multiple-notch filter from 1D multiple tone filter. The design of 1D multiple tone filter is based on the design of all-pass filter as discussed in [7].

The possibility of using 2D multiple-notch filter for reducing blocking artifact is fully examined. It is shown that 2D multiple-notch filter can eliminate the square grid. It can also reduce the blocking artifacts from DCT coded images. The concept of reducing blocking artifacts by 2D multiple-notch filter is based on the fact that the discontinuities due to block artifacts in decoded image have periodic structure which results in some peaks in DCT domain. These discontinuities are highlighted in gradient of the image. A 2D multiple-notch filter can kill these peaks to remove the false edges from the edge-map of blocky image. Discontinuities due to blocking artifacts are more visible in monotone area, so this filter can be applied directly in these areas. Thus, improvement in the performances of space-variant/adaptive filter by removing of false edges from the edge-map and the reduction of blocking artifacts directly in monotone area, are the new possible applications of 2D multiple-notch filter. In these applications, the reduction of discontinuity signifies that the blocking artifacts are reduced.

1.7.3 Design and applications of 2D FIR multiple-notch filter

The design approach of 2D multiple-notch filter has also been extended to FIR type. FIR filters are suitable for image processing applications as they cause less distortion due to their linear phase property. The drawback of FIR filter is that they cause more delay. A special 2D FIR multiple-notch filter is designed with an intention to remove blocking artifacts from DCT coded images. The design procedure for the 2D FIR multiple-tone filter is similar to IIR type of this filter but the desired 2D multiple-notch filter is the complementary filter of 2D multiple-tone filter. In this case, two 1D FIR multiple-tone filters are designed by windowed Fourier series method with Kaiser window. This filter is also applied for the reduction of blocking artifacts and removal of false edges from edge of blocky decompressed image. The results obtained in this case are better than IIR type of this filter as expected.

1.7.4 Smoothing of the Sub-image of DC Coefficients by Signal Adaptive Filter

The algorithm is based on the assumption that the correlation among the DC coefficients of neighboring block is high if all the blocks belong to monotone area. This algorithm reduces the blocking artifacts by exploiting the residual inter-block correlation which exists in received blocky image. In the approach, a DC sub-image is constructed by taking only the DC coefficient of each block in DCT coded image. A signal adaptive filter is applied to smooth the DC sub-image. The image blocks are classified as monotone block or edge block simply by comparing the absolute value of sum of the AC coefficient of the block with a threshold. This scheme shows significant reduction in blocking artifacts without much computational complexity. This can be verified by calculating block boundary discontinuity. The PSNR is slightly improved but the improvement is more at block boundary pixels.

1.7.5 Reduction of Block-boundary Discontinuities

Proposed algorithm is based on the assumption that artificial discontinuities at block boundaries are due to blocking artifacts and are more visible in monotone or slowly varying areas. The algorithm reduces the discontinuities in blocky image by capturing and removing the discontinuities in DCT domain. The algorithm also reduces the blocking artifacts significantly by selective attenuation of AC components corresponding to block boundary discontinuities. In order to capture the artificial discontinuities, the blocky image is re-divided into blocks with different block boundaries. To reduce the artificial discontinuities, the selected AC components of those new blocks which do not contain details, are heavily attenuated. The algorithm requires the computation of DCT of new blocks but the processing time is less because no filtering is required. Availability of fast algorithms for DCT computation further reduces the processing time.

The above two algorithms together reduce the blocking artifacts considerably. It is verified by comparing boundary PSNR and block-boundary discontinuity. It is found that improvement in PSNR for block boundary pixels is more as compared to over all PSNR. This result is attractive because discontinuities at block boundaries which are the most visually annoying effect, are reduced. Hence, this computationally efficient scheme reduces blocking artifacts considerably with slight improvement in PSNR.

1.7.6 Reduction of Block-boundary Discontinuities: Second Approach

A second approach for discontinuity reduction is proposed. In this algorithm, the discontinuities are captured in the same way but it uses the SVD based filtering scheme for their reduction. It reduces the blocking artifacts considerably but its computational complexity is slightly more because SVD algorithm has to be applied to each of the block. The PSNR achieved by this algorithm is also slightly less as compared to the first approach.

1.7.7 Blocking artifact reduction by eliminating some DCT coefficients of concatenated block of two adjacent blocks

This algorithm reduces the blocking artifacts by eliminating some selected DCT coefficients of concatenated block of two adjacent blocks. This DCT domain algorithm has low computational complexity, as no filtering is required. The availability of fast algorithm for DCT computation makes this algorithm suitable for low bit rate coding applications. The selection of first row and first column of the DCT of concatenated block further reduces the computation complexity. This computationally efficient algorithm also gives very good result in terms of PSNR, discontinuity measure and visual quality.

The performance analysis and simulation results show that the proposed techniques are very competitive compared to previously published works.

Motivations

Therefore the motivations behind the work presented in this thesis are:

- Uncompressed video and audio data are huge and there is a big problem for their storage and network communication. Therefore, data compression is required. As the compression ratio of lossless methods (e.g., Huffman, Arithmetic) is not high enough for image and video compression, a lossy compression scheme that can provide higher compression ratio is needed.
- Very good energy compaction and decorrelation properties of DCT motivated to work on the DCT based image compression scheme. The performance of DCT based compression scheme is limited by blocking artifacts. So, the main objective was to find a DCT based scheme that can minimize these blocking artifacts.
- Most of the existing popular standards for image compression also use DCT based image compression schemes. This was also one of the main reasons for taking up this problem. Although at the beginning a number of possibilities for modification of coding schemes are studied but looking at these existing standards the work is centered around the postprocessing of DCT coded images.
- DCT-based image compression is very popular and finds various applications. Improvement in quantization, encoding and postprocessing can increase the capabilities of DCT-based image compression scheme over other schemes in many applications.
- Low bit rate coding applications motivate to find computationally efficient algorithms for postprocessing of such images.

Organization of Thesis

Chapter 1 introduces various aspects of data compression with an overview of DCT based image compression scheme. Various methods of postprocessing of DCT coded images are discussed and a state-of-the-art survey on the subject is presented.

In *Chapter 2*, a hybrid scheme is presented which takes advantages of adaptive filtering in edge area and block boundary discontinuity algorithm in monotone area.

Chapter 3 presents an approach based on space-variant/ adaptive filtering. In this approach, a 2D IIR multiple-notch filter is designed from 1D multiple-notch filter. This filter is applied to reduce the blocking artifacts from DCT coded images either by improving the classification scheme or by directly filtering the blocking artifacts in monotone areas.

In *Chapter 4*, the design approach presented in *Chapter 3* of 2D multiple-notch filter is extended to FIR type filter. This filter is also applied to reduce the blocking artifacts from DCT coded images as in *Chapter 3*.

Chapter 5 is devoted to some new computationally efficient algorithms. Four algorithms to reduce the artifacts in DCT domain are presented.

Chapter 6 concludes the major contributions of this thesis and suggests the scope for future research work in this area.

Chapter 2

A Hybrid Scheme for the Postprocessing of DCT Coded Images

2.1 Introduction

In block discrete cosine transform (BDCT) based image compression schemes the reconstructed image from highly compressed data has noticeable degradation due to the blocking artifacts. In postprocessing of DCT coded image, filtering of image without considering the local image statistics often causes the loss of high frequency detail such as edges. Therefore, a space-variant or adaptive filtering techniques are used to overcome this problem. Both adaptive and space-variant filtering requires a classification scheme to categorize pixel into different class for adaptation. Then different spatial filters are used to remove coding artifacts according to class information. In these schemes, a lower order filter is preferred to save the processing time. However, to achieve better spatial adaptiveness, short-tap filters are preferred in smooth area near to edge but long-tap filters are required in larger smooth region. Thus, in these schemes the processing time for monotone block is more than that of edge block. Thus a better scheme that can reduce the over all processing time is required. In this Chapter, a hybrid scheme is proposed[1] in which the DCT coefficients of monotone block are compensated to achieve minimum block-boundary discontinuity whereas in edge blocks a signal adaptive filter is applied to perform the filtering along the edge. This scheme is named as hybrid scheme as the processing is done in both DCT as well as spatial domain by two different algorithms. The compensating DCT coefficients for monotone blocks are calculated from the DCT of the block-boundary pixel differences. In this calculation, those block-boundary pixel differences are made zero whose the neighboring block is an edge block. In proposed scheme, the edge information is extracted and used for the classification of image blocks. The signal adaptive filter also uses edge-map to perform the filtering approximately parallel to edge to avoid blurring. Thus, the blocking artifacts are reduced more efficiently by this scheme.

As discussed in *Chapter 1*, in BDCT based image compression, high compression ratio are usually achieved by discarding information about the BDCT coefficients that are considered unimportant and yields image that exhibit the visually annoying blocking artifact. It is done by the quantization of BDCT coefficients. This process is an irreversible one that results in degradation of coded image. The blocking artifact manifest itself as an artificial boundary among the pixels of adjacent blocks and constitutes a serious bottleneck for many important visual communication applications where the pleasing image is required at very high compression ratios. Blocking artifacts are the major degradation in block-based image coding techniques, especially at higher compression ratio. Thus, the objective of postprocessing is to maximally remove noise introduced by quantization process without sacrificing the image sharpness. Low pass filtering is inadequate to remove various types of noise present in different area of blocky image. Low pass filtering reduces grid noise in monotone area but it doesn't reduce the staircase noise. So, nonlinear space-variant or adaptive filter is required to reduce various types of noise. Several postprocessing algorithms have been proposed to reduce blocking artifacts of block coding system [1,3–5,22,24,27,56]. In non-linear space-variant filtering [1], the image is divided into monotone area and edge area using edge information obtained

[1] Part of this Chapter represents work accepted for presentation and publication, see [54, 83]

from detecting edge by gradient operator. Here two-dimensional (2D) lowpass filter is used to reduce grid noise in monotone area, whereas a directional one-dimensional (1D) filter is used to reduce staircase noise along the edges. In adaptive filtering [3,24,27,56], the coefficients of 2D filter are chosen by edge information of the image. No filtering is done at edge pixels. Weighted or un-weighted filtering is performed at the pixels in the monotone area or near the edge. In [56], 2D multiple-notch filter is used to reduce the blocking artifacts in monotone area. Both nonlinear space-variant filtering and adaptive filtering require classification of image blocks, which is based on available edge information extracted from the received blocky image. Hence the performance of space-variant or adaptive filtering scheme degrades. In references [2, 5], the blocking artifacts are reduced by processing the image in DCT domain itself.

2.2 Proposed Scheme

In postprocessing of DCT coded image, a good classification scheme is required because single algorithm cannot give the best performance in different types of regions. To maintain the sharpness of the decoded image filter coefficients must be selected carefully as the filtering without considering the local image statistics often cause the loss of high frequency detail such as edges. Hence, space-invariant lowpass filter is not suitable as it will blur the edge and degrade the image visual quality. Space-variant or adaptive filtering technique can be used to overcome this problem. An adaptive filtering technique uses classification and edge detection to categorize pixel into different class for adaptation. Then different spatial filters are used to remove coding artifacts according to class information. Classification of image segments is essential to both space-variant and adaptive filtering which attempts to exploit local statistics of image regions and the sensitivity of human eyes. As each block of image has been properly classified, one or more appropriate filters can be used to smooth out the coding artifacts. To avoid blurring, LPF is applied to areas that are not masked by the presence of detail information such as smooth region. A 2D separable lowpass FIR filter provides one popular choice to artifact reduction in smooth regions. As far as possible, lower order filter is taken to save the processing time. To achieve better spatial adaptiveness, the length of the LPF may vary. It is also found that the human visual system (HVS) is more sensitive to blocking artifacts in monotone regions as compared to edge regions. Therefore, a strong long-tap smoothing filter is required in monotone area. For smooth area near to edge, short-tap filters such as filter of size 3 × 3 are preferred.

Based on above discussion, a hybrid scheme for the postprocessing is being proposed in this Chapter. In the proposed scheme, the edge information is extracted and used for the classification of image blocks. For edge blocks, a signal adaptive filter performs the filtering along the edge to reduce the staircase noise. This filter also uses the same edge information (edge-map). In the monotone area, the DCT coefficients are compensated for loss of their accuracy using minimum block-boundary discontinuity criterion in transform domain itself. These two algorithms are discussed in the following two subsections.

2.2.1 DCT domain Block-boundary Discontinuity Minimization Algorithm for Monotone Area

In transform coding, the DCT coefficient is quantized with a quantization step size that is generally determined by the location of coefficient and color component. If no other noise exists, then quantization error for the coefficient is half of the corresponding quantization step size. Since the quantization processes is in transform domain, the quantization noise affects the pixel values over all the spatial locations. So, it is better to reduce it in DCT domain itself. Blocking artifacts are the result of quantization process required for image compression. These blocking artifacts are visible as an artificial boundary among the pixels of adjacent blocks. Thus, minimizing the discontinuity of pixel values over block boundaries can reduce these artifacts. This algorithm is applied in monotone area since blocking artifacts are more visible in these areas and does not contain high frequency details.

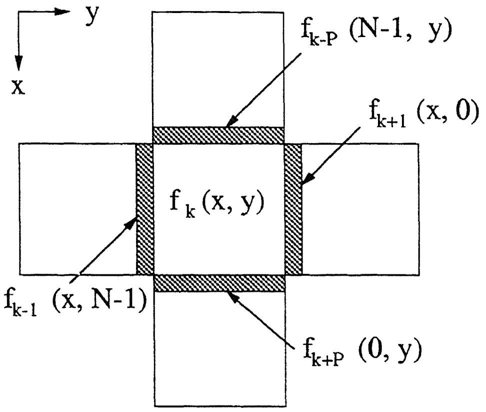

Figure 2.1: A block and its adjacent top, bottom, left and right blocks to calculate the block-boundary discontinuity.

In proposed scheme the minimum discontinuity of pixel values over block boundaries is achieved by compensating for the loss of accuracy of transform coefficients by the algorithm suggested by Jeon and Jeong in [5] with some modification. In their algorithm they have defined block-boundary discontinuity measure $D_k(f)$ for k^{th} block as the sum of squared pixel differences over the four block-boundaries to quantify the blocking artifacts.

$$\begin{aligned} D_k(f) = {} & \Sigma_{y=0}^{N-1}[f_{k-P}(N-1,y) - f_k(0,y)]^2 + \Sigma_{y=0}^{N-1}[f_{k+P}(0,y) - f_k(N-1,y)]^2 \\ & + \Sigma_{y=0}^{N-1}[f_{k-1}(x,N-1) - f_k(x,0)]^2 + \Sigma_{y=0}^{N-1}[f_{k+1}(x,0) - f_k(x,N-1)]^2 \end{aligned} \tag{2.1}$$

where f_{k-P}, f_{k+N}, f_{k-1} and f_{k+1} refer to pixels in the top, bottom, left an right blocks of the k^{th} block, respectively. The total block discontinuity is given by:

$$D(f) = \sum_{k=1}^{K} D_k(f) \tag{2.2}$$

In this scheme compensation signal $\Delta f(x, y)$ is added to the dequantized image $f_Q(x, y)$ to get resultant signal $\tilde{f}\,(x, y)$ as:

$$\tilde{f}\,(x, y) = f_Q(x, y) + \Delta f(x, y) \tag{2.3}$$

The compensating signal is estimated for each block to obtain the minimum block-boundary discontinuity. This is a constraint least square problem where the minimization is performed in DCT domain. In [5] the compensating DCT coefficients are calculated as:

$$\begin{aligned}
a_{00} &= \sqrt{N}[G_{k-P}(0) + G_{k+P}(0) + G_{k-1}(0) + G_{k+1}(0)]/4 \\
a_{01} &= \sqrt{N}[G_{k-P}(1) + G_{k+P}(1) + G_{k-1}(0) - G_{k+1}(0)]/[2 + 4\cos^2(\pi/2N)] \\
a_{10} &= \sqrt{N}[G_{k-P}(0) - G_{k+P}(0) + G_{k-1}(1) + G_{k+1}(1)]/[2 + 4\cos^2(\pi/2N)] \\
a_{11} &= \sqrt{N}[G_{k-P}(1) - G_{k+P}(1) + G_{k-1}(1) - G_{k+1}(1)]/4\sqrt{2}\cos(\pi/2N)]
\end{aligned} \tag{2.4}$$

where $G_k(r)$ is the r^{th} one dimensional DCT coefficient of pixel difference over block-boundary $g_{k\pm P}$ and $g_{k\pm 1}$ which are estimated simply by difference of dequantized values to further simplify the processing. To control degree of compensation weight factor λ is multiplied to the estimated compensating coefficients. In this case a weight factor near 0.5 is found to be appropriate.

In addition to applying this algorithm only in monotone area, some modifications have been made. One main difference between the proposed algorithm and the algorithm proposed in [5] is in the calculation of block-boundary differences. In this calculation, those block-boundary pixel differences are made zero whose the neighboring block is an edge block. This is based on the fact that characteristics of edge area is quite different from monotone area as we can observe that the artificial discontinuities at block-boundaries due to blocking artifacts are more visible in monotone or slowly varying areas. This modification improves the performance of the algorithm.

2.2.2 Spatial Domain Signal Adaptive Filtering for Edge Area

As discussed in [1], a directional filter is required to reduce staircase noise along the edges. Therefore, in proposed hybrid scheme a directional or signal adaptive filter is applied in edge area. This adaptive filtering scheme uses the edge-map obtained from an edge detection algorithm (Sobels, Canny operator etc.). Depending on this edge-map, some of the filter coefficient are made zero. In proposed signal adaptive filtering

A	B	C
D	E	F
G	H	I

$\frac{1}{16}$	$\frac{2}{16}$	$\frac{1}{16}$
$\frac{2}{16}$	$\frac{4}{16}$	$\frac{2}{16}$
$\frac{1}{16}$	$\frac{2}{16}$	$\frac{1}{16}$

Figure 2.2: Filtering mask of the signal adaptive filter.

(SAF), if the center E of filtering mask (see Fig 2.2) is at edge pixel of the block then all surrounding coefficients A, B, C, D, F, G, H, and I are made zero and thus the value of edge pixel remains unchanged. If the center of mask is at non-edge pixel in the block, then those surrounding values that are at edge pixels are decreased to zero whereas value at the center of mask is increased by the same amount.

2.2.3 Corner Outliers Detection and Replacement

As discussed in *Chapter 1*, corner outliers are visible at the cross point of M × M block when the corner pixel of one block is very large or very small as compared to corner pixels of the neighboring blocks. This condition is tested to detect the corner outliers by comparing each corner pixel with its neighbors. If the corner outliers exist, then the former and its neighbors are replaced by its weighted average to reduce this effect. The replacement scheme for this purpose is discussed in [3] is given below:

$$\begin{aligned} A' &= (4A + B + C + 2D + 4)/8 \\ A_1' &= (A' + 3A_1 + 2)/4 \\ A_2' &= (A' + 3A_2 + 2)/4 \end{aligned} \tag{2.5}$$

As shown in Fig. 2.3, the pixel A is detected as corner outliers and the pixels A, A_1 and A_2 is replaced by A', A_1' and A_2'.

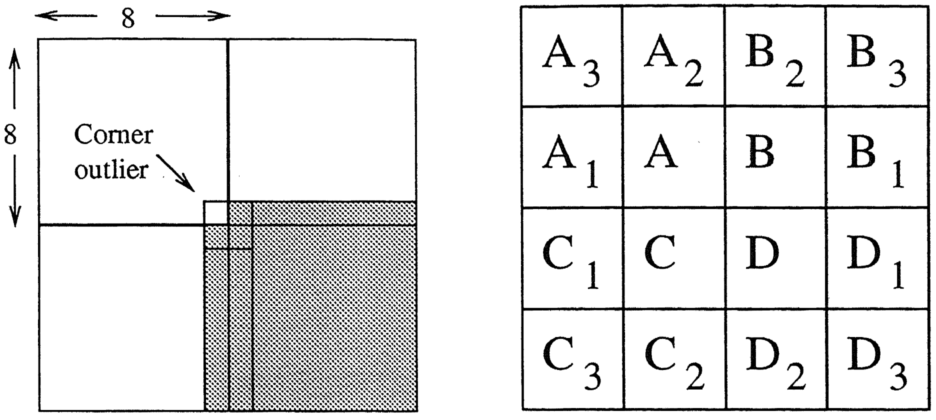

(a)

A_3	A_2	B_2	B_3
A_1	A	B	B_1
C_1	C	D	D_1
C_3	C_2	D_2	D_3

(b)

igure 2.3: (a) Presence of corner outliers. (b) Pixels used in weighted averaging for the duction of corner outliers.

.3 Results

this section, results of proposed algorithm applied on 256 × 256 Lenna image has been resented. The algorithm is implemented with MATLAB. Various results are given in able 2.1 in which the results of proposed algorithm are compared with baseline JPEG ke DCT decoded image. Peak signal to noise ratio (PSNR) is defined as:

$$PSNR(in\ dB) = 10\ log_{10}(\frac{255^2}{MSE}) \qquad (2.6)$$

Where 255 is the peak signal for 8 bit PCM and MSE is mean square error given by

$$MSE = \frac{1}{N^2}[\sum_{i=0}^{N-1}\sum_{j=0}^{N-1}(f_{mn} - \tilde{f}_{mn})^2] \qquad (2.7)$$

Vhere f_{mn} and $\tilde{f}_{mn}$ are the pixel values at position (m, n) of original and decoded mage respectively. As the PSNR is only the rough indicator of image quality and does ot reflects the blocking artifacts, two new discontinuity measures are defined. The lock-boundary PSNR (BPSNR) is defined in the same way as PSNR but only one pixel rom both side of block boundary are considered for the calculation of mean square

Table 2.1: Comparison of the performance of hybrid scheme on Lenna image.

Algorithms	*PSNR in dB at quality factor q*			*Boundary PSNR in dB at quality factor q*			*Boundary Discontinuity in (10^6) at quality factor q*		
	q=5	q=7	q=10	q=5	q=7	q=10	q=5	q=7	q=10
Original	-	-	-	-	-	-	4.28	4.28	4.28
DCT coded	25.32	26.75	28.09	15.02	16.51	17.96	10.9	9.22	7.93
Signal Adaptive filtering	25.17	26.12	27.11	15.15	16.16	17.22	8.89	7.85	7.07
block-boundary discontinuity minimization	25.60	27.00	28.40	15.52	16.88	18.31	8.92	7.67	6.65
Proposed algorithm	25.72	26.95	28.31	15.62	16.84	18.22	8.66	7.62	6.68

error (MSE) whereas the block-boundary discontinuity measure is defined as the sum of square of difference of pixel values across the four block-boundaries.

The performance of the proposed algorithm improves as compression ratio increases. The reduction of discontinuity signifies (see Table 2.1) blocking artifacts are reduced which can also be observed visually in Fig. 2.4, Fig. 2.5 and Fig. 2.6. These figures and Table 2.1 also shows that neither of the two algorithms used in hybrid scheme are able to give good results if they are used to process whole image. It can also be observed from Table 2.1 that the improvement in PSNR for block-boundary pixels is more as compared to over all PSNR.

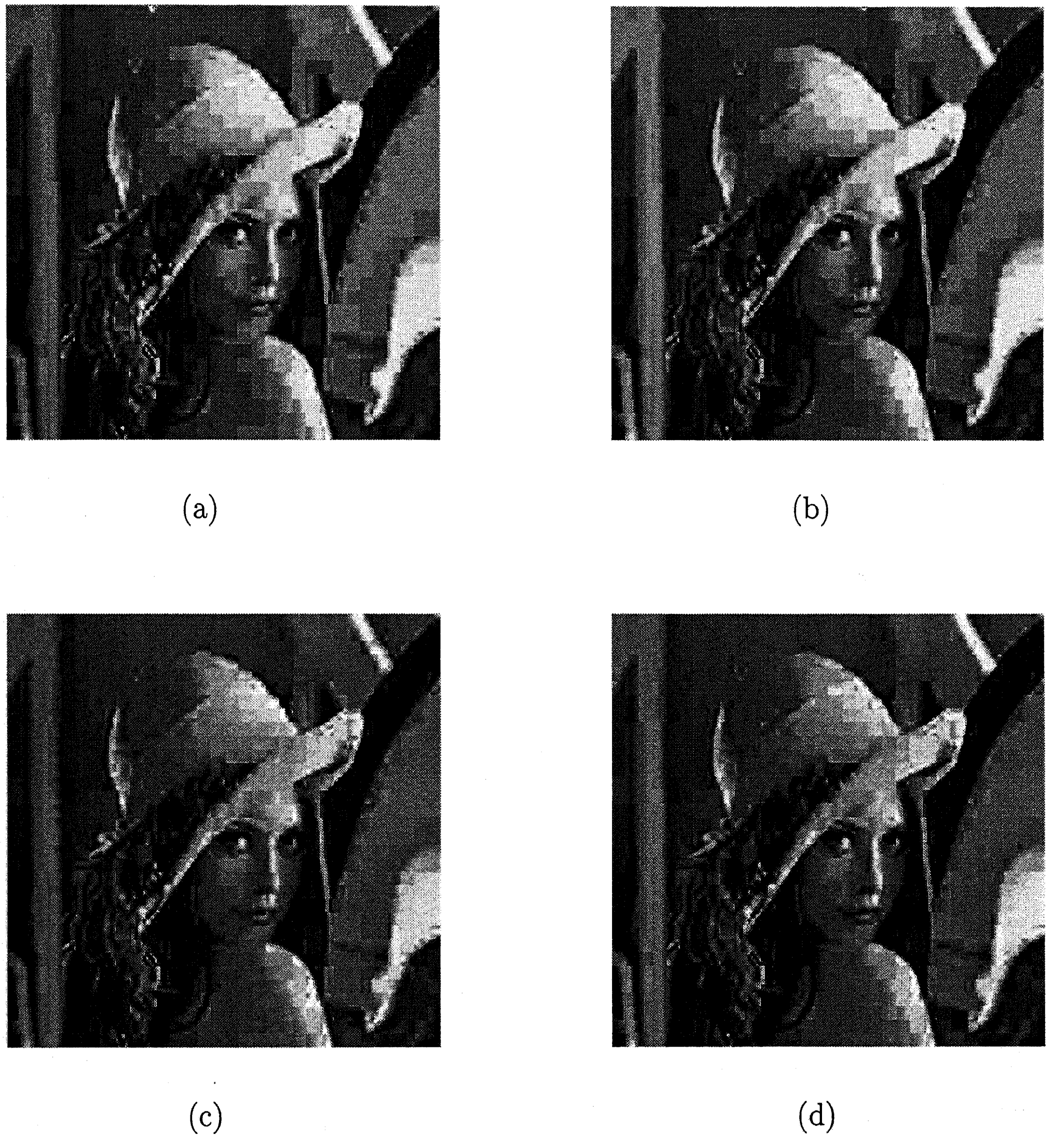

(a)

(b)

(c)

(d)

Figure 2.4: Reconstructed Lenna image (compressed at Quality Factor 5) by various algorithm (a) Simple DCT decoded, (b) Postprocessed by signal adaptive filtering, (c) Postprocessed by block-boundary discontinuity minimization algorithm, (d) Postprocessed by proposed hybrid scheme.

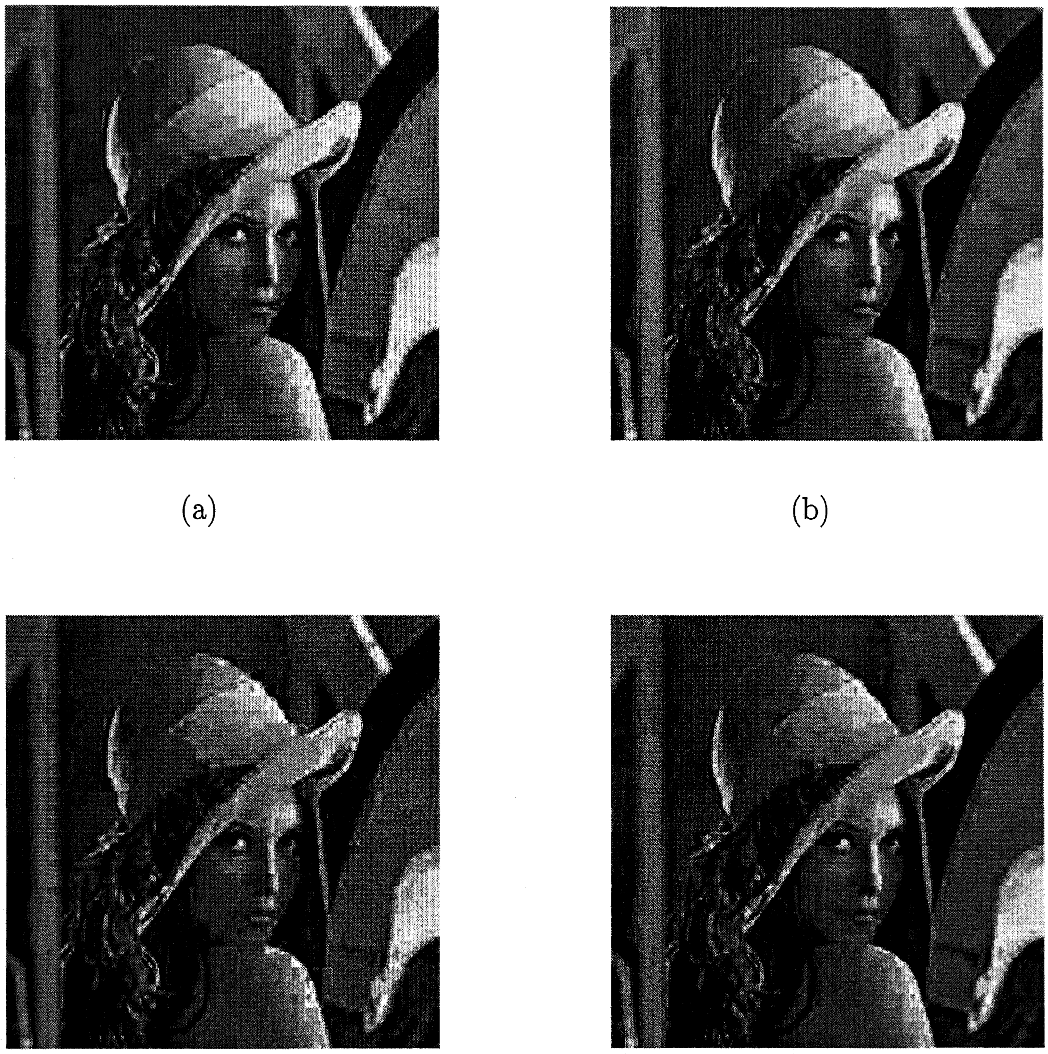

(a)

(b)

(c)

(d)

Figure 2.5: Reconstructed Lenna image (compressed at Quality Factor 7) by various algorithm (a) Simple DCT decoded, (b) Postprocessed by signal adaptive filtering, (c) Postprocessed by block-boundary discontinuity minimization algorithm, (d) Postprocessed by proposed hybrid scheme.

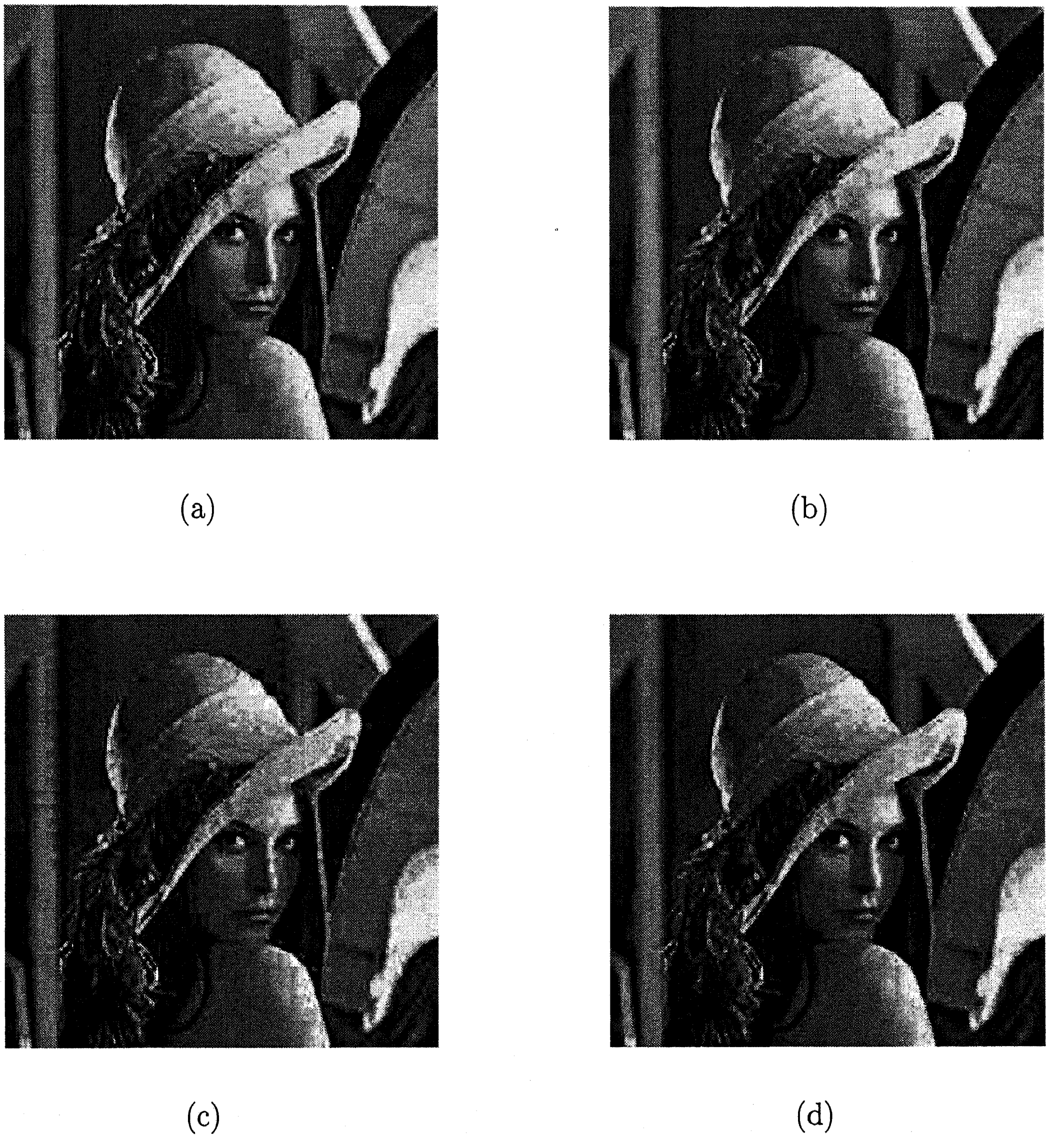

Figure 2.6: Reconstructed Lenna image (compressed at Quality Factor 10) by various algorithm (a) Simple DCT decoded, (b) Postprocessed by signal adaptive filtering, (c) Postprocessed by block-boundary discontinuity minimization algorithm, (d) Postprocessed by proposed hybrid scheme.

2.4 Conclusions

In this Chapter a hybrid scheme for postprocessing of DCT coded image is proposed which takes the advantage of adaptive filtering in edge area and block-boundary discontinuity minimization algorithm in monotone area. Thus, the processing of image is done in both spatial and transform domain. In this algorithm, in order to reduce the processing time, a lower order signal adaptive filter is applied in edge area whereas block-boundary discontinuity minimization algorithm is used in monotone area. Block-boundary discontinuity minimization algorithm reduces the blocking artifacts with low computational cost. Thus, proposed algorithm reduces the blocking artifacts considerably without introducing much blurring in the edge area. The results are verified by comparing boundary PSNR and block-boundary discontinuity (see Table 2.1). This can also be observed from the results presented in Fig. 2.4, Fig. 2.5 and Fig. 2.6. These results also show that neither of the two algorithm used in hybrid scheme can give good results if they are applied to process complete image. It is found that improvement in PSNR for block-boundary pixels is more as compared to over all PSNR. This result is attractive because discontinuities at block-boundaries, which are the most visually annoying effect, are reduced. Thus, this hybrid scheme reduces blocking artifacts considerably without introducing much blurring in the edge areas. This scheme also provides slight improvement in PSNR.

Chapter 3

Design and applications of 2D IIR multiple-notch filter

3.1 Introduction

The reconstructed image from highly compressed JPEG data has noticeable degradation due to blocking artifacts. Linear, space-invariant filtering is inadequate to remove these artifacts. So, space-variant or adaptive filtering is required. These schemes are based on edge information extracted from the received blocky image, which contain false edges due to blocking artifacts. Based on analysis in frequency domain, it has been found that artifacts in decoded image have periodic structure. These periodic-textures become more obvious after gradient operation since discontinuities due to block coding are highlighted in gradient image. According to signal processing theory, periodic texture will result in some peaks in frequency domain. Here, peaks are due to false edges in gradient image or due to blocking discontinuities in decoded image. A two-dimensional (2D) multiple-notch filter can kill these peaks to reduce the artificial edges due to blocking artifacts in gradient image. In this Chapter[1], a 2D IIR multiple-notch filter is designed from one-dimensional (1D) multiple-tone filter using simple algebraic method. This approach is an extension of method used by Pei *et al.* [6] in the domain of 2D. Since discontinuities

[1] Part of this Chapter represents work published before, see [56]

due to blocking artifacts are more visible in monotone area, this filter can be applied directly in these areas to remove them. Thus, improvement in the performance of space-variant/adaptive filter by removing of false edges from edge of blocky decoded image and reduction of blocking artifacts directly in monotone area, are the new possible applications of multiple-notch filter which are considered in this Chapter. The filtering is performed in DCT domain to reduce the computational complexity.

3.2 Objective

In BDCT based image compression, as discussed in *Chapter 1*, the blocking artifacts are main cause of degradation, especially at higher compression ratio. Low pass filtering is inadequate to remove various types of noise present in different area of blocky image. Low pass filtering reduces grid noise in monotone area but it does not reduce the staircase noise. So, non-linear space-variant or adaptive filter is required to reduce various types of noise. These schemes require classification of image, which is based on available edge information extracted from the received blocky image. This edge information also contains false edges due to blocking artifacts. Hence the performance of space-variant or adaptive filtering scheme degrades.

Several postprocessing algorithms [1,3–5,22,24,27,56] have been proposed to reduce blocking effect of block coding system which are discussed in brief in *Chapter 1*. In non-linear space-variant filtering [1], first the image is divided into monotone area and edge area using edge information obtained from gradient thresholding and then a suitable filter is applied in each of these two areas. In adaptive filtering [3,24,27,56], the coefficients of 2D filter are chosen by edge information of the image. Weighted or unweighted filtering is performed at the pixels in the monotone area or near the edge but the edge pixel remains unaffected.

Based on analysis in frequency domain [8], it has been found that blocking artifacts in decoded image appears periodic in the structure. Artifacts are expected to have periodic texture because block size is fixed in block coding. This kind of texture hides hin the image and it is difficult to detect them. However, this periodic-texture omes more obvious after gradient operation since discontinuities due to block coding ighlighted in gradient image. According to signal processing theory, periodic texture l result in some peaks in frequency domain. Thus, periodic texture can be detected re conveniently in frequency domain. In case of the DCT coded image, the artificial es in the gradient of the decompressed image are due to the blocking artifacts. These ficial edges result in multiple peaks in DCT domain. Thus, a 2D-multiple notch filter equired to kill these peaks to reduce the artificial edges in the gradient image.

In this Chapter, the design of 2D multiple-notch filter is considered and the possibility ısing it for the reduction of blocking artifact, which is the main objective of this work, been discussed. Proposed scheme for blocking artifact reduction is based on the ce-variant/ adaptive filtering but the use of 2D IIR multiple-notch filter is new. This ır is applied for artificial edge removal to improve the classification scheme of space-ant/ adaptive filtering. In addition to this, it can also be applied in removing the cking artifacts in monotone area directly as artificial discontinuities due to blocking facts are more visible in these areas. The design of 2D IIR multiple-notch filter will discussed in section 3.5 whereas its applications will be discussed in section 3.7. In ion 3.4 the review of the design of 1D multiple-notch filter has been presented as the gn of 2D IIR multiple-notch filter is based on this. In the following section 3.3, the ring in DCT domain is briefly discussed.

3 Filtering in DCT domain

problem of 2D filtering in DCT domain is an important problem in the area of cessing and manipulating of images and video streams compressed by DCT-based hod. Convolution multiplication property (CMP) for DCT is given in [57–62]. Like volution multiplication property for discrete Fourier transform (DFT) converts the ring operation to simple element-by-element multiplication, CMP property of DCT also be used to get similar results. First Chen and Fralick [57] gave the CMP for

CT which was used for lowpass filtering by Ngan and Clarke in [58]. Then, Chitprasert d Rao [59] derived a much simpler CMP. They proposed two approaches. In first pproach, a multiplication in spectral domain results in a circular convolution in spatial omain plus a constant DC term. Their second approach is even simpler in which the ultiplication of the DCT of signal sequence with the DFT of filter sequence results circular convolution of the folded signal sequence and the filter sequence. Most of e works on CMP do not implement linear convolution, but rather a convolution with folded input sequence, called symmetric convolution. The convolution-multiplication roperty can be used in filtering the images. To filter 256×256 pixels of test image, a lock size of 8 × 8 may be selected. To perform filtering with a separable 3 × 3 2D lter, first each of the 1D filter is Fourier transformed by 16 point DFT. The resulting equency responses are real and even. Then 2D frequency responses are created by ultiplication of the 1D versions. Finally 8 × 8 DCT of test images are multiplied by e filter matrices.

Symmetric convolution is the convolution mode of discrete trigonometric transforms DTT) [60]. The DCT is one member of DTT family. Symmetric convolution can be ficiently computed by taking inverse DTT of element-by-element product of forward TT's of the inputs. We must use the appropriate type of DTT for each type of mmetric convolution. Symmetric convolution provides the systematic way to convolve mmetric FIR filters with symmetrically extended data. These various possibilities f symmetrically extending the two sequences at both ends result in various types of mmetric convolutions.

3.4 Review of design of 1D IIR Multiple-notch Filter

he design of 1D multiple-notch filter is available in [7], [49]. These techniques are lso discussed in brief in *Chapter 1.* In these approaches 1D multiple-notch filter is esigned from the allpass filter. The specifications of notch filter is first transformed nto that of all-pass filter and effective approach to design this desired all-pass filter is developed. All-pass filter A(z) is designed such that the phase response A(ω) satisfies 2M requirements, then (1+A(z))/2 are the desired notch filter. Here 2M is the order of the filter. The design method proposed by Joshi and Dutta Roy [49] is similar to the method proposed by Pei *at el.* [7]. In [49], 1D multiple-notch filter is realized by the cascade of second order allpass filter. Now, the design approach proposed by Pei in *at el.* [7] will be discussed in detail. The input of notch filter has the following form:

$$x(n) = s(n) + \sum_{k=1}^{M} A_k \sin(n\omega_{Nk} + \phi_k) \tag{3.1}$$

$$= s(n) + d(n) \tag{3.2}$$

where M is number of sinusoidal interferences, s(n) is the desired signal and d(n) is sum of all sinusoidal interferences, ω_{Nk} is frequency for k=1, 2, ..., M. To remove these sinusoidal interferences, the specifications of ideal notch filter is given by

$$H(e^{jw}) = \begin{cases} 0 & for \quad \omega = \omega_{Nk}, \quad k = 1, 2, 3, ..., M \\ 1 & otherwise \end{cases} \tag{3.3}$$

Specification Transformation

The specifications of notch filter are first transformed into that of all-pass filter using the relation $H(z) = (1 + A(z))/2$. As a result, the notch filter design problem reduces to an allpass filter design problem. The transfer function of 2M order allpass filter A(z) is given by

$$A(z_i) = \frac{a_{2Mi} + ... + a_{1i}z_i^{-2M+1} + z_i^{-2M}}{1 + a_{1i}z_i^{-1} + ... + a_{2Mi}z_i^{-2M}} \tag{3.4}$$

As magnitude response of A(z) is equal to unity for all frequency, its frequency response can be written as

$$A(e^{j\omega}) = e^{j\theta_A(\omega)} \tag{3.5}$$

where $\theta_A(\omega)$ is the phase response. Thus the frequency response of notch filter can be written as

$$H(e^{j\omega}) = \frac{1}{2}(1 + e^{j\theta_A(\omega)}) \tag{3.6}$$

he $\theta_A(\omega)$ of a stable allpass filter is 0 when $\omega = 0$, $-2M\pi$ when $\omega = \pi$, and is required) decrease monotonically with increasing frequency. Thus, when ω goes from 0 to π adians, the phase $\theta_A(\omega)$ goes from 0 to $-2M\pi$. Therefore

1. There exits M frequency points $\omega_1 < \omega_2 < ... < \omega_M$ such that $\theta_A(\omega_n) = -(2n-1)\pi$, or $H(e^{j\omega_n}) = 0$ for n=1, 2, ...M.
2. There exits M frequency points $\omega_1^{(1)} < \omega_2^{(1)} < ... < \omega_M^{(1)}$ such that $\theta_A(\omega_n^{(1)}) = -(2n-1)\pi + \frac{\pi}{2}$, or $\mid H(e^{j\omega_n^{(1)}}) \mid = \mid \frac{1}{2}(1-j) \mid = \frac{1}{\sqrt{2}}$ for n=1, 2, ...,M.
3. There exits M frequency points $\omega_1^{(2)} < \omega_2^{(2)} < ... < \omega_M^{(2)}$ such that $\theta_A(\omega_n^{(2)}) = -(2n-1)\pi - \frac{\pi}{2}$, or $\mid H(e^{j\omega_n^{(2)}}) \mid = \mid \frac{1}{2}(1+j) \mid = \frac{1}{\sqrt{2}}$ for n=1, 2, ...,M.
4. There exits M+1 frequency points $0 = \omega_1^{(3)} < \omega_2^{(3)} < ... < \omega_M^{(3)} = \pi$ such that $\theta_A(\omega_n^{(3)}) = -(2n)\pi$, or $H(e^{j\omega_n^{(3)}}) = 1$ for n=1, 2, ...,M.

hen H(z) is forth-order notch filter, i.e. for M=2, following assignments of the phase $_A(\omega)$ are needed

) $\theta_A(\omega_{Nn}) = -(2n-1)\pi$

) $\theta_A(\omega_{Nn} - BW_n/2) = -(2n-1)\pi + \pi/2$

) $\theta_A(\omega_{Nn} + BW_n/2) = -(2n-1)\pi - \pi/2$

here n=1, 2,...M and notch frequency points ω_{Nn} satisfies $\omega_{N1} < \omega_{N2} < ... < \omega_{NM}$. oreover, if BW_n is very small, $\theta_A(\omega_{Nn}) = -(2n-1)\pi$ and $\theta_A(\omega_{Nn} - BW_n/2) =$ -$(2n-1)\pi + \pi/2$, then to a first order approximation it can be shown that

$$\theta_A(\omega_{Nn} + BW_n/2) \approx -(2n-1)\pi - \pi/2 \tag{3.7}$$

hus for small rejection bandwidth BW_n, the above three assignment reduces to the ollowing two assignments

1) $\theta_A(\omega_{Nn}) = -(2n-1)\pi$

2) $\theta_A(\omega_{Nn} - BW_n/2) = -(2n-1)\pi + \pi/2$

ter suitable arrangement, these two assignments are equivalent to the following contion in 2M frequency-sampling points. If the frequency points are

$$\omega_i = \omega_{N[\frac{i+1}{2}]} - \frac{1}{2}(1-(-1)^{mod(i,2)})\frac{BW_{[\frac{i+1}{2}]}}{2} \tag{3.8}$$

en the desired phase response is specified by

$$\theta_A(\omega_i) = -(2[\frac{i+1}{2}]-1)\pi + \frac{1}{2}(1-(-1)^{mod(i,2)})\frac{\pi}{2} \tag{3.9}$$

ıere i=1,2,...2M and $[x]$ denotes the largest integer which is smaller than or equal to and $mod(x,2)$ denotes the remainder when x is divided by 2. Thus the specifications notch filter have been transformed into specifications of allpass filter.

esign Procedure

ıe phase response of of A(z) can be written as

$$\theta_A(\omega) = -2M\omega + 2\arctan(\frac{\sum_{k=1} 2M a_k \sin(k\omega)}{1+\sum_{k=1} 2M a_k \cos(k\omega)}) \tag{3.10}$$

ɔm equation (3.9), the phase response $\theta_A(\omega)$ given at 2M points ω_i, i=1,2,...2M, we tain a set of equations as

$$\frac{\sum_{k=1} 2M a_k \sin(k\omega_i)}{1+\sum_{k=1} 2M a_k \cos(k\omega_i)} = \tan(\beta_i) \quad i = 1,2,...,2M \tag{3.11}$$

ıere $\beta_i = \frac{1}{2}[\theta_A(\omega_i) + 2M\omega_i]$. After some manipulations, this expression can be written

$$\sum_{k=1}^{2M}[\sin(k\omega_i) - \tan(\beta_i)\cos(k\omega_i)]a_k = \tan(\beta_i) \quad i = 1,2,...,2M \tag{3.12}$$

ich is a set of linear equation in the filter coefficients a_k. The set of linear equation matrix form can be given by

$$\mathbf{Qa} = \mathbf{p} \tag{3.13}$$

ere

$$\mathbf{a} = [a_1, a_2, ...a_{2M}]^T$$

$$\mathbf{p} = [tan\beta_1, tan\beta_2, ...tan\beta_{2M}]^T$$

and the elements of matrix **Q** are given by:

$$q_{ik} = sin(k\omega_i) - tan\beta_i cos(k\omega_i) \quad i = 1, 2, ..., 2M \;\; k = 1, 2, ..., 2M \tag{3.14}$$

By solving these linear simultaneous equations, the desired solution is given as

$$\mathbf{a} = \mathbf{Q}^{-1}\mathbf{p} \tag{3.15}$$

Thus the realization of notch filter H(z) is equivalent to realization of allpass filter A(z).

$$H(z) = [1 + A(z))]/2 \tag{3.16}$$

Due to mirror image symmetry relation between the numerator and denominator polynomials of allpass filter, the notch filter can be realized by computationally efficient lattice structure.

3.5 Design of 2D IIR Multiple-notch Filter

In proposed approach, the 2D IIR multiple-notch digital filter is designed from one-dimensional (1D) multiple-tone (narrow bandpass) filter. The 1D multiple-tone filter is designed from allpass filter [7] in the similar way as discussed in *section 3.4*. The design approach of 2D IIR multiple-notch filter is based on the concept used in [6] for the design of 2D IIR single-notch filter. This approach is discussed in *Chapter 1* where the 2D single-notch filter is designed by cascading 2D-parallel line filter with 2D straight-line filter. In proposed approach, a special 2D multiple-notch filter is obtained by cascading 2D multiple vertical-line filter with 2D multiple horizontal-line filter. The block diagram of 2D IIR multiple-notch filter of proposed method is shown in Fig. 3.1. From the block diagram it is clear that the design of two multiple-parallel line filters are required to design a 2D multiple-notch filter. The specifications of 2D multiple-notch filter is given by:

$$H_i(e^{j\omega_1}, e^{j\omega_2}) = \begin{cases} 0, & for \;\; (\omega_1, \omega_2) = (\omega_{1N_k}, \omega_{2N_k}) \\ 1, & otherwise \end{cases} \tag{3.17}$$

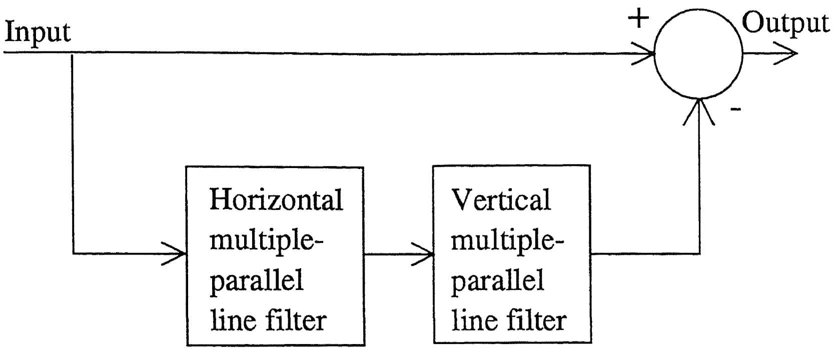
Input
Output
+
-
Horizontal multiple-parallel line filter
Vertical multiple-parallel line filter

Figure 3.1: Block diagram of a 2D IIR multiple-notch filter.

where k=1,2,......M; for M notch frequencies. Now to design such filter, simple algebraic method is used. In this method we start with writing the specifications of corresponding 2D multiple-parallel line filters as:

$$H_i(e^{j\omega_1}, e^{j\omega_2}) = \begin{cases} 1, & for \ \ \omega_i = \pm\omega_{iN_k} \\ 0, & otherwise \end{cases} \tag{3.18}$$

where i=1,2 corresponds to vertically parallel multiple-line filter and horizontally parallel multiple-line filter, respectively. These kind of filters can be designed by choosing $H(z_1, z_2)$ as:

$$H_i(z_1, z_2) = H_{mtf}(z)|_{z=z_i} \qquad for \quad i = 1,2 \tag{3.19}$$

where $H_{mtf}(z)$ is a 1D multiple-tone filter and $i = 1,2$ corresponds to vertically and horizontally parallel multiple-line filter, respectively. Thus multiple parallel line filters can be obtained using 1D multiple-tone filter, which can be designed from allpass filter. As discussed in *section 3.4*, if the allpass filter $A(z)$ is designed such that the phase response A(ω) satisfies 2M requirements, then $(1 - A(z))/2$ are the desired multiple-tone filter. Here $2M$ is the order of the filter. Thus

$$H_{mtf} = [1 - A(z)]/2 \tag{3.20}$$

where A(z) is allpass filter whose transfer function is given by :

$$A(z_i) = \frac{a_{2Mi} + ... + a_{1i}z_i^{-2M+1} + z_i^{-2M}}{1 + a_{1i}z_i^{-1} + ... + a_{2Mi}z_i^{-2M}} \tag{3.21}$$

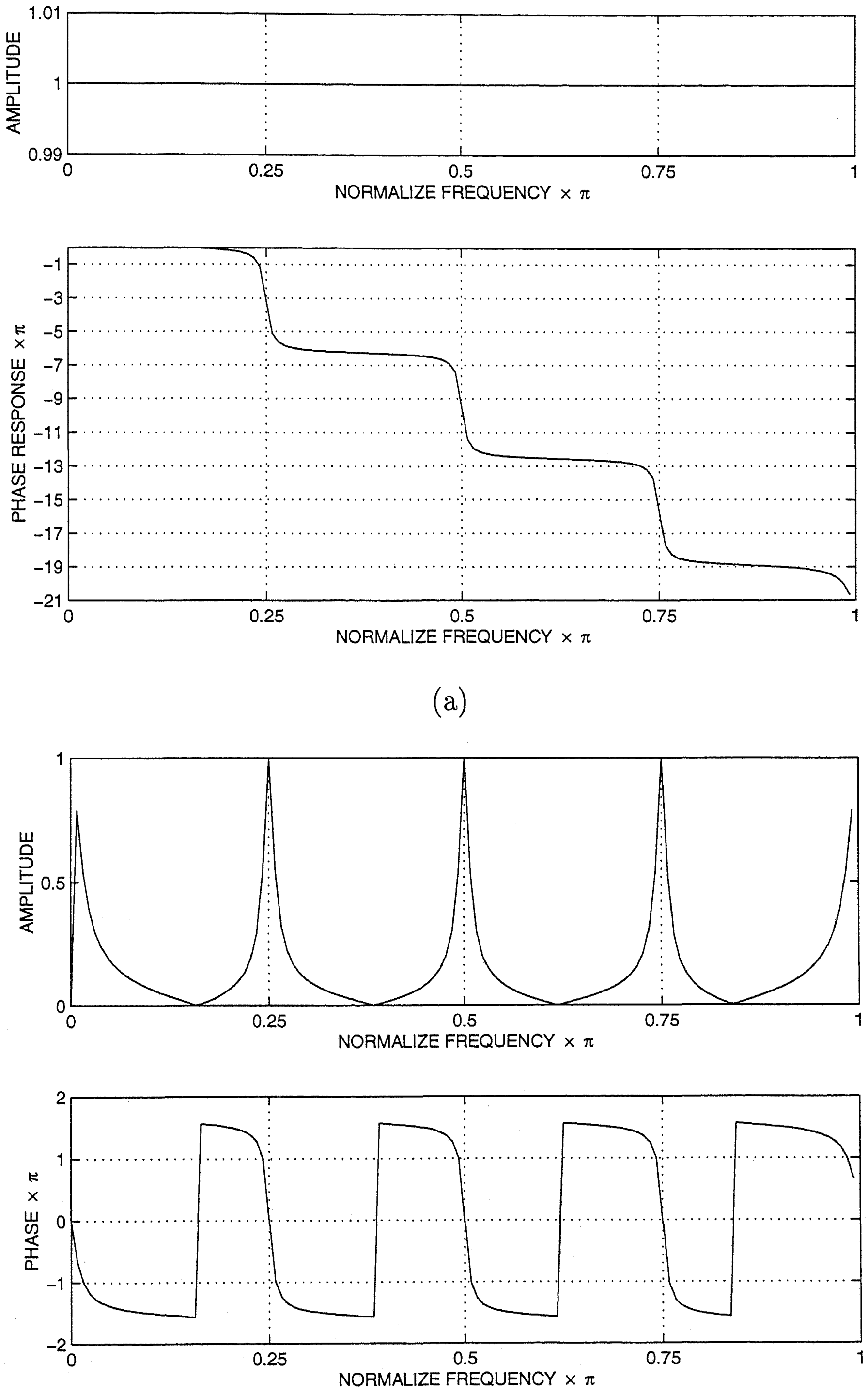

(a)

(b)

Figure 3.2: Frequency response of (a) 1D IIR allpass filter and (b) 1D IIR multiple-tone filter.

Where $i = 1, 2$ and $2M$ is the order of the each allpass filter to get M notch frequencies. The coefficients of allpass filter $A(z)$ can be obtained using method proposed in [7].

Thus realization of proposed notch filter is based on the realization of an allpass ilter. The desired 2D multiple-notch filter can be obtained from these properly designed ertical parallel line filter $H_1(z_1, z_2)$ and multiple horizontal line filter $H_2(z_1, z_2)$. The ransfer function of 2D multiple-notch filter is given by:

$$H_N(z_1, z_2) = 1 - H_1(z_1, z_2)H_2(z_1, z_2) \tag{3.22}$$

The frequency response of the 1D multiple-tone filter and corresponding allpass filter re shown in Fig. 3.2. The block diagram of 2D multiple-notch filter is shown in Fig. 3.1 vhereas its amplitude response is shown in Fig. 3.3 (a).

3.6 Design Example

n this section, a design example has been presented which was performed with MATAB.

p 1: The notch frequencies for a 2D multiple-notch filter are calculated from the block size. The notch frequencies and corresponding bandwidths of this filter are selected for the block size of 8 × 8 as

$\omega_1 = 0$	$BW_1 = 0.02\pi$
$\omega_2 = 0.25\pi$	$BW_2 = 0.01\pi$
$\omega_3 = 0.50\pi$	$BW_3 = 0.01\pi$
$\omega_4 = 0.75\pi$	$BW_4 = 0.01\pi$
$\omega_5 = \pi$	$BW_5 = 0.02\pi$

In this case, these frequencies and bandwidths are used in the design of two identical 1D multiple-tone filter.

p 2: Using method proposed in [7], we obtain the filter coefficients of eighth-order allpass filter as:

$a_1 = 1.9201$	$a_2 = 1.8806$
$a_3 = 1.8869$	$a_4 = 1.8622$
$a_5 = 1.8300$	$a_6 = 1.8437$
$a_7 = 1.7969$	$a_8 = 1.8622$
$a_9 = 1.7969$	$a_{10} = 1.8622$

ep 3: 1D multiple-tone filter coefficients are obtained from equation (3.20). The frequency response of this filter along with the corresponding allpass filter is shown in Fig. 3.2.

ep 4: Using proposed method, we obtain the transfer function of 2D multiple-notch filter from $H_{mtf}(z)$. The amplitude response of this filter is shown in Fig. 3.3 (a).

ep 5 : DCT coefficient of block size $M \times M$ is multiplied by filter matrix of equal size.

3.7 Applications of 2D multiple-notch filter

This filter can be used for the removal of single or multiple sinusoidal interferences. As discussed earlier, the discontinuities at block boundaries of decoded image are due to blocking artifacts, which have the periodic structure and results in some peaks in DCT domain. A 2D multiple-notch filter can be used to kill these peaks to reduce the blocking artifacts from DCT coded images in the following two ways.

3.7.1 Improvement in the performance of space-variant/ adaptive filter by removal of false edges from edge-map of blocky image

It is obvious from the property of DCT and it can also be observed that the DCT of square grid of line spacing of eight in both horizontal and vertical direction has peaks at a interval of 64 in both directions. This grid can be removed by killing these peaks by suitable notch filter. Here, this fact is verified as shown in Fig. 3.3 (b) and Fig. 3.3 (c). The notch frequencies for this multiple-notch filter are calculated from block size. It has

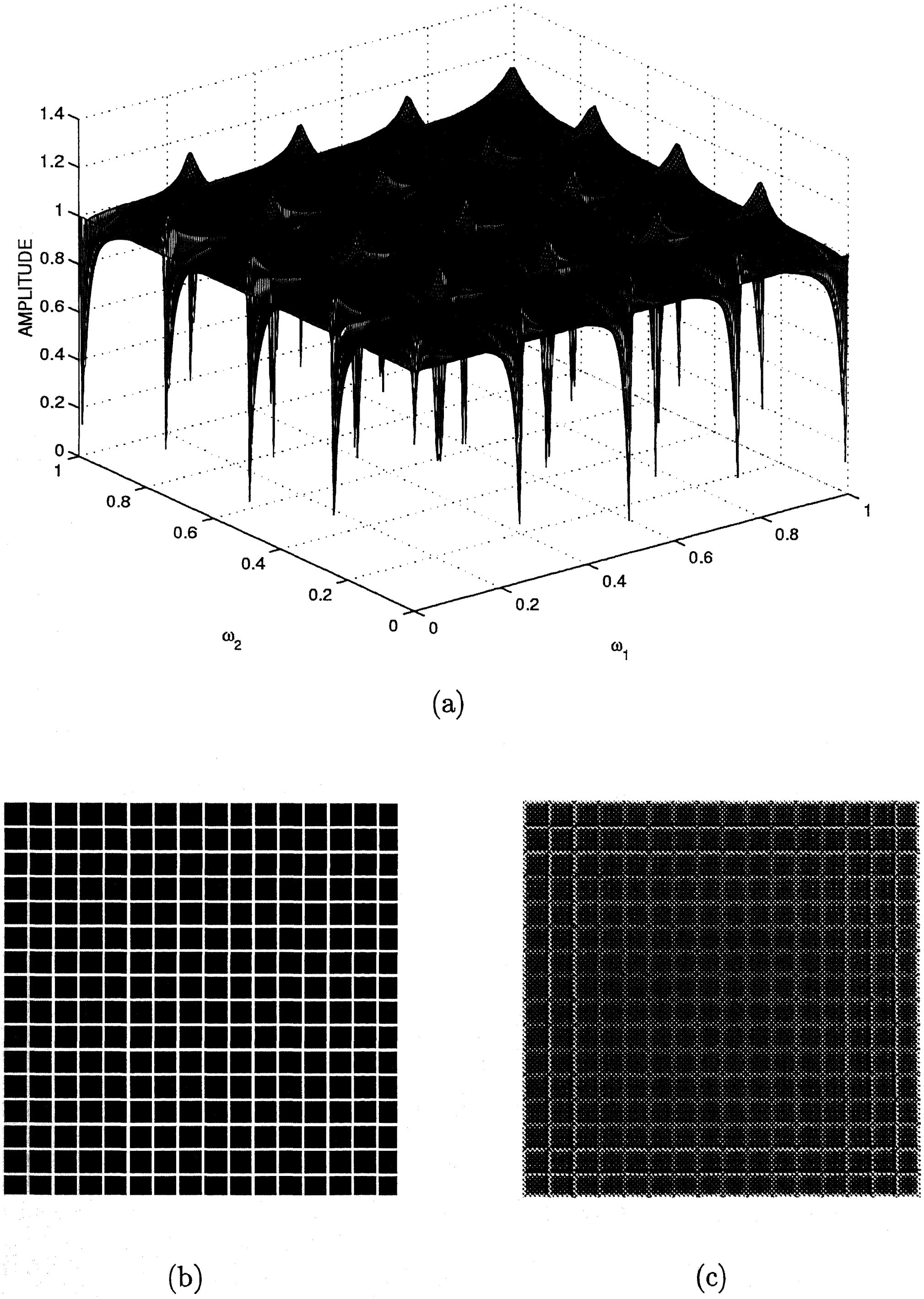

(a)

(b)

(c)

igure 3.3: False edge filtering by 2D IIR multiple-notch filter. (a) Amplitude response f 2D IIR multiple-notch filter, (b) Square grid, (c) Filtered grid with threshold at half f the maximum value.

also been observed that as the grid of lines due to blocking artifact in the edge-image is not complete, these peaks remain at the same position but their spread increases. So, at high compression ratio, when grid in the edge-map of DCT coded image is visible, this grid or false edges can be removed using proposed 2D multiple-notch filter. This fact is tested for DCT coded 256 × 256 Lenna image and found to be correct as shown in Fig. 3.4 and Fig. 3.5.

3.7.2 Reduction of blocking artifacts using 2D multiple-notch filter

At high compression ratio, the discontinuities due to blocking artifacts are more pronounced in monotone area so this filter can be applied directly in these areas. In proposed space-variant/adaptive filtering approach, 2D multiple-notch filter and signal adaptive filter is applied in the monotone area and edge area, respectively. In space-variant/adaptive filtering, the image is first divided into monotone area and edge area then in monotone area lowpass filter is applied whereas in edge area directional or signal adaptive filter is applied. A 2D multiple-notch filter can be applied in monotone area because the periodic texture due to blocking artifacts are more visible in monotone areas as compared to edge areas. Moreover, the actual edges are blurred if the same filter is applied in edge areas. Therefore, in this algorithm a signal adaptive filter discussed in *Chapter 2* is used in edge area.

Another advantage of this scheme is low computational complexity as filtering is performed in DCT domain. The results are shown in Fig. 3.6. These results show that blocking artifacts can be reduced by this method. However, the improvement is limited to high compression ratios because these periodic textures due to blocking artifacts hides in DCT domain at low compression ratios.

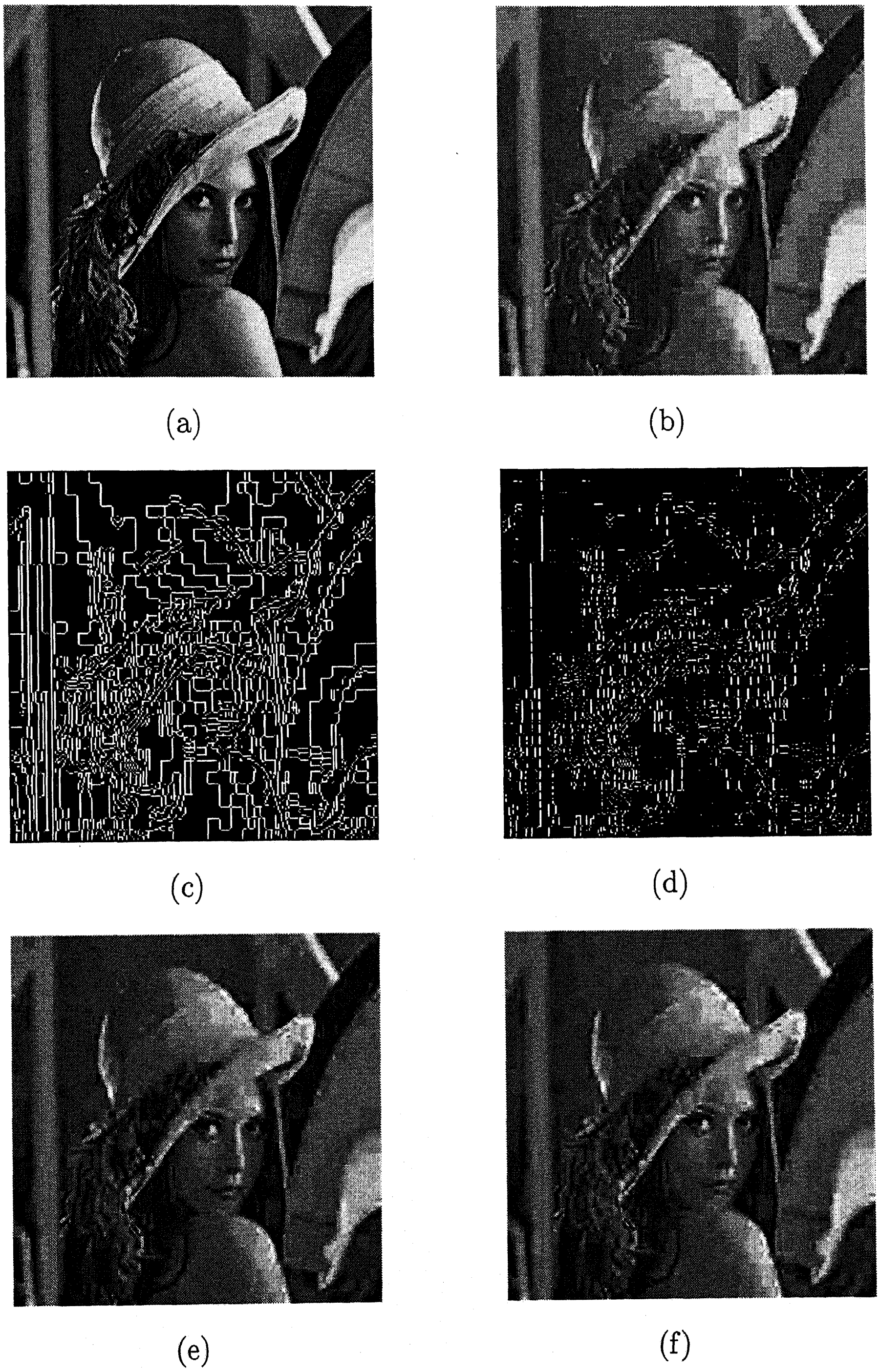

(a) (b)

(c) (d)

(e) (f)

Figure 3.4: Postprocessing of decompressed Lenna image at quality factor= 5. (a) Original. (b) Before postprocessing. (c) Edge-map. (d) Edge-map in (c) is filtered by 2D IIR multiple-notch filter. (e) Postprocessed by space-variant algorithm with filtered edge-map. (f) Postprocessed by space-variant algorithm without filtered edge-map.

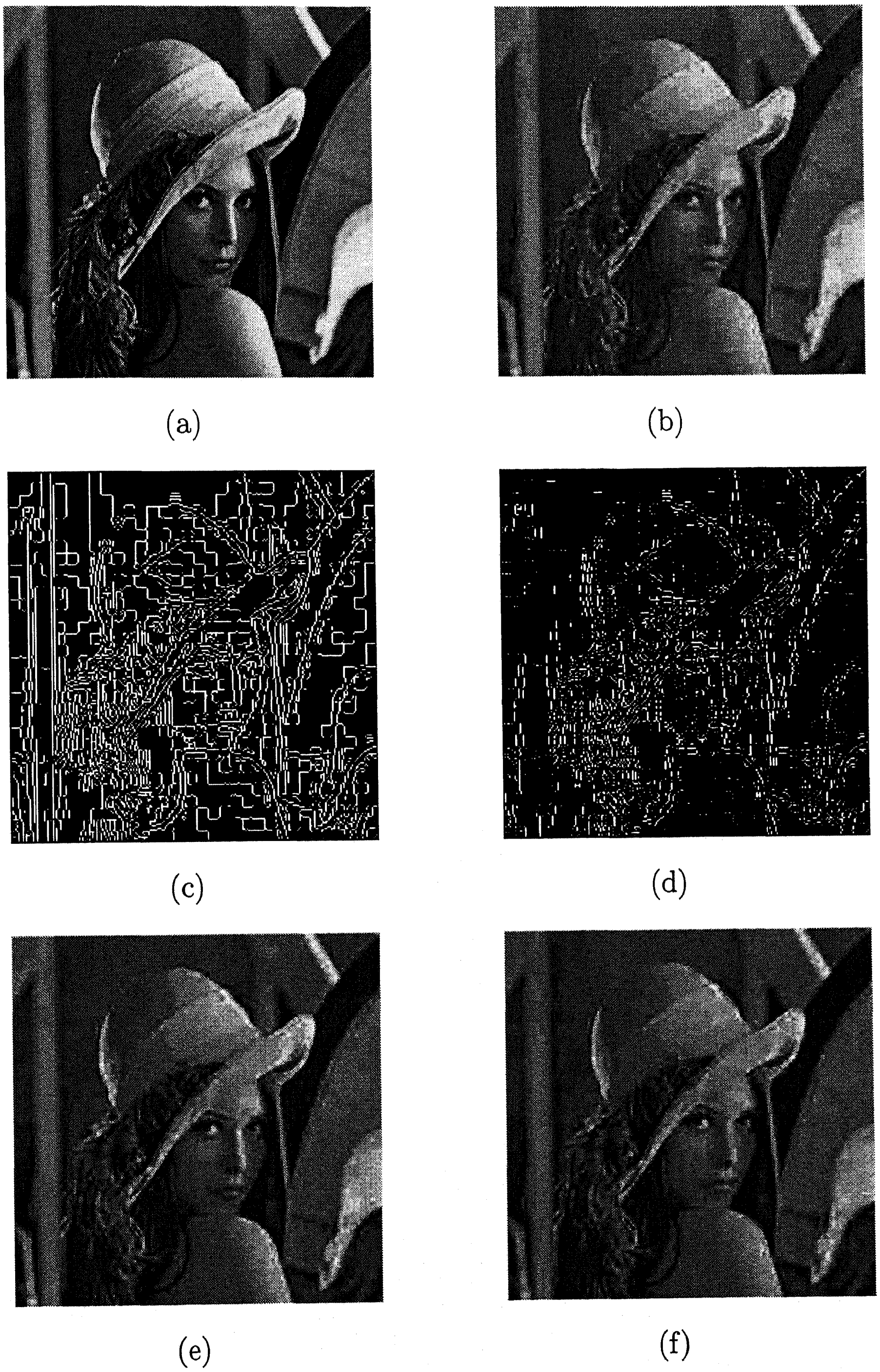

(a)

(b)

(c)

(d)

(e)

(f)

Figure 3.5: Postprocessing of decompressed Lenna image at quality factor=7. (a) Original. (b) Before postprocessing. (c) Edge-map. (d) Edge-map in (c) is filtered by 2D IIR multiple-notch filter. (e) Postprocessed by space-variant algorithm with filtered edge-map. (f) Postprocessed by space-variant algorithm without filtered edge-map.

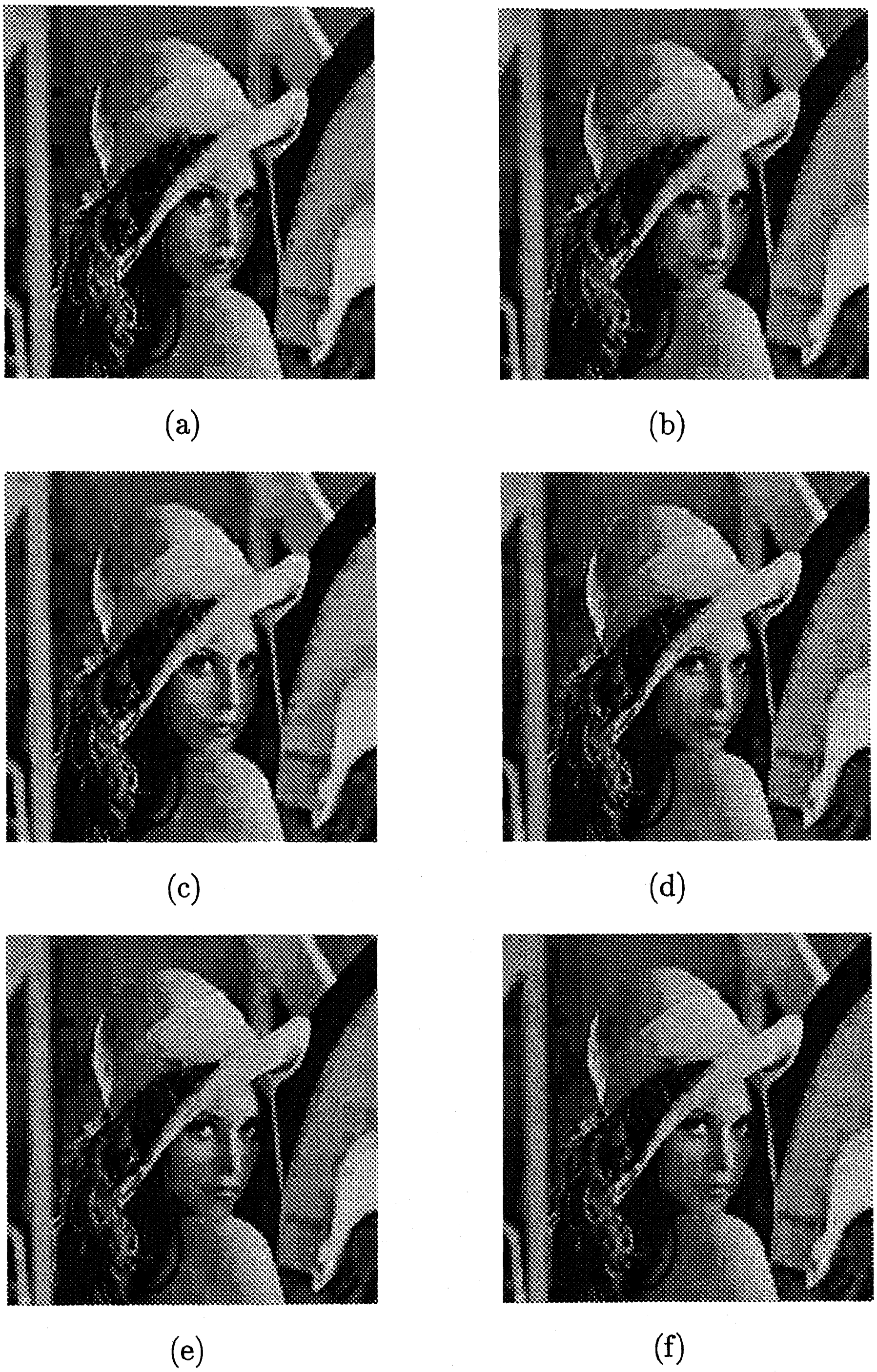

(a)

(b)

(c)

(d)

(e)

(f)

Figure 3.6: Postprocessing of Lenna image compressed at quality factor 5 in (a), (b), (c) and compressed at quality factor 7 in (d), (e), (f) by various algorithms; where (a) and (d) Before postprocessing, (b) and (e) Processed by 2D IIR multiple-notch filter with Signal Adaptive filter (SAF), and (c) and (f) Processed by Gaussian LPF with SAF

Table 3.1: Comparison of the performances of various space-variant algorithms on Lenna image.

Algorithms	*PSNR in dB at quality factor q*			*Boundary PSNR in dB at quality factor q*			*Boundary Discontinuity in* (10^6) *at quality factor q*		
	q=5	q=7	q=10	q=5	q=7	q=10	q=5	q=7	q=10
Original	-	-	-	-	-	-	4.28	4.28	4.28
DCT coded	25.32	26.75	28.09	15.02	16.51	17.96	10.9	9.22	7.93
2D IIR multiple notch filter with SAF	26.00	27.41	28.78	16.37	17.75	19.19	5.66	4.96	4.31
Gaussian LPF with SAF	26.11	27.49	28.90	16.60	17.92	19.41	4.97	4.61	3.92

3.8 Results

In this *section*, the results of various algorithms applied on reconstructed blocky 256×256 Lenna image have been presented. These algorithms are implemented with MATLAB. The results of two algorithms are compared with baseline JPEG like DCT decoded image. Peak SNR (PSNR) is defined in *Chapter 2*. As discussed in *Chapter 2*, the PSNR is only the rough indicator of image quality and does not reflects the blocking artifacts, two new discontinuity measures are defined. The block boundary PSNR (BPSNR) is defined in the same way as PSNR but only one pixel from both side of block boundary are considered for the calculation of mean square error (MSE) whereas the block boundary discontinuity measure is defined as the sum of square of difference of pixel values across the four block boundaries. Using these measures the performance of various proposed algorithms are compared.

It can be seen from Fig 3.3 that 2D multiple-notch filter can eliminate the square grid. This filter can also remove the false edges from the edge-map of blocky lenna image as shown in Fig. 3.4 and Fig. 3.5. These figures also show the result of postprocessing of DCT coded image by the space-variant filtering algorithm which uses the 2D multiple-notch filter for false edge removal in its classification scheme. In the second application of 2D multiple-notch filter as discussed in *subsection 3.7.2*, the reduction of discontinuity signifies that blocking artifacts are reduced which can also be observed visually in Fig. 3.6. It can also be seen from Table 3.1 that the improvement in PSNR for block boundary pixels is more as compared to over all PSNR.

3.9 Conclusion

In this Chapter, a simple algebraic method is used to design 2D IIR multiple-notch filter. In this approach, at first two 1D multiple-tone filters are designed as per the specifications of 2D multiple-notch filter and then these two 1D multiple-tone filters are used to obtain 2D multiple-vertical line and 2D multiple-horizontal line filter. Finally, cascade of these two filters, as shown in Fig. 3.1, gives the desired 2D multiple-notch filter. The design of 1D multiple-tone filter is based on the design of allpass filter. In this Chapter a design example and two new applications of 2D multiple-notch filter are discussed. It is found that the reduction of blocking artifacts and removal of false edges from edge-map of blocky DCT coded image are the new possible application of 2D multiple-notch filter. Furthermore, the space-variant filtering method can be improved with a more efficient multiple-notch filter.

Chapter 4

Linear-phase 2D FIR Multiple-notch Filter for Reducing Blocking Artifact from DCT Coded Images

4.1 Introduction

The design and applications of 2D IIR multiple-notch filter is discussed in *Chapter 3*, where it was found that this filter could be used for reducing the blocking artifacts from DCT coded images. In this Chapter the design of FIR multiple-notch filter and its application in reducing the blocking artifacts from DCT coded images will be discussed. As the filter is used for reducing blocking artifacts from DCT coded images, it is meaningful to design multiple-notch filter with linear-phase, which provides less distortion as compared to the filters with non-linear phase. The Blocking artifacts are the major problem with DCT coded image, which is discussed in *Chapter 1*. Space-variant or adaptive filtering is required to reduce these artifacts. These schemes are based on edge information extracted from blocky image, which contain false edges due to blocking artifacts. Based on analysis in frequency domain, it has been found that artifacts in decoded image have periodic structure that corresponds to discontinuities due to block coding. These discontinuities are highlighted in gradient image. According to signal processing theory, periodic texture will result in some peaks in frequency domain, which are either due to false edges in gradient-image or due to boundary discontinuities in decoded image. A two-dimensional (2D) multiple-notch filter can kill these peaks to reduce these artifacts. In this Chapter[1], 2D linear-phase FIR multiple-notch filter is designed. Discontinuities due to blocking artifacts are more in monotone area so this filter can be applied directly in these areas. As discussed in *Chapter 3*, improvement in the performance of space-variant/adaptive filter by removal of false edges from edge-map of blocky image and the reduction of blocking artifacts directly in monotone area, are also the new possible applications of 2D FIR multiple-notch filter. Computational complexity is less because the filtering is performed in DCT domain.

4.2 Objective

The objective of work presented in this Chapter is once again the reduction of coding artifacts. Thus, let us begin with recalling the causes of coding artifacts and their reduction methods. The blocking artifacts are the major degradation in block-based image coding techniques, especially at higher compression ratio. One main reason of blocking artifacts is that blocks are encoded and quantized independently without considering the correlation between adjacent blocks. High compression ratios are achieved by quantization process in which the information about less important BDCT coefficient is discarded.

As discussed in [1], space-invariant lowpass filter is not suitable because it will blur the edge and degrade the image visual quality. It is also found that the human visual system (HVS) is more sensitive to blocking artifacts in monotone regions than edge regions. Therefore, a strong smoothing filter is required in monotone area. In edge regions the smoothing operation tends to introduce undesirable blur, so smoothing of a few pixels around block boundaries by directional lowpass filter is sufficient. The information about local image characteristics can be extracted from image by edge detection. Thus, one of

[1] Part of this Chapter represents work communicated for publication, see [63]

the best approach of reducing blocking artifact is to classify the image blocks into various categories and each is processed by one or two-dimensional filter. Hence, space-variant or adaptive filtering depending on local image characteristics is preferable. A number of postprocessing algorithms have been proposed in [1–4, 22–29, 56] to reduce blocking effect of block coding system as discussed in *Chapter 1*. In non-linear space-variant filtering [1], the image is classified into monotone area and edge area and then a suitable filter is applied in each of the classified area to reduce over all noise introduced in the image. In adaptive filtering [3, 24, 27, 56], the coefficients of 2D filter are chosen by edge information of the image.

As discussed earlier, that both non-linear space-variant filtering and adaptive filtering require classification of image, which is based on available edge information extracted from the received blocky image. This edge information also contains false edges due to blocking artifacts. Hence the performance of space-variant or adaptive filtering scheme may degrade due to misclassification. Hung at el. [8] proposed a scheme for removing false edges from Fourier transformed image using notch filter, as discussed in *Chapter 3*. In this scheme, based on analysis in frequency domain, it was found that blocking artifacts in decoded image appears periodic in the structure. These artifacts are expected to have periodic texture because block size is fixed in block coding but this kind of texture hides in the image and is difficult to detect them. However, these periodic-textures become more obvious after gradient operation as discontinuities due to block coding is highlighted in gradient image. According to signal processing theory, periodic texture will result in some peaks in frequency domain, which are repeated after regular spacing and corresponds to false edges due to blocking artifacts.

This Chapter also deals with the design and applications of 2D multiple-notch filter but here the filter has finite impulse response (FIR). As discussed in *Chapter 3*, a notch filter highly attenuates a particular frequency and leaves the other relatively unchanged. So, a 2D multiple-notch filter can kill these peaks to reduce the artificial edges due to blocking artifacts in the gradient image. As there are multiple peaks in the frequency transformed (DCT coded) image, 2D multiple-notch filter is required to remove it.

Since this filter is used for reducing blocking artifacts from DCT coded images, it is meaningful to design multiple-notch filter with linear-phase which provides less distortion as compared to the filters with non-linear phase. A linear-phase is particularly important in image processing application as demonstrated in [64]. In this Chapter, we start with a review of design of 1D FIR notch filter in section 4.3. Section 4.4 explains the design of 2D multiple-notch filter. In section 4.5, design example is discussed. In section 4.6, two new applications of proposed filter are highlighted where as in section 4.7, the results have been presented to compare the proposed algorithm with the space-variant/ adaptive filtering algorithm. Finally, conclusions are given in section 4.8.

4.3 Review of the Design of 1D FIR Notch Filter

Digital notch filters are the effective means for eliminating narrow-band or sinusoidal interferences in signal processing applications such as power line interference and cancellation in electrocardiograms (ECG). A notch filter highly attenuates a particular frequency component in the input signal while leaving nearby frequency components relatively unchanged. Design of FIR digital notch filter is discussed in [9, 50]. **Yu** *et al.* [9] investigated some approaches for designing 1D linear-phase FIR notch filters, which are based on the modification of several established design techniques [65] of linear-phase FIR band selective filters. In this section, various existing techniques for designing linear-phase band selective filter with finite impulse response (FIR) filter are discussed. The commonly used methods for designing linear-phase FIR notch filter are

(1) Windowed Fourier Series,

(2) Frequency sampling approach,

(3) Optimal FIR filter design approach.

The aim of filter design is to make a reasonable choice of the coefficients of the transfer function such that the response of resulting filter is a satisfactory approximation of the desired response. The notch filter is a very narrow band-stop filter. Ideally, bandwidth of notch filter should be zero with passband magnitude equal to unity and attenuation

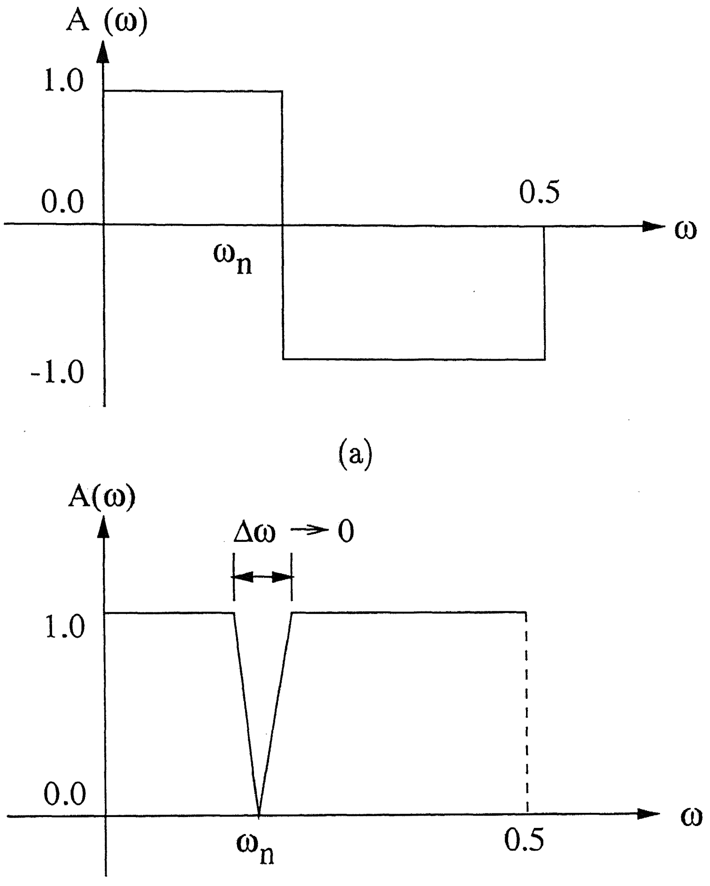

(a)

(b)

Figure 4.1: Amplitude response of ideal linear-phase notch filter (a) Type 1 (b) Type 2

.

at notch frequency should be infinite but in practice it has non-zero transition band and passband ripples. To provide the linear-phase, the notch filter must be a FIR filter with symmetric impulse response. Due to linear-phase requirement of FIR filter and the amplitude response requirements of notch filter, the length of a digital notch filter must be odd i.e. $N = 2M + 1$. The frequency response of a linear-phase FIR filter is given by

$$H(\omega) = A(\omega)e^{j\theta(\omega)} \tag{4.1}$$

where $A(\omega)$ is a real even function called the amplitude function to distinguish it from the magnitude function $|H(\omega)|$ and $\theta(\omega)$ is the phase function which is a linear function of $\omega(\theta = \omega M)$. The linear-phase notch filter is completely characterized by $A(\omega)$ and its impulse response is a non causal sequence a(n) which is symmetric about origin. The causal sequence $h(n)$ is given by

$$h(n) = a(n - M) \tag{4.2}$$

Linear-phase notch filter can be divided into two types: Ideal Type 1 filter has a 180^o phase shift at the notch frequency ω_n as shown in Fig. 1 (a) whereas Type 2 linear-phase notch filter has exact linear-phase and there is no difference between magnitude function $|H(\omega)|$ and amplitude function $A(\omega)$ as shown in Fig. 1 (b). Magnitude function $|H(\omega)|$ of both type of filter are same.

The ideal Type 1 linear-phase notch filter is the amplitude-shifted version of an ideal lowpass filer. If $A_n(\omega)$ is the amplitude response of ideal linear-phase notch filter, then amplitude function of corresponding low pass filter $A_l(\omega)$ are related with it as

$$A_n(\omega) = \pm[2A_l(\omega) - 1] \tag{4.3}$$

The non causal response of two filters are related as

$$a_n(n) = \pm[2a_l(n) - \delta(n)] \tag{4.4}$$

This relationship is based on the concept of complementary filter. The complementary filter transfer function $G(z)$ is defined as

$$H(z) = z^{-(N-1)/2} - G(z) \tag{4.5}$$

where $N-1$ is order of $H(z)$ which is assumed to be even. If $H(z)$ is a Type 2 linear-phase notch filter with notch frequency at ω_n, $G(z)$ is an extremely narrow-band bandpass filter called a tone filter. Thus design of a notch filter can be executed as the design of a tone filter and then converted to notch filter using above equation.

4.3.1 Windowed Fourier Series design approach

The frequency response of a linear-phase FIR filter, $H(\omega)$, is a periodic function of ω with a period 2π. Thus, the impulse response of this filter is given by the Fourier series coefficients of $H(\omega)$ of infinite length which leads to unrealizable filter. In this design method, the approximate version of $H(\omega)$ is obtained by truncating the infinite impulse response to finite impulse response by windowing. The window functions are used to improve the convergence of the Fourier series in the vicinity of discontinuities where the well-known Gibbs' phenomenon is present.

Type 1 linear-phase notch filter

Thus, if $a_i(n)$ are the Fourier series coefficients of the given ideal amplitude function $A_i(\omega)$, then the coefficient are weighted by a selected windowing function $w(n)$.

$$a(n) = a_i(n).w(n) \tag{4.6}$$

The amplitude function is given by

$$A(\omega) = (1/2\pi)\int_{-\pi}^{\pi} A_i(\theta)W(\omega-\theta)d\theta \tag{4.7}$$

A desirable property of window function is that the function is of finite duration in the time domain and should also have most of the energy concentrated at low frequencies in its Fourier transform. Kaiser window function is very good approximation to this condition. Kaiser window is optimal window in the sense that it has the minimum spectral energy beyond some specified frequency. Thus, in windowed Fourier series approach, most frequently used window is Kaiser window and which can also be used for designing the FIR notch filter. Transition bandwidth and passband ripple determines the required length of the filter. Required passband ripples are obtained by the selection of window parameters. The filter attenuation is obtained by the choice of the parameter α of the Kaiser window as

$$\alpha = \begin{cases} 0.1102(A-8.7), & 50 \leq A \\ 0.5842(A-21)^{0.4} + 0.07886(A-21), & 21 < A < 50 \\ 0, & A \leq 21 \end{cases} \tag{4.8}$$

where A is the required ripple δ of the lowpass filter in decibels

$$A = -20\ log_{10}(\delta) \tag{4.9}$$

Kaiser also developed the relation between attenuation A and lowpass filter of length N

$$N \approx (A - 7.95).2\pi/14.36\Delta\omega \tag{4.10}$$

This formula is modified in [9] for linear-phase notch filter as

$$N \approx (A - 1.93).2\pi/14.36\Delta\omega \tag{4.11}$$

Type 2 linear-phase notch filter

Type 2 linear-phase notch filter can be considered as an complement of an FIR tone filter. Ideal tone filter has very narrow rectangular frequency response $B_i(\omega)$ centered at $\pm\omega_n$ and having bandwidth $\Delta_i\omega$ tending to be zero. The convolution integral can be written as

$$B(\omega) = \frac{1}{2\pi}\int_{-\omega_n-(\Delta_i\omega/2)}^{-\omega_n+(\Delta_i\omega/2)} B_i(\theta)W(\omega-\theta)d\theta + \frac{1}{2\pi}\int_{\omega_n-(\Delta_i\omega/2)}^{\omega_n+(\Delta_i\omega/2)} B_i(\theta)W(\omega-\theta)d\theta \tag{4.12}$$

For small $\Delta_i\omega$, frequency response of tone filter can be written as

$$B(\omega) \approx (\Delta_i\omega/2\pi)[B_i(\omega_n)W(\omega-\omega_n) + B_i(-\omega_n)W(\omega+\omega_n)] \tag{4.13}$$

The normalization of tone filter response can be done using $B_i(\omega_n) = B_i(-\omega_n)$ and the value $B(\omega_n)$.

$$B(\omega)/B(\omega_n) = [W(\omega-\omega_n) + W(\omega+\omega_n)]/[W(0) + W(2\omega_n)] \tag{4.14}$$

From this equation it can be seen that the tone filter response is equal to the shifted window spectra. The response of notch filter $A(\omega)$ can be given by

$$A(\omega) = 1 - [W(\omega-\omega_n) + W(\omega+\omega_n)]/[W(0) + W(2\omega_n)] \tag{4.15}$$

The impulse response of the notch filter is then

$$a_n(n) = \delta(n) - 2bw(n)cos(\omega_n n) \tag{4.16}$$

where $b = 1/[W(0) + W(2\omega_n)]$. Thus, filter response is shifted window spectrum. The design of Type 2 linear-phase notch filter is reduced to the determination of the window with main lobe width equal to $\Delta\omega$ and the window ripple equal to δ. The formula is developed by Yu *et al.* in [9], for the design of Type 2 linear-phase notch filters using Kaiser window. The approximate formula giving relationship between α and the attenuation A is given by

$$\alpha = \begin{cases} 0.1284(A + 0.4551), & 50.1943 < A \\ 0.1517(A - 4.7071), & 20.5278 < A \leq 50.1943 \\ 0.7798(A - 12.9164)^{0.4} & \\ \quad +0.0842(A - 12.9164), & 12.9164 < A \leq 20.5278 \\ 0, & A \leq 12.9164 \end{cases} \tag{4.17}$$

A practical formula for the required width derived by them is given by

$$N \approx (A + 6.35)/11.87\Delta\omega \tag{4.18}$$

4.3.2 Frequency sampling design approach

This is the most straightforward method of designing linear-phase FIR filter. The main idea of frequency sampling design approach is that a desired frequency response can be approximated by sampling it at N evenly spaced points and obtaining the interpolated frequency response that passes through the frequency samples. An FIR filter can be uniquely specified by giving either the impulse response $h(n)$ or, equivalently, the Discrete Fourier Transform (DFT) coefficients $H(k)$. DFT samples $H(k)$ for an FIR sequence can be regarded as the samples of the filter's z-transform, evaluated at N points equally spaced around the unit circle. Thus, amplitude response $A(\omega)$, specified at N equidistant points or frequency samples, gives the coefficients for the recursive FIR filter realization. It becomes computationally efficient method if coefficients A_k are zeros or ones. Therefore a typical lowpass filter consists of choosing $A_k = 1$ in the passband and $A_k = 0$ in the stopband and optimization of samples $0 < A_k < 1$ in the transition band. The optimization based on adjustment of all samples results in optimum filter.

4.3.3 Optimal FIR filter design approach

This method is one of the most powerful 1D FIR digital filter design techniques proposed by Park and McClellan, which is based on Remez exchange algorithm. These designs are based on the optimization of a weighted Chebyshev error norm. McClellan *et al.* in 1973 [66] have developed useful program based on direct application of Chebyshev approximation theory to the linear-phase FIR filter design problem, and using Remez exchange algorithm. Main function of this program is to find equiripple behavior over the set of frequency bands, such as stopbands and passbands for band selective linear-phase FIR filters. Using this approach, an optimal linear-phase notch filter can be designed in two parts: first the realization of the infinite attenuation at the notch frequency with prefilter and second, the design of the corresponding equalizer which is cascaded with the prefilter to achieve the passbands equiripples characteristics.

4.4 Design of 2D FIR Multiple-notch Filter

The design of notch filter is discussed in [6,7,9,48–50,56]. In [9], various methods of the design of 1D FIR notch are discussed. They have also discussed the design of 2D notch filter from 1D notch filter. From the literature, it is difficult to find straightforward way to design two-dimensional filter. Several method of designing 2D FIR filter from 1D FIR filter exists with less computing time but the resulting filter is not optimum, although they can be very good. First step is to approximate the frequency response of 2D filter as separable into two 1D filters and then 1D filter are designed using a suitable design technique. If the 1D filters are optimum then 2D filter will also be optimal. Rabiner *et al.* in [67] proposed an approach for converting 1D linear-phase FIR filter design into 2D linear-phase filter designs. Design of FIR or nonrecursive filter involves determining a finite set of impulse response coefficients such that filter characteristics satisfy the prescribed specifications. This is a problem of polynomial approximation.

However, in this Chapter, a simple algebraic method is used to design a special 2D multiple-notch filter. In proposed method, which is based on [6], the 2D multiple-notch

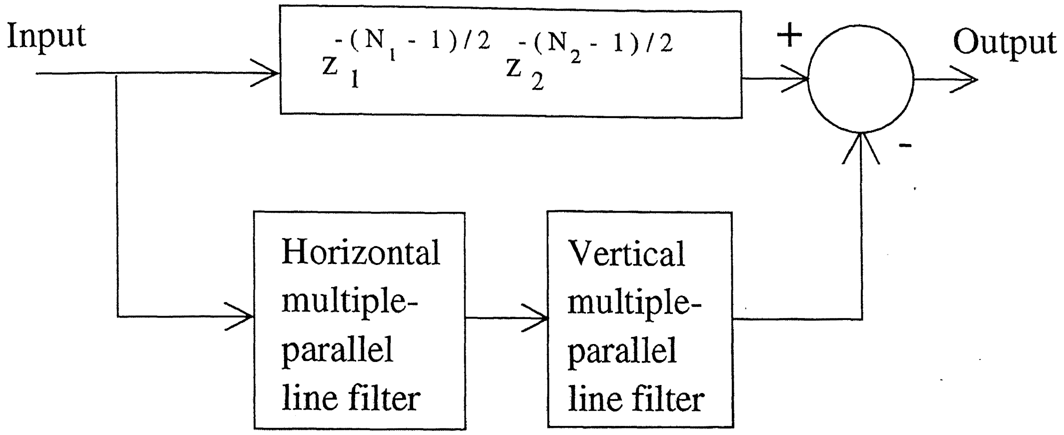
Input
$z_1^{-(N_1-1)/2} z_2^{-(N_2-1)/2}$
+
-
Output
Horizontal multiple-parallel line filter
Vertical multiple-parallel line filter

Figure 4.2: Block diagram of a 2D FIR multiple-notch filter.

filter is designed in following steps

1. Two 1D FIR multiple-tone (narrow band pass) filters are designed using well-known windowed Fourier series design approach.

2. 2D multiple-parallel line filters are obtained from these 1D FIR multiple-tone filters with their narrow pass-bands at appropriate frequencies based on the specifications of desired 2D multiple-notch filter.

3. Cascading these two 2D multiple-parallel line filter gives a 2D FIR multiple-tone filter.

4. The complementary filter of 2D linear-phase FIR multiple-tone filter is 2D linear-phase FIR multiple-notch filter.

5. Finally, the notch at DC (zero frequency) of 2D multiple-notch filter is replaced by nearly all-pass filter to preserve the DC component of the image block, which contains the important information about the image.

To design 2D multiple-notch filter, we start with the specifications of the desired 2D

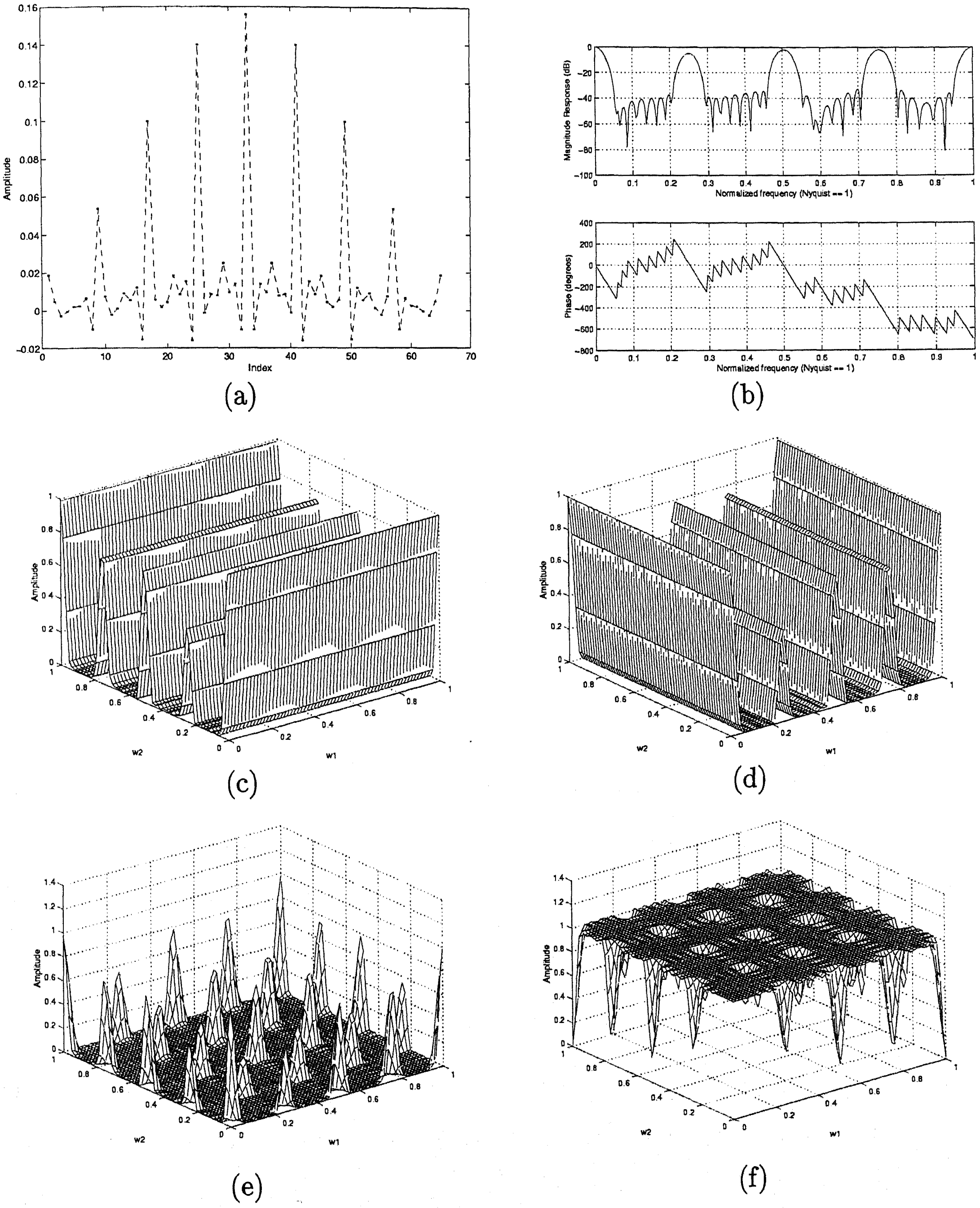

Figure 4.3: (a) Impulse response of 1D FIR multiple-notch filter (b) Frequency response of 1D multiple-notch filter. (c) Amplitude response of horizontal multiple-parallel line filter. (d) Amplitude response of vertical multiple-parallel line filter. (e) Amplitude response of 2D FIR multiple-tone filter. (f) Amplitude response of 2D FIR multiple-notch filter.

multiple-notch filter, which are given by:

$$H_i(e^{j\omega_1}, e^{j\omega_2}) = \begin{cases} 0, & for \ \ (\omega_1, \omega_2) = (\omega_{1N_k}, \omega_{2N_k}) \\ 1, & otherwise \end{cases} \tag{4.19}$$

where k=1,2,......M; for M notch frequencies. For the design of such filter, a simple algebraic method is used. The specifications of corresponding 2D multiple-parallel line filters are:

$$H_i(e^{j\omega_1}, e^{j\omega_2}) = \begin{cases} 1, & for \ \ \omega_i = \pm\omega_{iN_k} \\ 0, & otherwise \end{cases} \tag{4.20}$$

where $i = 1, 2$ corresponds to vertically-parallel multiple-line filter and horizontally-parallel multiple-line filter, respectively. This kind of filters can be designed by taking:

$$H_i(z_1, z_2) = H_{mtf}(z)|_{z=z_i} \qquad for \quad i = 1,\ 2 \tag{4.21}$$

where $H_{mtf}(z)$ is 1D multiple-tone filter and $i = 1, 2$ corresponds to vertically and horizontally-parallel multiple-line filter, respectively. The well-known windowed Fourier series design approach is used to design 1D multiple-tone filter. This approach is discussed in *section 4.3*. The most frequently used window function for FIR filter design is the Kaiser window, which is also used here to design linear-phase multiple-tone filter. The 2D multiple-tone filter can be obtained by cascading of these properly designed vertically-parallel multiple-line filter $H_1(z_1, z_2)$ and horizontally-parallel multiple-line filter $H_2(z_1, z_2)$. The transfer function of 2D multiple-tone filter is given by:

$$H_t(z_1, z_2) = H_1(z_1, z_2)H_2(z_1, z_2) \tag{4.22}$$

As in the case of 1D linear-phase filters, a frequency-shifted window is a linear-phase FIR tone filter and its complimentary filter is a linear-phase notch filter. $A(z_1, z_2)$ and $B(z_1, z_2)$ are complementary [68] with respect to all pass function $z_1^{-M}z_2^{-N}$ if

$$A(z_1, z_2) + B(z_1, z_2) = z_1^{-M}z_2^{-N} \tag{4.23}$$

where $2M + 1$ and $2N + 1$ is the order of the two filter. The linear-phase 2D FIR multiple-notch filter can be obtained as the complementary filter of $H_t(z_1, z_2)$.

$$H_N(z_1, z_2) = z_1^{-(N_1-1)/2}z_2^{-(N_2-1)/2} - H_t(z_1, z_2) \tag{4.24}$$

where $N_1$and N_2 are the length of two 1D multiple-tone filter. The block diagram of 2D multiple-notch filter is shown in Fig. 4.2 whereas its amplitude response is shown in Fig. 4.3 (f).

4.5 Design Example

In this section, a design example has been presented which was performed with MATLAB.

Step 1: The notch frequencies are selected for the block size of 8 × 8 as:

$$\omega_1 = 0.25\pi \qquad BW_1 = 0.02\pi$$

$$\omega_2 = 0.50\pi \qquad BW_2 = 0.03\pi$$

$$\omega_3 = 0.75\pi \qquad BW_3 = 0.03\pi$$

$$\omega_4 = 0.99\pi \qquad BW_4 = 0.04\pi$$

These frequencies and bandwidths are also taken for the design of 1D multiple-tone filter.

Step 2: 1D FIR multiple-tone filter is designed using MATLAB function with Kaiser window and we obtain the filter coefficients of 64^{th} order filter. The impulse response (filter coefficients) is shown in Fig. 4.3 (a) whereas the frequency response of 1D multiple-tone filter is shown in Fig. 4.3 (b).

Step 3: We obtain the transfer function of 2D multiple-tone filter $H_t(z1, z2)$ by cascading 2D multiple-parallel line filters $H_i(z1, z2)$ as shown in Fig. 4.2 .

Step 4: The linear-phase 2D FIR multiple-notch filter can be obtained as the complementary filter of $H_t(z1, z2)$. Amplitude response shows the notches at desired frequencies.

Step 5: DCT coefficient of block size $M \times M$ is multiplied by 2D filter matrix of equal size. Where M is also the order of both 1-D filters.

4.6 Applications of 2D Multiple-notch Filter

In [6] 2D IIR single-notch filter is used for single or multiple sinusoidal-interferences. Proposed 2D multiple-notch filter can also be used for the removal of single or multiple sinusoidal-interferences. As discussed in *Chapter 3*, 2D IIR multiple-notch filter can be used for reducing blocking artifacts from the DCT coded image. Thus, 2D FIR multiple-notch filter can also be used for reducing blocking artifacts from the DCT coded image in the similar way as the 2D IIR multiple-notch filter. These applications have been discussed below.

4.6.1 Removal of false edges from the edge-map of blocky DCT coded image

As discussed earlier, space-variant/ adaptive filtering requires a classification of image regions into different categories to apply a suitable filter in the corresponding region. Thus the performance of these algorithms is based on classification scheme which is based on edge information extracted from the received blocky image. Thus performance of these algorithms can be improved by removing the false edges from the edge-map of blocky DCT coded image. It is obvious from the property of DCT and it can also be observed that the DCT of square grid of line spacing of eight in both horizontal and vertical direction has peaks at an interval of 64 in both directions. This grid can be removed by killing these peaks by suitable notch filter. In this work this fact is verified as shown in Fig. 4.4 (a-d). The notch frequencies for this multiple-notch filter are calculated from block size. In case of actual images, it is observed that as the grid of lines in the edge image is not complete, the peaks remain at the same position but their spread increases. So, at a very high compression ratio, when grid in the edge map of DCT coded image is visible, this grid or false edges can be removed using this proposed 2D multiple-notch filter. This fact was verified with DCT coded 256 × 256 Lenna image and was found to be correct as shown in Fig. 4.4 (e) and Fig. 4.4 (f). Thus, false edges from the edge-map of blocky DCT coded image can be removed by 2D FIR

Table 4.1: Comparison of the performances of various space-variant algorithms on Lenna image.

Algorithms	*PSNR in dB at quality factor q*			*Boundary PSNR in dB at quality factor q*			*Boundary Discontinuity in (10^6) at quality factor q*		
	q=5	q=10	q=20	q=5	q=10	q=20	q=5	q=10	q=20
Original	-	-	-	-	-	-	4.28	4.28	4.28
DCT coded	25.31	28.09	30.79	15.0	17.94	20.93	10.9	7.95	5.98
Multiple-notch filter with SAF	26.1	28.84	31.12	16.49	19.22	21.42	5.57	4.28	3.57
Gaussian LPF with SAF	26.1	28.88	31.20	16.57	19.32	21.52	5.23	4.00	3.33

multiple-notch filter and the performance of space-variant/ adaptive filtering could be improved.

4.6.2 Reduction of blocking artifacts by using multiple-notch filter in monotone areas

In space-variant/adaptive filtering, the image regions are first classified into monotone area and edge area and then in the former low pass filtering is performed whereas in the latter directional or signal adaptive filter is applied. In proposed scheme, the same signal adaptive filter is applied in edge area but a 2D FIR multiple-notch filter is applied in place of lowpass filter in monotone area. The 2D FIR multiple-notch filter is applied directly in monotone area because the periodic textures due to blocking artifacts are more visible in these areas as compared to edge areas. The 2D FIR multiple-notch filter is not applied to the complete image as periodic texture due to blocking artifacts hide

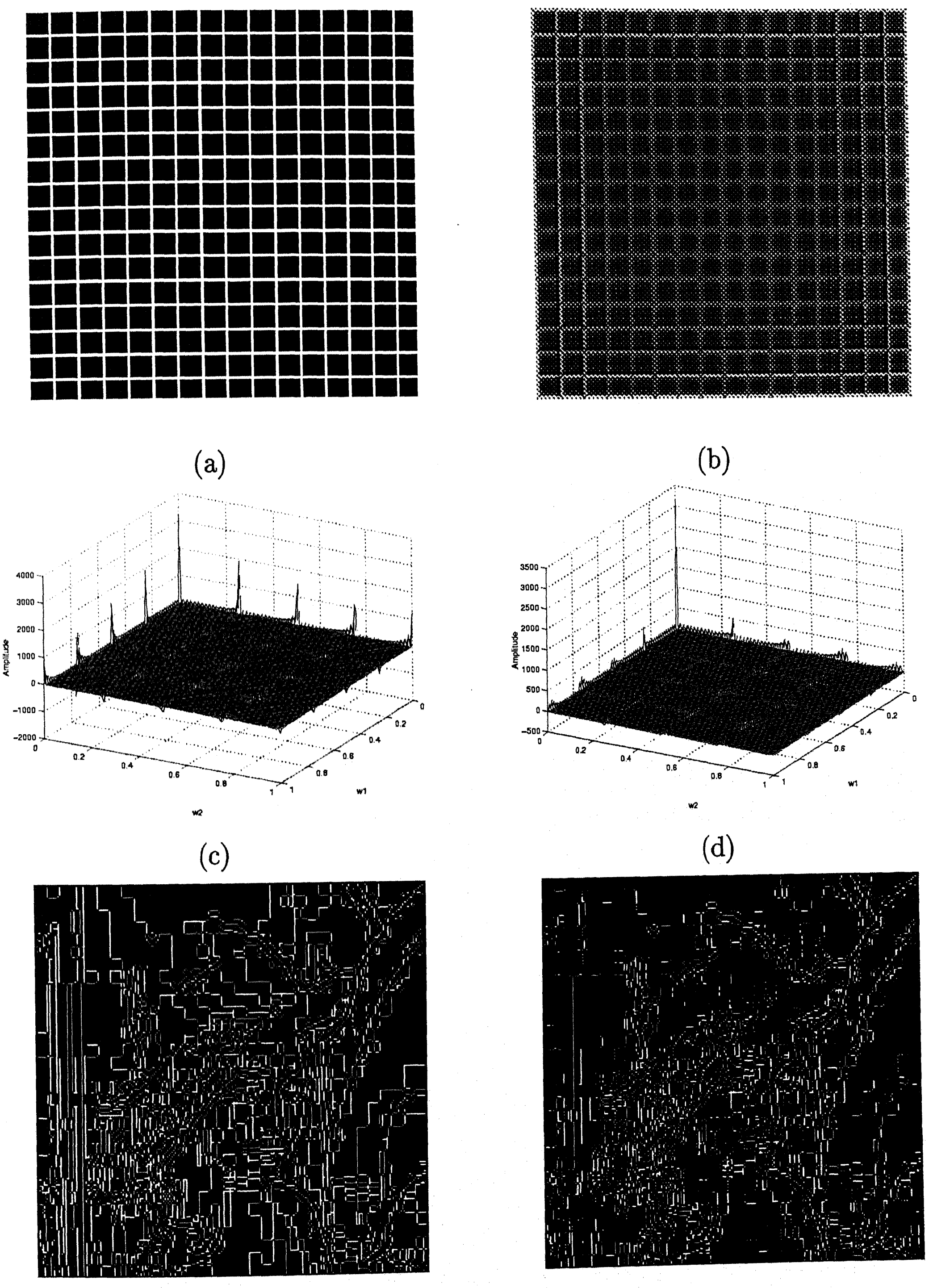

(a) (b)

(c) (d)

(e) (f)

Figure 4.4: False edge filtering by 2D FIR notch filter. (a) Square grid. (b) Filtered grid with threshold at half of the maximum value. (c) Square grid in DCT domain. (d) Filtered grid in DCT domain. (e) Edge of Lenna image. (f) Filtered edge in (e).

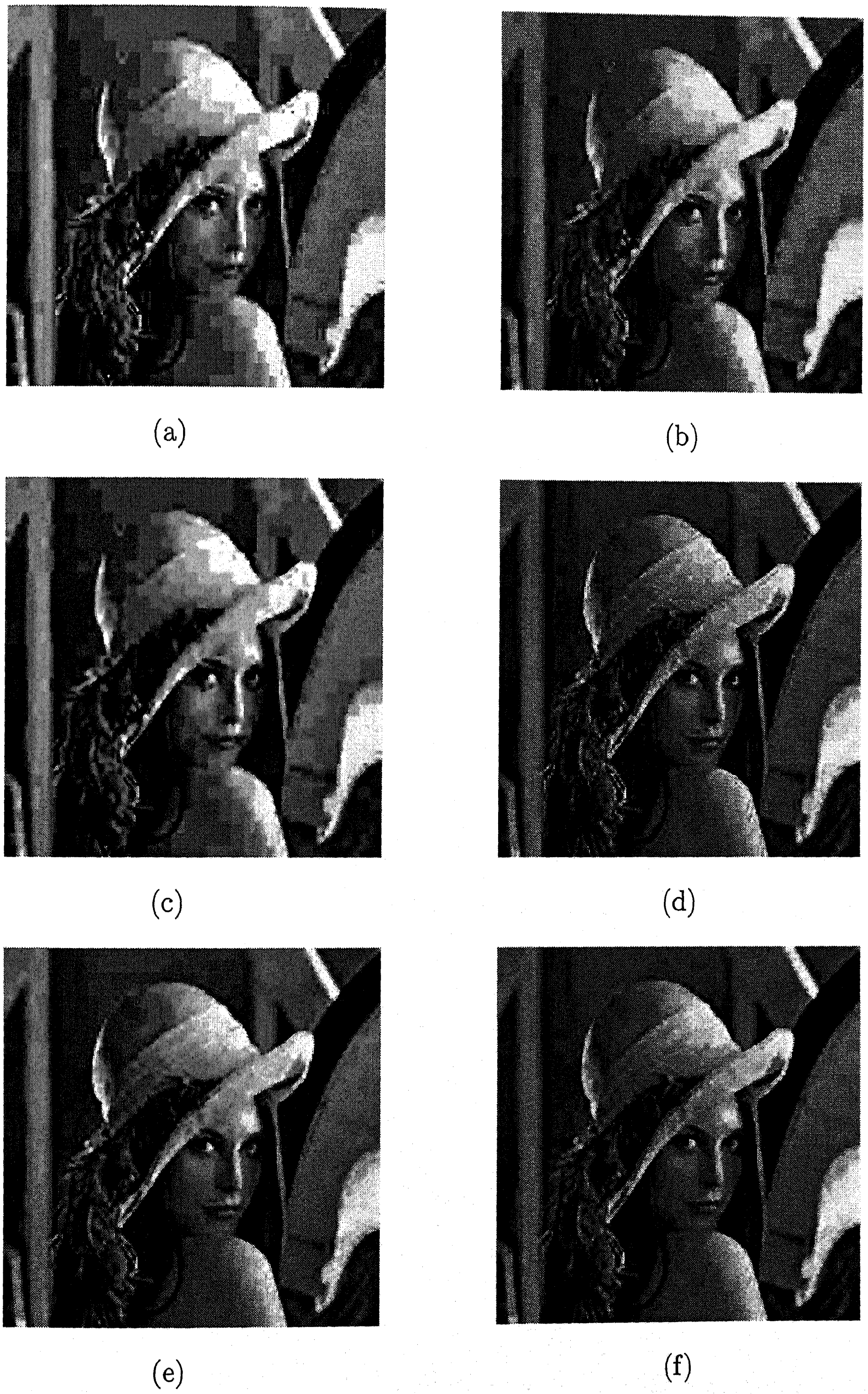

(a)

(b)

(c)

(d)

(e)

(f)

Figure 4.5: Postprocessing of Lenna image at quality factor 5 in (a), (b), (c) and (d), (e), (f) at quality factor 10 by various algorithms. Here, (a) and (d) Before postprocessing, (b) and (e) Processed by 2D FIR multiple-notch filter with signal adaptive filter (SAF), and (c) and (f) Processed by Gaussian LPF with SAF

in DCT domain especially in edge area which is due to the masking effect of human visual system. Moreover, actual edges are also blurred if the same filter is applied in edge areas. In this scheme, spatial domain signal adaptive filtering algorithm is used in edge area to avoid blurring. The filtering mask for this two-dimensional signal adaptive filter is given by

$$\begin{bmatrix} A & B & C \\ D & E & F \\ G & H & E \end{bmatrix} \equiv \begin{bmatrix} 1/16 & 2/16 & 1/16 \\ 2/16 & 4/16 & 2/16 \\ 1/16 & 2/16 & 1/16 \end{bmatrix} \qquad (4.25)$$

This filtering scheme is already discussed in *Chapter 2*. The results given in Fig. 4.5 shows that blocking artifacts can be reduced by this method. However, the improvement is limited to high compression ratios because these periodic textures due to blocking artifacts hides in DCT domain at low compression ratios.

4.7 Results

The filter is designed according to the approach discussed in *section 4.4* and is implemented using MATLAB. The MATLAB functions are used for the design of 1D FIR multiple-notch filter with Kaiser window. The block diagram of 2D FIR multiple-notch filter is shown in Fig. 4.2 whereas its amplitude response is shown in Fig. 4.3 (f). These plots of Fig. 4.3 show that all 1D and 2D filters are obtained as per the design approach discussed in section 4.4. The 2D FIR multiple-notch filter has the notches at desired frequencies and the passbands ripples not very large.

Now, in the rest of this section, the results of various algorithm applied on reconstructed blocky 256 × 256 Lenna image have been presented. These algorithms were implemented with MATLAB. Various results are given in Table 4.1. The results of two algorithms are compared with baseline JPEG like DCT decoded image. As the PSNR is only the rough indicator of image quality and does not reflects the blocking artifacts, two new discontinuity measures are defined. Various performance measures such as Peak SNR (PSNR), block boundary PSNR (BPSNR), block boundary discontinuity have already been defined in *Chapter 2*.

The reduction of discontinuity signifies that (see Table 4.1) blocking artifacts are reduced which can also be observed visually in Fig. 4.5. It can also be seen from Table 4.1 that the improvement in PSNR for block boundary pixels is more as compared to over all PSNR.

4.8 Conclusions

In this Chapter, design and some new applications of 2D FIR multiple-notch filter are discussed. FIR filters are suitable for image processing applications as they causes less distortion due to their linear-phase property. The drawback of FIR filter is that they cause more delay. In this work, a special 2D FIR multiple-notch filter is designed with an intention to remove blocking artifacts from DCT coded images. For the design of this type of filter, first a 2D FIR multiple-tone filter is obtained from 1D FIR multiple-tone filter. In proposed design approach, a simple algebraic method is used in which first a 2D vertical and horizontal multiple-parallel line filters are obtained from 1D multiple-tone filter and then a 2D FIR multiple-tone filter is obtained by cascading these two filters. Finally, the desired 2D multiple-notch filter is the complementary filter of 2D multiple-tone filter as shown in Fig. 4.2. Reduction of blocking artifacts and removal of false edges from edge-map of blocky image to improve the performance of space-variant/ adaptive algorithm are the new possible applications of 2D FIR multiple-notch filter that are considered in this work. Furthermore, the space-variant filtering method can be improved with a more efficient 2D FIR multiple-notch filter.

Chapter 5

Computationally Efficient Algorithms for Reducing Blocking Artifacts

5.1 Introduction

Most of the image compression standards use block discrete cosine transform (BDCT) in their image compression scheme due to its excellent energy compaction and decorrelation properties. DCT is used to exploit the spatial correlation for image compression. In BDCT based image compression, the image degradation becomes visible when compression ratio exceeds certain level. These degradations manifest themselves as blocking artifacts due to the rigid block partitioning of the image and ringing noise around edges due to coarse quantization. Both effects are visually annoying and have substantial impact on the subjective quality of image. Blocking artifacts are visible because the inter-block correlation is not taken into account during encoding and quantization process of DCT coefficients. At higher compression ratios, since very few coefficients are encoded and each coefficient must be represented at a very coarse level of quantization, the blocking artifacts are more visible.

Several postprocessing algorithms [1–4,22–29] have been proposed to reduce blocking effect of block coding system as discussed in *Chapter 1.* Out of these algorithms space-variant / adaptive filtering techniques are more attractive as they try to exploit the local statistics of the image. In these algorithms, the classification of image areas is used to capture the non-stationary behavior of the image. Classification is based on available edge information extracted from the received blocky image. Hence the performance of space-variant or adaptive filtering scheme degrades. Furthermore, the need of strong filter in monotone area and week directional filter in edge area makes it complex. In references [2, 4, 5], the blocking artifacts are reduced by processing the image in DCT domain itself.

In this Chapter [1], four simple but effective algorithms for reducing blocking artifacts from DCT coded images are proposed. In original image, a large inter-block correlation exits between adjacent blocks and some amount of it remains in the blocky decoded image. To exploit the existence of large inter-block correlation between adjacent blocks, a signal adaptive filter is applied to DC component of DCT coded image. To further reduce the discontinuities, the image is re-divided into blocks in such a way that the corner of the original blocks comes at the center of new blocks. These discontinuities are reflected as AC component in the DCT of new blocks. The AC components of those blocks, which do not contain details, can be attenuated to reduce discontinuities. The performances of both the algorithms improve as compression ratio increases. These DCT domain algorithms are computationally efficient since fast algorithms for the computation of DCT are available. In third algorithm, a second approach for discontinuity reduction is proposed which is based on SVD based filtering scheme. This algorithm is also very effective for reducing blocking artifacts. Fourth algorithm proposed in this Chapter is again a DCT domain algorithm, which reduces the blocking artifacts by eliminating some DCT coefficients of concatenated block of two adjacent blocks. This algorithm has low computational complexity, as no filtering is required. In this Chapter, transform domain processing is discussed in section 5.2. Proposed four algorithms are described

[1] Part of this Chapter represents work accepted for presentation and publication in [55] and communicated in [84]

in section 5.3. In section 5.4, the results have been presented. Finally, conclusions are given in section 5.5.

5.2 Processing in Transform domain

In DCT based image coding, the compressed image is in transform domain. Thus processing in DCT domain itself has low computational complexity. Following are the advantage of processing the image in DCT domain.

1. To get processed image back in JPEG like format, IDCT-DCT calculation can be avoided. It can be shown that the computational complexity of filtering in DCT domain is significantly smaller than that of the straightforward approach, of converting back to the uncompressed domain, convolving in the spatial domain, and re transforming to the DCT domain.

2. Distribution of noise in transform domain is random so its energy is spread over all the locations where as most of the signal energy is concentrated in a very narrow band, thus the effect of noise can be minimized.

3. Quantization results in large number of DCT coefficients as zero. This property can be used to reduce the computational complexity.

5.3 Proposed Algorithms for Blocking Artifact Reduction

Blocking artifacts are mainly due to independent coding of different blocks of an image. In original image a large inter-block correlation exits between blocks and some amount of it remains in the blocky decoded image. This residual inter-block correlation can be used for correcting the value of DC coefficient. In this Chapter, a signal adaptive filter is applied to sub-image of DC components of the DCT coded image. This filtering scheme is based on the idea that the DC components of blocks in monotone area are not changing very rapidly and therefore in monotone areas, smoothing of DC components can be performed to exploit the residual inter-block correlation. The DC components of those blocks, which contain details, remain unchanged. This scheme reduces blocking artifacts without affecting much on peak signal to noise ratio (PSNR). The main advantage of this scheme is its low computational complexity. To further reduce the discontinuities in blocky image, the latter is divided into blocks in such a way that the corners of the original blocks come at the centers of new blocks. These discontinuities are reflected as AC component in the DCT of new blocks. The AC components of those blocks, which do not contain details, can be attenuated to reduce these discontinuities. Another advantage of this algorithm is that it also reduces the corner outliers. The performance of both the algorithms improve as compression ratio increases.

Four algorithms are proposed in this section. In first subsection, filtering of DC component by signal adaptive filter is discussed whereas in second subsection the block-boundary discontinuity reduction algorithm is described. In the third subsection, a SVD bases discontinuity algorithm is discussed. Finally, in fourth subsection, another new DCT domain algorithm is discussed which reduces the blocking artifacts by eliminating some of the DCT coefficients of a concatenated block consisting of two adjacent blocks.

5.3.1 ALGORITHM 1: Filtering of DC Component by Signal Adaptive Filter

This algorithm is based on the assumption that the correlation among the DC coefficients of neighboring blocks are high if all the blocks belong to monotone area. In this algorithm, first a DC sub-image is constructed by taking only the DC coefficient of each block in DCT coded image and then a signal adaptive filter is applied to smoothen this DC sub-image. Filtering mask of this filter is shown in Fig. 5.1. Initial value of mask at center is taken as 0.75 whereas the value at other place is 0.0625. Experimentally it is found that these values are giving good results. The image blocks are classified as monotone block or edge block simply by comparing the absolute value of the sum of the

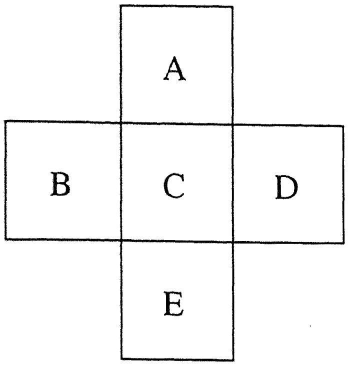

Figure 5.1: Filtering mask of the Signal Adaptive Filter.

AC coefficients of the block with a threshold.

In this adaptive filtering scheme, if the center C of filtering mask is at DC component corresponding to edge block in DC sub-image then all surrounding coefficients A, B, D and E are made zero and this value remains unchanged. Since the blocking artifacts are more visible in monotone areas, it is assumed here that DC values corresponding to monotone block is more correlated with the DC value of neighboring blocks but it is not so for the DC value that corresponds to edge block. Thus, the DC components corresponding to edge blocks are excluded from the filtering. If the center of mask is at DC component corresponding to monotone block, then those surrounding values that correspond to DC component of edge blocks are decreased to zero whereas weight of center of mask is increased by the same amount. These filtered values of DC coefficients are fed in original image blocks and then inverse DCT is performed to reconstruct the image. This scheme shows significant reduction in blocking artifacts without much computation complexity. This can be verified by calculating block boundary discontinuity. The PSNR is slightly improved but the improvement is more at block boundary pixels. These results are given in Table 5.1.

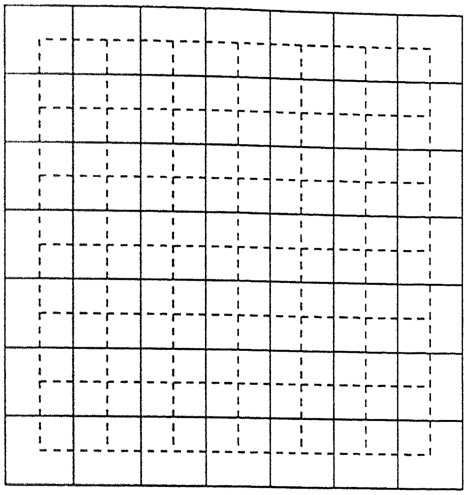

Figure 5.2: Original (solid line) and new position (dotted line) of blocks used for reducing discontinuities in algorithm 2 and 3.

5.3.2 ALGORITHM 2: Reduction of Block Boundary Discontinuities

Proposed algorithm is based on the observation that artificial discontinuities at block boundaries are due to blocking artifacts and are more visible in monotone or slowly varying areas. Thus, this algorithm is also applied in monotone areas. The blocky image is re-divided into new blocks such that it captures the maximum artificial discontinuities. In order to reduce discontinuities, the AC components corresponding to discontinuities are identified and then selected AC components of those new blocks, which do not contain details, are heavily attenuated. Although this algorithm requires the computation of DCT of new block, the processing time is less because no filtering is required. Availability of fast algorithms for DCT computation further reduces the processing time. This algorithm has following steps

1) Division of blocky image into new blocks

The blocky image is re-divided into blocks in such a way that the corner of the original blocks comes at the center of new blocks as shown in Fig. 5.2. This type of re-division captures the maximum artificial discontinuities in new blocks. These discontinuities are reflected as AC component in the DCT of new blocks.

2) Classification of blocks

To protect actual edges, the discontinuity algorithm is applied to monotone blocks only. Thus, the classification of new blocks into edge block and monotone block is required. Classification of block can be performed in DCT domain by examining the values of DCT coefficients. In the proposed algorithm, a DCT based block classification scheme is used in which the sum of absolute values of AC components is used to classify the blocks into monotone block and edge block. The average of sum of absolute values of AC components for all blocks is taken as the threshold for the classification. A block is considered as monotone block if the sum of absolute values of AC components for that block is below the threshold value.

3) Discontinuity Reduction

From the formula of DCT it can be shown that when only the DCT coefficients in the top row are non-zero then all the pixels in each column has equal values in spatial domain or *vise-versa*. Similarly, if the DCT coefficients in the first column are non-zero then all the pixels in each row have equal values in spatial domain. These facts and trends support that monotone blocks having artificial edges have higher values in first row or column [3] because they may have vertical, horizontal or both types of edges/discontinuities due to blocking artifacts. The spatial block $\mathbf{f} = \{f_{ij}\}$ can be transformed to the frequency (DCT) block $\mathbf{F} = \{F_{uv}\}$ as:

$$F_{uv} = C_{uv} \sum_{i=0}^{N-1} \sum_{j=0}^{N-1} f_{ij} D_{ij}^{uv} \qquad for \quad 0 \leq u, v \leq (N-1) \tag{5.1}$$

Where

$$D_{ij}^{uv} = cos(\frac{(2i+1)u\pi}{2N})cos(\frac{(2i+1)u\pi}{2N}) \tag{5.2}$$

Where C_{uv} = 2/N for u $\neq$ 0 and v $\neq$ 0; $C_{uv} = \sqrt{2}/N$ for either u = 0 or v = 0; and C_{uv} = 1/N for both u = 0 and v = 0. Here F_{00} is DC component whereas vertical ($\mathbf{F_v}$), horizontal ($\mathbf{F_h}$) and remaining AC components ($\mathbf{F_{ac}}$) are:

$$\mathbf{F_v} = [F_{01}, F_{02}, ...F_{0(N-1)}]$$

$$\mathbf{F_h} = [F_{10}, F_{20}, ...F_{(N-1)0}]^T$$

$$\mathbf{F_{ac}} = \{F_{uv}, N-1 \geq u, v \geq 1\}_{(N-1)(N-1)} \tag{5.3}$$

Quantized and decoded block can be written as:

$$\tilde{f}_{ij}= \sum_{i=0}^{N-1}\sum_{j=0}^{N-1} C_{uv}\, \tilde{F}_{ij}\, D_{ij}^{uv} \tag{5.4}$$

Where $\tilde{F}_{uv}$ is the quantized DCT coefficient of F_{uv}.

The blocking effect can be estimated for monotone blocks using transform coefficients as they are estimated in [2]. Let current, left, right, top and bottom blocks are denoted by C, L, R, T and B respectively. Blocking effect occurs along the boundary of successive smooth blocks in the spatial domain, thus vertical blocking effect can be estimated as:

$$S_v^{(L)} = (\sum_{j=0}^{N-1} |B_j^{(L)}|^p)^{1/p} \tag{5.5}$$

Where $B_j^{(L)}$ is the boundary difference given by:

$$B_j^{(L)} = \tilde{f}{}^{(C)}_{j,0} - \tilde{f}{}^{(L)}_{j,N-1} \tag{5.6}$$

This boundary difference in DCT domain can be given by:

$$B_j^{(L)} = \sum_{u=0}^{N-1}\sum_{v=0}^{N-1} C_{uv}\, \tilde{F}{}^{(C)}_{uv}\, D_{j0}^{uv} - \sum_{u=0}^{N-1}\sum_{v=0}^{N-1} C_{uv}\, \tilde{F}{}^{(L)}_{uv}\, D_{ij}^{j(N-1)} \tag{5.7}$$

The boundary difference in DCT domain can be divided into DC, V, H, AC components. The contributions of these components to vertical boundary difference is discussed in [2]. We can draw following conclusions to apply the results in proposed algorithm:

(a) Boundary difference contributed by DC component depends on the difference of DC levels of two adjacent blocks. Since we have already minimized this component by first algorithm, so we can neglect it.

(b) Boundary difference contributed by V component is major part that greatly affects the blocking effect along the vertical direction.

(c) Boundary difference contributed by H and AC components produce high frequency variations along the vertical direction and results in perceptible invisible blocking effects. So they can be neglected.

(d) Similarly it can be shown that boundary difference contributed by H component is a major part that greatly affects the blocking effect along the horizontal direction.

In proposed algorithm, based on the above discussion, the DCT coefficients of first two rows and columns of monotone blocks are heavily attenuated whereas the DCT coefficients of edge blocks are less attenuated to reduce artificial discontinuities. Here second row and second column are also selected for attenuation because experimentally we found that vertical and horizontal discontinuities in blocky image have strong showings in first two columns and rows, respectively, in DCT domain.

5.3.3 ALGORITHM 3: Reduction of Block Boundary Discontinuities: Second Approach

In this algorithm the first two-steps i.e. division of blocky image into new blocks and classification of blocks remain the same but the third step i.e. the approach for the reduction of discontinuity is different. The second approach of discontinuity reduction is based on block-based, non-linear filtering algorithm. This filtering approach is based on singular value decomposition (SVD) algorithm. Linear filtering is used to remove the additive noise but their major drawback is that they tend to blur the edges. Non-linear filtering based on SVD method has been successfully used in past for various noise removal applications [69–71]. This technique does not require any additional *a priori* information. It is well known that random noise is hard to compress whereas ordered information is not. Thus, lossy compression of noisy signal, with allowed loss set equal to the noise strength provides the required filtering of the signal. Proposed SVD-based filtering can effectively reduce the discontinuities while preserving the edge details. SVD algorithm can be viewed as a lossy compression scheme. For monotone blocks, the discontinuities are hard to compress as compared to smooth area therefore SVD algorithm allows to filter out these discontinuities. Derivation of the optimum threshold to distinguish significant and insignificant singular values for reducing discontinuity is still a problem with this approach, which must be investigated. The threshold calculation requires the additional signal strength due to discontinuities. The theory of SVD-based filtering is discussed below.

Any $m \times n$ real-valued matrix A can be decomposed uniquely as

$$A = U\Sigma V^T = \sum_{i=0}^{n} \alpha_i \mathbf{u}_i \mathbf{v}_i^T \tag{5.8}$$

where U and V are orthogonal matrices with column vectors $\mathbf{u}_i$ and $\mathbf{v}_i$ and $\Sigma =$ diag(α_1,α_2,...,α_n) is a diagonal matrix. The diagonal elements of Σ can be arranged in descending order and are called the singular values of A. Thus, SVD provides the rank r of a matrix, which is equal to the number of non-zero singular values of the matrix. If rank of the matrix A is r then

$$\alpha_1 \geq \alpha_2 \geq ... \geq \alpha_r > \alpha_{r+1} = ... = \alpha_n = 0 \tag{5.9}$$

For additive noise model, observation matrix B is equal to $A + E$, where E is a random noise matrix of full rank. So, the last (n-r) singular values of B are small but not necessarily zero.

Let B be an $M \times N$ image divided into $k \times k$ image subblocks B_k. Each subblock can be expressed as weighted sum of basis images and weights are the singular values. Setting "nonsignificant" singular values to zero results in lossy compression. The amount of loss is controlled by a threshold value ϵ. The effectiveness of algorithm depends upon the value of ϵ. If ϵ is very small then most of the noise remains but if ϵ is very large then image information is lost. Thus, the main steps of SVD-based filtering algorithm are

(1) Divide image B into subblocks B_k.

(2) Apply SVD to each subblock and set the singular values less than a threshold ϵ to zero.

$$B_k = U\Sigma V^T = \sum_{i=0}^{n} \alpha_i \mathbf{u}_i \mathbf{v}_i^T \tag{5.10}$$

If Σ' is resultant diagonal matrix of singular value after threshold then the reconstructed block will be

$$B_k' = U\Sigma' V^T = \sum_{i=0}^{r} \alpha_i \mathbf{u}_i \mathbf{v}_i^T \tag{5.11}$$

(3) Replace B_k with B_k', where B_k' is resultant block after setting the singular values less than a threshold ϵ to zero.

(4) Apply step (2) an (3) to all the blocks and reconstruct the image.

Note that this algorithm is applied to new blocks obtained by re-division of blocky image into block as discussed in *step 1* of discontinuity reduction algorithm. It is found that the reduction in blocking artifacts cannot be achieved with the original blocks. This approach reduces the blocking artifacts more efficiently but its computational complexity is more because SVD algorithm has to be applied to each of the block.

5.3.4 ALGORITHM 4: Blocking artifact reduction by eliminating some DCT coefficients of concatenated block of two adjacent blocks

As we know that edge component causes the high frequency components in the transformed domain. Thus, examining the DCT coefficients of the block itself can identify the monotone blocks. As discussed in *Chapter 1*, the discontinuities in monotone area are due to blocking artifacts. These discontinuities also cause the high frequency components in DCT domain. Thus, these discontinuities are reflected as high frequency components in the DCT of concatenated block of two or more neighboring monotone blocks. It is also found that there exists a relationship between the DCT coefficient of two monotone blocks and that of concatenated block. The DCT coefficients due to blocking artifacts are present in the concatenated block but not in individual block. Therefore, from the relationship between the DCT coefficients of monotone block of different sizes we can detect the high frequency components due to blocking artifacts and thus we can eliminate them to reduce the blocking artifacts. It is well known that N-point DCT $C(k)$ is closely related with the 2N-point discrete Fourier Transform (DFT) $F(k)$ for symmetrically extended sequence.

$$C(k) = e^{j(\pi k/2N)}F(k) \tag{5.12}$$

To find the relationship between $N \times N$ 2D DCT and $2N \times N$ 2D DCT we extend the results obtained in [4, 39]. The two adjacent rows $u(n)$ and $v(n)$ are concatenated as $w(n)$ and their DCT are given by $U(k)$, $V(k)$ and $W(k)$, respectively, as

$$U(k) = \alpha(k)\sum_{n=0}^{N-1} u(n)\cos[\frac{\pi(2n+1)k}{2N}] \tag{5.13}$$

$$V(k) = \alpha(k)\sum_{n=0}^{N-1} v(n)\cos[\frac{\pi(2n+1)k}{2N}] \tag{5.14}$$

$$W(k) = \frac{1}{\sqrt{2}}\alpha(k)\sum_{n=0}^{2N-1} w(n)\cos[\frac{\pi(2n+1)k}{4N}] \tag{5.15}$$

where $\alpha(k) = \sqrt{\frac{1}{N}}$ for $k = 0$ and $\alpha(k) = \sqrt{\frac{2}{N}}$ for other values. $W(k)$ can be expressed as

$$W(k) = \begin{cases} \frac{1}{\sqrt{2}}[U(k/2) + (-1)^{k/2}V(k/2)], & for \quad k = 0, 2, 4, ... \\ \frac{1}{\sqrt{2}}\alpha(k)\sum_{n=0}^{N-1}\{u(n)\cos[\frac{\pi(2n+1)k}{4N}] & \\ \quad +(-1)^{(k-1)/2}v(n)\cos[\frac{\pi(2n+1)k}{4N}]\} & for \quad k = 1, 3, 5, ... \end{cases} \tag{5.16}$$

From the above equation it is clear that the $2k^{th}$ DCT coefficient of W depends only on the k^{th} DCT coefficients of U and V whereas the odd numbered DCT coefficients of W are expressed as a weighted sum of $u(n)$ and $v(n)$. Thus, only the odd numbered DCT coefficients of W are affected by the discontinuities in the block. Thus, actual nonzero coefficients due to signal are kept within the range two times larger than those of U and V. For concatenated 2D blocks, actual nonzero DCT coefficients are present within the range two times larger than those of DCT coefficients of constituent block for all rows and column. The coefficients beyond this range are the coefficients due to the blocking artifacts. In proposed algorithm, the DCT coefficients in the first row and first column that are beyond this range are eliminated. Only first row and first column are selected because of the effect of vertical and horizontal discontinuities which has greater values in these locations as discussed in subsection 5.3.2. This algorithm has low computational complexity, as no filtering is required. The availability of fast algorithm for DCT computation makes this algorithm suitable for low bit rate coding applications. The selection of first row and first column for elimination further reduces the computation time. Following are the main steps of this algorithm.

Step 1. ***Identification of block as monotone block:*** Actual edges are blurred due to elimination of high frequency components. To protect the actual edges, this algorithm requires the identification of monotone blocks. In proposed algorithm, we selected only first row and first column for elimination of some DCT coefficients. Therefore, this step can be bypassed. In fact, in implementation of this algorithm, this step is ignored because this algorithm doesn't produces much undesirable blur as discussed above.

Step 2. ***Joining two horizontally adjacent monotone block and transforming the concatenated block in DCT domain:*** The two horizontally adjacent monotone block of size $M \times M$ are concatenated into one block of size $2M \times M$. The DCT coefficients due blocking artifacts are present in the concatenated block but not in individual block. The $2M \times M$ DCT of concatenated block gives the global characteristics.

Step 3. ***Finding the maximum non-zero valued index for the concatenated block for elimination of DCT coefficients corresponding to blocking artifacts:*** The global frequency characteristics in two adjacent blocks are similar to local ones in each block. This concept is used in identifying and eliminating the coefficients due to blocking artifacts in the concatenated block. For two blocks, the index of first row and first column are found by checking them for non-zero values. The maximum non-zero valued index for any row or column of a block is defined as the location beyond which all the DCT coefficients are zero. For concatenated

5.4 Results

In this section, results of various algorithm applied on 256 × 256 Lenna image are presented. These algorithms are implemented with MATLAB. To get blocky image at different quality factors, a baseline JPEG like algorithm is implemented and then this blocky image is postprocessed by various algorithms. Various results are given in Table 5.1. Various quality measures are calculated to see the performances of these algorithms. The results of two algorithms are compared with baseline JPEG like DCT decoded image. Peak SNR (PSNR) is defined in *Chapter 2*. Subjective quality of an image depends on the properties of human visual system (HVS), as discontinuities are more visible in monotone or slowly varying areas. Therefore, the PSNR is only the rough indicator of image quality and does not reflect the blocking artifacts. Two new discontinuity measures are defined as discussed in *Chapter 2*. The block boundary PSNR (BPSNR) is defined in the same way as PSNR but only one pixel from both side of block boundary are considered for the calculation of MSE whereas the block boundary discontinuity measure is defined as the sum of square of difference of pixel values across the four block boundaries.

Filtering of sub-image consisting of DC components by signal adaptive filter reduces blocking artifacts with very low computational cost whereas the selective attenuation of AC component corresponding to block boundary discontinuities shows significant reduction in blocking artifacts. Finally corner outliers detection and replacement algorithm is applied to further improve the performance. The performance of both the algorithms improves as compression ratio increases. The reduction of discontinuity signifies that (see Table 5.1) blocking artifacts are reduced and it can also be observed visually in Fig. 5.3 and Fig. 5.4. It can also be seen from Table 5.1 that the improvement in PSNR for block boundary pixels is more as compared to over all PSNR.

The second approach for discontinuity reduction is proposed in algorithm 4. It reduces the blocking artifacts more efficiently but its computational complexity is more because SVD algorithm is to be applied to each of the block. PSNR achieved by this

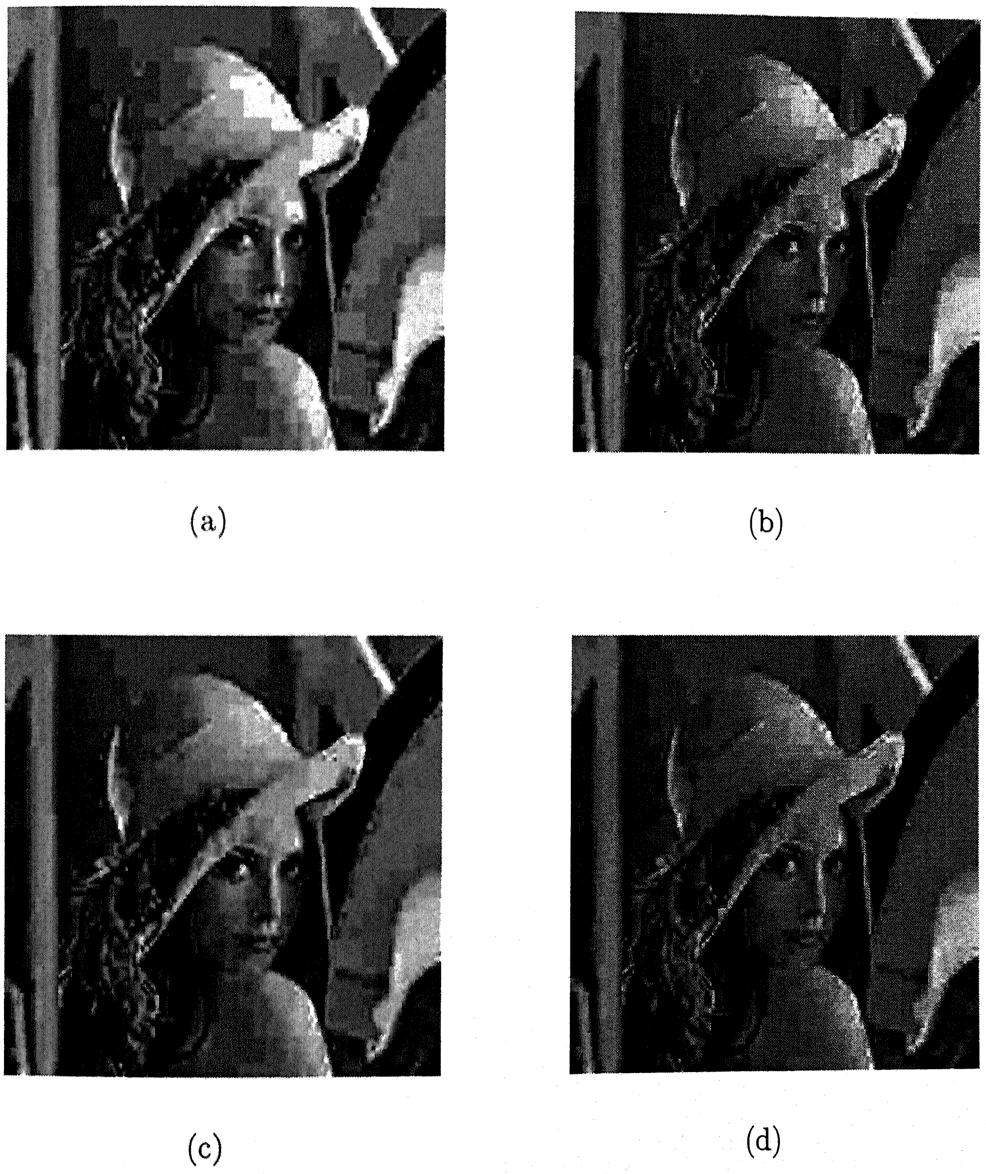

(a)

(b)

(c)

(d)

Figure 5.3: Postprocessing of Lenna image compressed at quality factor of 5 by various algorithms. (a) Before postprocessing. (b) DC component filtered. (c) Discontinuity reduction. (d) Corner outliers removed.

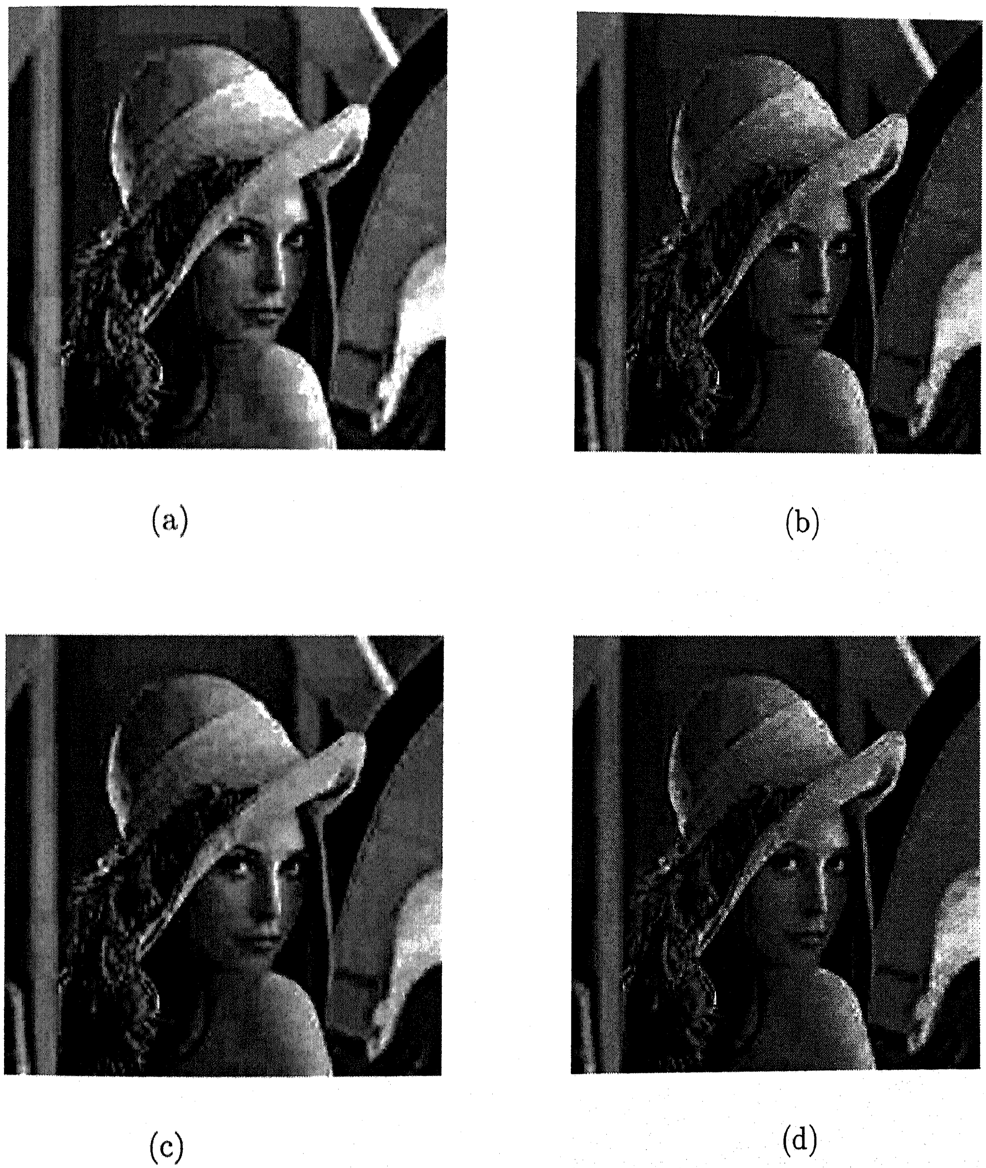

(a)

(b)

(c)

(d)

Figure 5.4: Postprocessing of Lenna image compressed at quality factor of 9 by various algorithms. (a) Before postprocessing. (b) DC component filtering by algorithm 1. (c) Discontinuity reduction by algorithm 2. (d) Corner outliers removed.

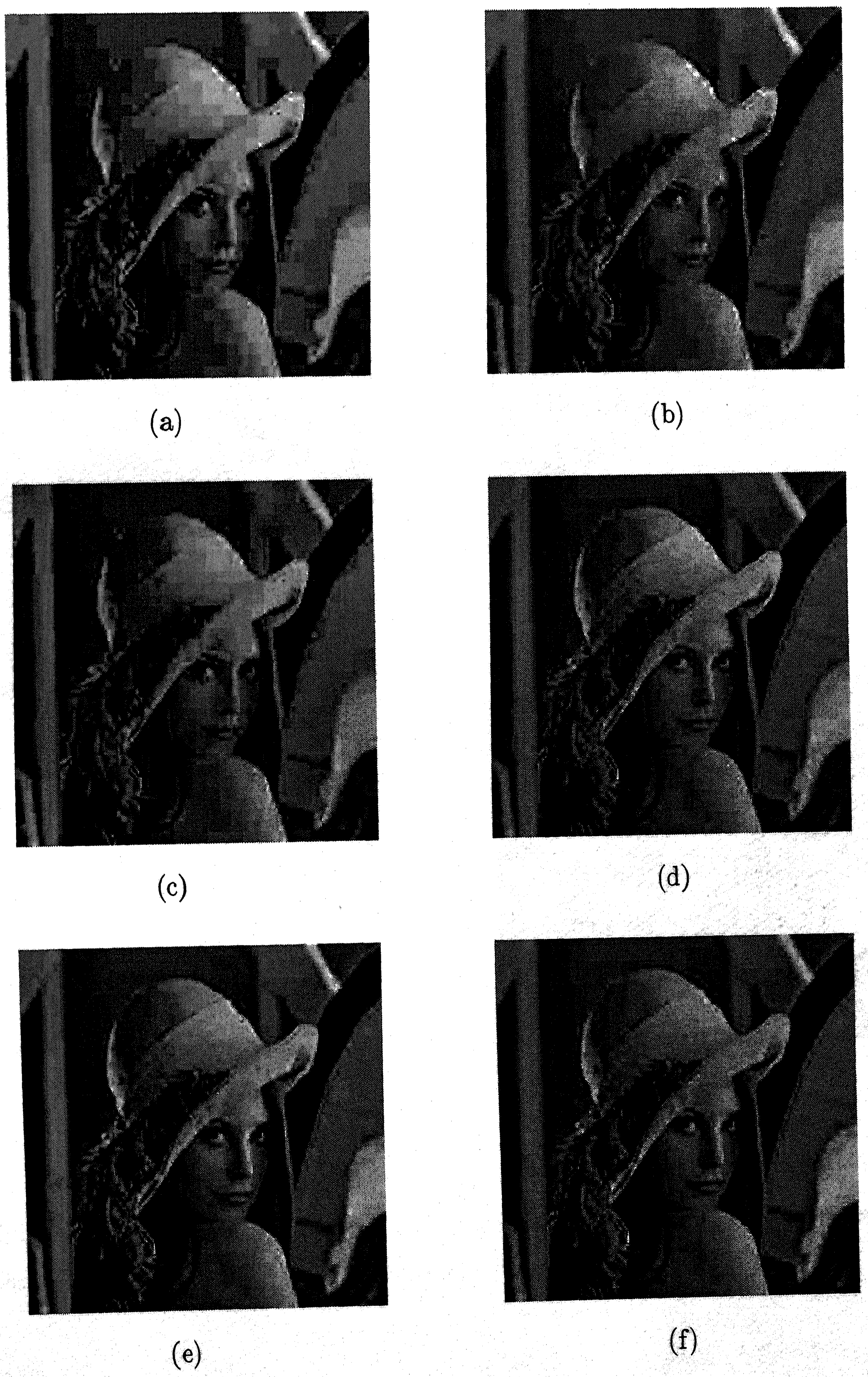

Figure 5.5: Postprocessing of Lenna image compressed at quality factor of 5 in (a), (b) and (c) and 9 in (d), (e) and (f) by various algorithms. (a) and (d) Before postprocessing. (b) and (e) Discontinuity reduction by algorithm 2. (c) and (f) Discontinuity reduction by SVD filtering (Algorithm 3).

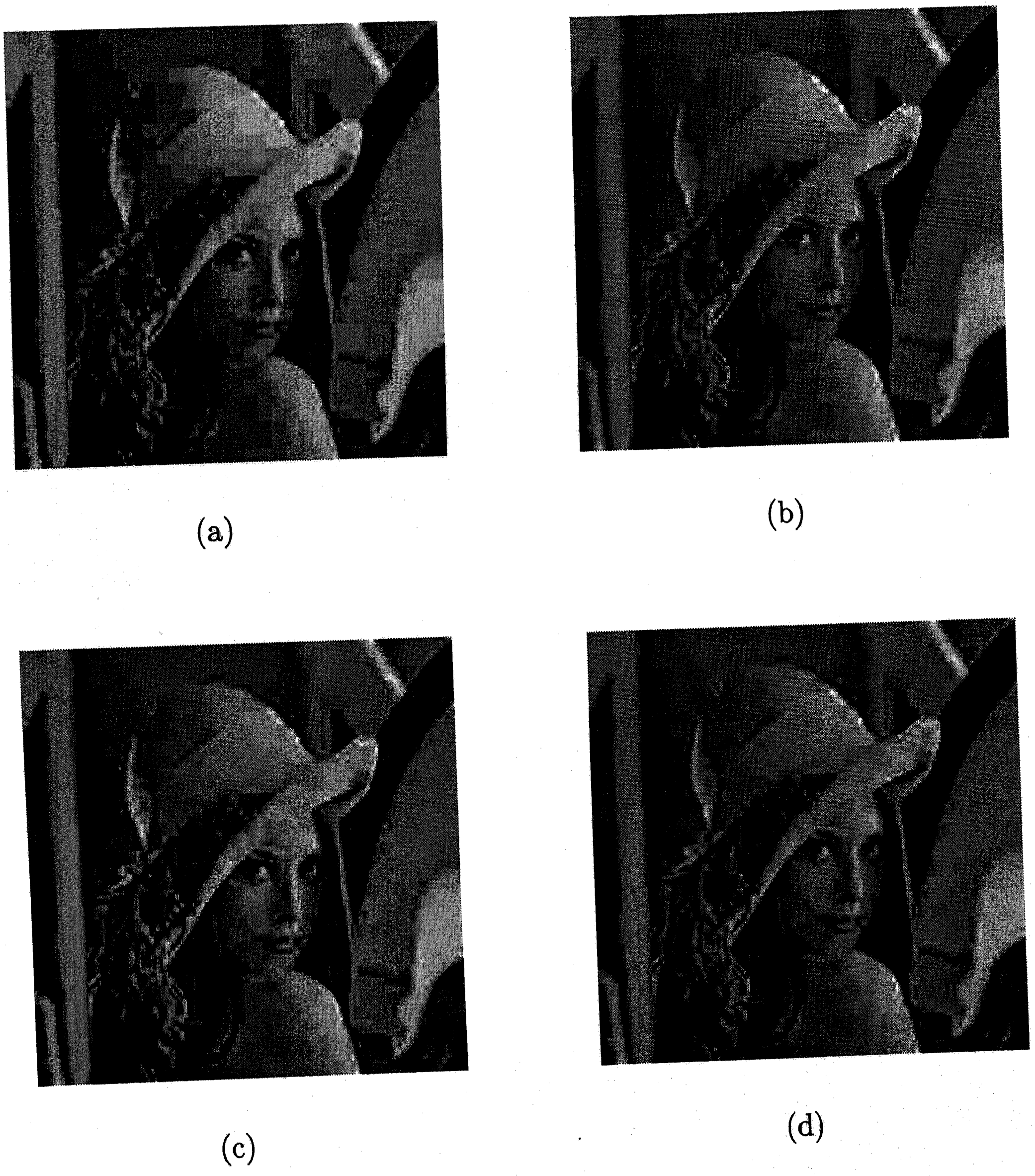

(a)

(b)

(c)

(d)

Figure 5.6: Postprocessing of Lenna image compressed at quality factor of 5 by various algorithms. (a) Before postprocessing. (b) Discontinuity reduction by algorithm 2 (c) Algorithm 4. (d) Algorithm 4 with corner outliers removed.

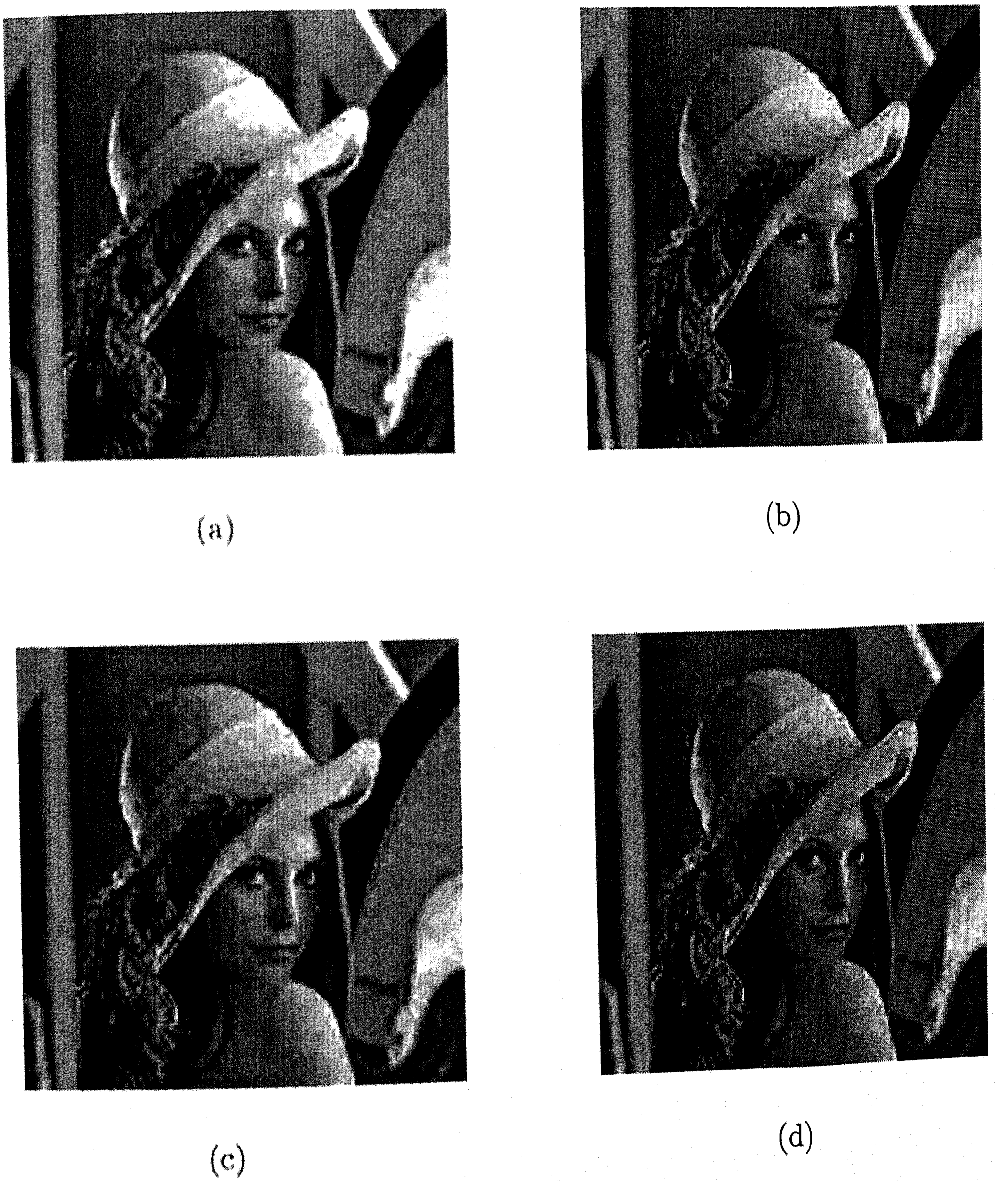

(a)

(b)

(c)

(d)

Figure 5.7: Postprocessing of Lenna image compressed at quality factor of 9 by various algorithms. (a) Before postprocessing. (b) Discontinuity reduction by algorithm 2 (c) Algorithm 4. (d) Algorithm 4 with corner outliers removed.

Table 5.1: Comparison of the performances of proposed computationally efficient algorithms on Lenna Image.

Algorithms	*PSNR in dB at quality factor q*			*Boundary PSNR in dB at quality factor q*			*Boundary Discontinuity(in 10^6)at quality factor q*		
	q=5	q=9	q=12	q=5	q=9	q=12	q=5	q=9	q=12
Original	-	-	-	-	-	-	4.28	4.28	4.28
DCT coded	25.32	27.71	28.80	15.02	17.54	18.71	10.9	8.20	7.19
DC component filtering: Algorithm 1	25.42	27.71	28.82	15.13	17.56	18.73	10.4	8.06	7.13
Discontinuity reduction: Algorithm 2	25.60	27.87	28.95	15.45	17.85	18.95	9.47	7.46	6.71
Algorithm 2 with corner outliers reduction	25.75	27.98	29.00	15.89	18.20	19.15	7.74	6.19	5.69
Discontinuity reduction: Algorithm 3	25.45	27.71	28.77	15.26	17.74	18.82	9.95	7.58	6.76
Algorithm 3 with corner outliers reduction	25.60	27.81	28.80	15.71	18.08	19.01	8.22	6.37	6.12
Blocking Artifact reduction: Algorithm 4	25.55	27.79	28.85	15.29	17.63	18.77	9.58	7.87	7.00
Algorithm 4 with corner outliers reduction	25.71	27.91	28.91	15.76	18.01	18.97	7.87	6.55	5.96

algorithm is also slightly less as compared to the first approach. The results from this algorithm are presented in Table 5.1 and Fig. 5.5.

Finally, the fourth algorithm proposed in this Chapter is also implemented with MATLAB. This computationally efficient algorithm also gives very good result in terms of PSNR, discontinuity measure and visual quality. The performance and results of this algorithm are presented in Fig. 5.6, Fig. 5.7 and Table 5.1. It is clear from these results that this algorithm also gives very good performance with minimum computational complexity.

5.5 Conclusions

In this Chapter, four simple yet effective algorithms for reducing blocking artifacts from DCT coded image are proposed. Although these algorithms look very simple but they are able to reduce blocking artifacts significantly without much computational complexity. The performance of these algorithms is better at high compression ratios; therefore they are suitable for low bit rate video coding applications. In first algorithm the signal adaptive filter is applied to sub-image consisting of DC components of DCT coded image. This algorithm reduces the blocking artifacts with very low computational complexity. In second algorithm the blocking artifacts are reduced significantly by selective attenuation of AC components corresponding to block boundary discontinuities. These results are verified by comparing boundary PSNR and block-boundary discontinuity (see Table 5.1). This can also be observed from the results presented in Fig. 5.3 and Fig. 5.4. It is found that improvement in PSNR for block boundary pixels is more as compared to over all PSNR. This result is attractive because discontinuities at block boundaries, which are the most visually annoying effect, are reduced. Hence, these computationally efficient schemes reduce blocking artifacts considerably with slight improvement in PSNR.

In third algorithm proposed in this Chapter, the discontinuity reduction is based on SVD-based filtering scheme. It reduces the blocking artifacts more efficiently but its computational complexity is more because SVD algorithm has to be applied to each of the block. This algorithm is very effective for reducing blocking artifacts but PSNR achieved by this algorithm is also slightly less as compared to the first approach.

Fourth algorithm proposed in this Chapter is again a DCT domain algorithm, which reduces the blocking artifacts by eliminating some DCT coefficients of concatenated block of two adjacent blocks. This algorithm has low computational complexity, as no filtering is required. The availability of fast algorithm for DCT computation makes this algorithm suitable for low bit rate coding applications. The selection of first row and first column for elimination further reduces the computation time. The results show that this algorithm provides very good performance with minimum computational complexity.

Chapter 6

Conclusions and Future scope

6.1 General

In this Chapter we summarize the results obtained in this thesis and present our conclusions along with the suggestions for research in the area of DCT based coding and postprocessing. In this work, a number of postprocessing algorithms are proposed. All these algorithms are implemented in MATLAB and some of these are also implemented in C. The reason for using MATLAB was to save the time in writing the long code for implementation of the various algorithms. The various functions available in image processing toolbox are used. First, to make the platform for the work, a simple baseline JPEG like algorithm for lossy image compression is implemented. Almost all the stages of this algorithm i.e. dividing the image into blocks, taking DCT of each block, their quantization and inverse quantization at different quality factors, IDCT and reconstruction of image, are implemented. Some more programs are written for finding the number of bits required to encode the quantized image and the calculation of various performance measures such as PSNR, boundary PSNR and block-boundary discontinuity. With this preliminary work, all of the proposed algorithms are implemented. To get decompressed blocky image at different quality factors, a baseline JPEG like algorithm is implemented and this image is postprocessed by various algorithms. The results of various algorithms proposed in this work are already given at the end of the each Chapter.

6.2 Summary and Main findings

In this thesis work, a number of algorithms for postprocessing of DCT coded images are proposed. These algorithms are implemented with MATLAB and they are applied to process the decompressed Lenna image to compare the performances. The performances of these algorithms are verified by comparing the PSNR, boundary PSNR and block-boundary discontinuity with baseline JPEG like scheme. The corner outliers reduction scheme improves the performance of all proposed algorithms. In this section, these algorithms are summarized.

In *Chapter 2* we proposed a hybrid scheme for the postprocessing of DCT coded images. This scheme is named as hybrid as the processing is performed in both DCT as well as in the spatial domain by two different algorithms. This algorithm includes the advantage of adaptive filtering in edge area and block-boundary discontinuity minimization algorithm in monotone area. Thus, the processing of image is performed in both spatial and transform domain. In this algorithm, a lower order signal adaptive filter is applied in edge area to reduce the processing time. This scheme uses the block-boundary discontinuity minimization algorithm in monotone area, which also does not have much computational cost. Corner outliers reduction scheme further improves the performance.

In this scheme, the DCT coefficients of monotone block are compensated to achieve minimum block-boundary discontinuity. These compensating DCT coefficients for monotone blocks are calculated from the DCT of the block-boundary pixel differences. In this calculation, those block-boundary pixel differences are made zero whose neighboring block is an edge block. In proposed scheme, the edge information is extracted and used for the classification of image blocks. For edge blocks, a signal adaptive filter is applied to perform the filtering along the edge. This filter also uses the same edge information (edge-map) to perform the filtering approximately parallel to edge to avoid blurring. It has been found that the performance of the proposed algorithm improves as compression ratio increases. The reduction of discontinuity signifies that the blocking artifacts are reduced. The improvement in PSNR for block-boundary pixels is more as compared to over all PSNR, which also indicates the same. It has also been observed that neither of the two algorithms used in the hybrid scheme are able to give good results if they are used to process the whole image.

In *Chapter 3* we developed the design method for 2D IIR multiple-notch filter and some new applications are being proposed. In proposed design approach, a simple algebraic method is used to design the 2D IIR multiple-notch filter. In this approach, first two 1D multiple-tone filters are designed as per the specifications of 2D multiple-notch filter and then these two filters are used to obtain 2D multiple-vertical line filter and 2D multiple-horizontal line filter. Finally, cascade of these two filters gives the desired 2D multiple-notch filter. The design of 1D multiple tone filter is based on the design of all-pass filter as discussed in [7].

Then, a design example and new applications of 2D multiple-notch filter are discussed. It is shown that 2D multiple-notch filter can eliminate the square grid. It can also reduce the blocking artifacts from DCT coded images. The concept of reducing blocking artifacts by 2D multiple-notch filter is based on the fact that the discontinuities due to block artifacts in block decoded image have periodic structure which ultimately results in some peaks in the DCT domain. These discontinuities are highlighted in gradient of the image. A 2D multiple-notch filter can kill these peaks to reduce blocking artifacts. Discontinuities due to blocking artifacts are more visible in the monotone area, so this filter can be applied directly in these areas. Thus, improvement in the performances of space-variant/adaptive filter by the removal of false edges from the edge-map of blocky image and the reduction of blocking artifacts directly in monotone area, are the new possible applications of 2D multiple-notch filter. In these applications, the reduction of boundary PSNR and block-boundary discontinuity signifies that the blocking artifacts are reduced.

In *Chapter 4* we extended the design approach of 2D multiple-notch filter to FIR type filter. FIR filters are suitable for image processing applications as they cause less distortion due to their linear phase property. The drawback of FIR filter is that they cause more delay. In this work, a special 2D FIR multiple-notch filter is designed with an intention to remove blocking artifacts from DCT coded images.

The design procedure for the 2D FIR multiple-notch filter is similar to the procedure that is used for the design of 2D IIR multiple-notch filter. However, the desired 2D multiple-notch filter is a complementary filter of 2D multiple-tone filter. In this case, two 1D FIR multiple-tone filters are designed by windowed Fourier series method with Kaiser window. The filter is designed and implemented using MATLAB. Various plots show that all 1D and 2D filters are obtained as per the design approach. The 2D FIR multiple-notch filter has the notches at desired frequencies and the passband ripples are also not very large. This filter is also applied for the reduction of blocking artifacts and removal of false edges from edge of blocky decompressed image. The filter is applied on decompressed blocky Lenna image and the comparison of performance and visual observations signifies that blocking artifacts are reduced.

In *Chapter 5*, four simple and effective algorithms for reducing blocking artifacts from DCT coded images are being proposed. Although these algorithms look very simple but they are able to reduce blocking artifacts significantly without much computational complexity. The performance of these algorithms is better at high compression ratios; therefore these are suitable for low bit rate video coding applications.

First algorithm proposed in *Chapter 5* reduces the blocking artifacts by exploiting the residual inter-block correlation, which exists in the received blocky image. For this purpose a signal adaptive filter is used to smoothen out a sub-image of DC coefficients of all the blocks. This algorithm reduces the blocking artifacts with a very low computational complexity. Second algorithm reduces the block-boundary discontinuities due to blocking artifacts by capturing and removing them in the DCT domain. The blocking artifacts are reduced significantly by selective attenuation of AC components due to block boundary discontinuities. These two algorithms together reduce the blocking artifacts considerably. It has been verified by comparing boundary PSNR and block-boundary discontinuity. It has been found that improvement in PSNR for block boundary pixels is more as compared to over all PSNR. This result is attractive because discontinuities at block boundaries, which are the most visually annoying effect, are reduced. Hence, this computationally efficient scheme reduces the blocking artifacts considerably with slight improvement in PSNR. In the third algorithm, a second approach for discontinuity reduction is proposed which uses the SVD based filtering scheme. In this algorithm, the block-boundary discontinuities due to blocking artifacts are captured in the same way but the SVD based filtering scheme is used for their reduction. It reduces the blocking artifacts considerably but its computational complexity is slightly more because SVD algorithm has to be applied to each monotone block. The PSNR achieved by this algorithm is also slightly less as compared to the first approach.

Fourth algorithm proposed in *Chapter 5* is again a DCT domain algorithm. It reduces the blocking artifacts by eliminating some selected DCT coefficients of concatenated block of two adjacent blocks. This algorithm has low computational complexity, as no filtering is required. The availability of fast algorithm for DCT computation makes this algorithm suitable for low bit rate coding applications. In this algorithm, only the first row and first column are selected for elimination which further reduces the computation time. The results show that this algorithm provides very good performance with minimum computational complexity.

6.3 Conclusions

DCT based image compression is very popular and found various applications till date, thus efficient postprocessing of such image has become an important research topic. This thesis addresses various postprocessing issues that may arise in practice: (i) reduction of coding artifacts; and (ii) computationally efficient methods to make algorithm suitable for real time applications such as video and still image decoding. Main finding of this thesis is that the coding artifacts can be reduced efficiently by postprocessing. At higher compression ratios, the coding artifacts are more visible and they can be reduced more efficiently than the existing postprocessing algorithms. Various aspects of DCT based image compression and post processing methods are studied with a state-of-art survey on the subject. A number of new postprocessing algorithms for reducing the coding artifacts are proposed in this work.

The first contribution of the thesis is to develop a hybrid scheme for postprocessing by clubbing the good things of several existing algorithms. Smoothing artificial discontinuities due to blocking artifacts improves the image quality whereas smoothing actual image edges degrades it. Thus, objective was to satisfy these two conflicting requirements as simply as possible. Proposed hybrid scheme takes advantages of adaptive filtering and a method for the recovery of loss of accuracy of DCT coefficients. In this algorithm, no filtering is required in monotone area but only the computation of compensating coefficients is required. Performance of this algorithm is better than space-variant filtering. This scheme reduces blocking artifacts considerably without introducing much blur in edge areas and also it provide slight improvement in PSNR.

The second contribution of the thesis is the design of 2D multiple-notch filter and some of its new applications in reducing blocking artifacts. The design method for both FIR and IIR filter of this type are developed. The possibility of using this filter for reducing blocking artifact is fully examined. For this purpose, this filter is applied to improve the performance of the space-variant/adaptive filtering method. It is found that the performance of space-variant filtering can be improved by including the proposed 2D multiple-notch filter for false edge removal in its classification scheme. Reduction of the blocking artifacts directly in monotone area is the second application suggested for this filter. The application of 2D multiple-notch filter for reducing blocking artifact is new and it is found that the performance of the space-variant algorithm utilizing 2D multiple-notch filter are comparable to existing algorithms. Thus, 2D multiple-notch filter has been successfully applied for reducing the blocking artifacts. To reduce the computational complexity, the filtering is performed in DCT domain. The results obtained in case of FIR filter are better than IIR filter, as expected.

The third contribution of the thesis is to provide four computationally efficient algorithms for postprocessing of DCT coded images. In literature several powerful postprocessing algorithms have been developed to reduce blocking artifacts but even a very simple algorithm can be too complex for real time applications such as video and still image decoding. These simple algorithms can improve visual quality with improvement in PSNR and are competitive to the many deblocking algorithms reported in literature. Four algorithms are proposed in *Chapter 5*. First algorithm reduces the blocking artifacts by exploiting the residual inter-block correlation, which exists in received blocky image. Second algorithm further reduces the block-boundary discontinuities in blocky image by capturing and removing the discontinuities in the DCT domain. The performance of both the algorithms improves as compression ratio increases. These DCT domain algorithms are computationally efficient since fast algorithms for the computation of DCT are available. In third algorithm for block-boundary discontinuity reduction, the discontinuities are captured in the same way but it uses the SVD based filtering scheme for their reduction. It reduces the blocking artifacts considerably but its computational complexity is slightly more because SVD algorithm has to be applied to each of the monotone block. Thus, this algorithm is very effective for reducing the blocking artifacts but its performance in terms of PSNR and computational complexity is slightly poor as compared to first approach of discontinuity reduction. Fourth algorithm reduces the blocking artifacts by eliminating some DCT coefficients of concatenated block of two adjacent blocks. This DCT domain algorithm has low computational complexity, as no filtering is required. The availability of fast algorithm for DCT computation makes this algorithm suitable for low bit rate coding applications. The selection of first row and first column of the DCT of concatenated block further reduces the computation complexity. This computationally efficient algorithm also gives very good result in terms of PSNR, discontinuity measures and visual quality.

The performance analysis and simulation results show that the proposed techniques are very competitive as compared to previously published works.

6.4 Future Scope

For the hybrid scheme, some more computationally efficient algorithm as suggested in *Chapter 5* can be used in monotone area. In signal adaptive filtering for edge area, the trade off between quality and complexity is required.

For 1D notch filter design, several well-known techniques are available in the literature but there is a very little work in case of 2D notch filer. The optimum method for the design of 2D multiple-notch filter is required. The uses of this filter in some other applications have to be investigated.

As we discussed in this thesis, the transform domain algorithm are very effective for postprocessing. More investigations are required to develop some more computationally efficient algorithms. The processing of DCT components due to edges may give smooth edges. This can be investigated for the further development of these algorithms.

Finally, the testing of these algorithms for the postprocessing of still image and low bit rate video sequence in real time is required.

Alternative DCT based coder such as a coder based on embedded zero tree scheme or a coder with variable size and variable shape blocks, can remove some of the drawbacks of conventional DCT based coder.

Appendix A

Standard JPEG Encoding

A.1 Introduction

There is an increasing effort to achieve standardization in image compression. Members from both the International Telecommunication Union (ITU) and the International Organization for Standardization (ISO) are working together to establish a joint international standard. As a result, IS (International Standard) 10918 has been established for both international organizations. This standard is known as JPEG, the Joint Photographic Experts Group. The goal of JPEG has been to develop a general method for image compression, which will be as close as possible to the state of the art in image compression. JPEG includes two basic compression methods: a DCT-based lossy compression method and a predictive method for lossless compression. In this Appendix, an overview of the lossy JPEG method is presented.

JPEG has been recognized as the most popular and efficient coding scheme for continuous tone still images, both monochrome and color. JPEG specifies one or more algorithm for image compression for each of the various modes. The four encoding modes are:

- Sequential encoding: Sequential mode is the most common mode of operation. The image is encoded in raster scan fashion left-to-right/top-to-bottom and is based on DCT. The baseline system belongs to this category.

- Progressive encoding: The image is encoded in multiple scans at the same spatial resolution for applications in which the channel bandwidth is narrow and, therefore, the transmission time may be long, but the viewer prefers to view the image contents in multiple coarse-to-fine stages.

- Lossless encoding: The image is encoded to guarantee exact recovery of every source sample value. The lossless method within JPEG is fully independent of transform-based coding. Instead, it uses differential coding to form prediction residuals that are then coded with either a Huffman coder or an arithmetic coder.

- Hierarchical encoding: The image is encoded at multiple spatial resolutions, so that lower-resolution images may be accessed and displayed without having to decompress the image at a higher spatial resolution.

Required coding techniques for JPEG are based on 2D (8 × 8) DCT. The DCT was chosen for two reasons, compression capability and the availability of commercial hardware chips. JPEG works best on natural images (scenes). It compresses the red-green-blue parts of a color image as three separate grayscale images - each compressed to a different extent, if desired. This is a widely used method of image compression which is based on performing the Discrete Cosine Transform (DCT) on 8 × 8 blocks of pixels. The JPEG standard prescribes a strict format for the encoded data stream, thereby allowing the use of a simple decoder to reconstruct the image. The JPEG method is designed to exploit limitations of the human eye. The information that is not perceived well by the eye is discarded.

It is based on the fact that human eyes are more sensitive to small changes in brightness than in color. JPEG compression relies on several things.

- Mostly the important signal energy of a picture lies at low frequencies.

- The human eye has less sensitivity to representation errors in high frequencies.

- In a small 8 × 8 block only a few important frequencies are present.

JPEG uses lossy compression scheme in which the data is thrown away during compression. The discarded data is in the form of higher frequency spatial information in the image, which is less visible. Most pictures usually have large areas of only low frequency components (flat borders, out-of-focus areas, sky, etc). JPEG also relies on limitations of the human eye's ability to perceive detail by not throwing away high frequencies, but just coding it crudely and letting your eye "fill-in" the proper details. It has also the ability to only encode the "important" frequencies although not many encoders take advantage of this. When this compressed data is stored as a file and then re-opened, the image exhibits error, or JPEG artifacts. If the compression ratio is large, these artifacts show up as clearly visible blocking, with patterns sometimes seen in the blocks. The baseline JPEG algorithm partitions the image into 8×8 pixel blocks. The pixel data in each block are processed using a discrete cosine transform (DCT), which generates a frequency representation of the 8×8 block. The DCT coefficients are quantized, and the integer coefficients Huffman coded. The quantization eliminates DCT coefficients with small amplitudes, thus discarding the higher frequency data that these coefficients represent. This loss of data by quantization and coding is responsible for the high compression ratios that the JPEG scheme is capable of, but is also responsible for varying degrees of loss of image information. The block diagram of the baseline JPEG compression scheme is shown in Fig. A.1 where as its simplified version is given in *Chapter 1.* The baseline algorithm consists of the following six stages:

1. Transformation in color space.
2. Subsampling.
3. Discrete Transform Coding.
4. Quantization.
5. Data compression.
6. File construction.

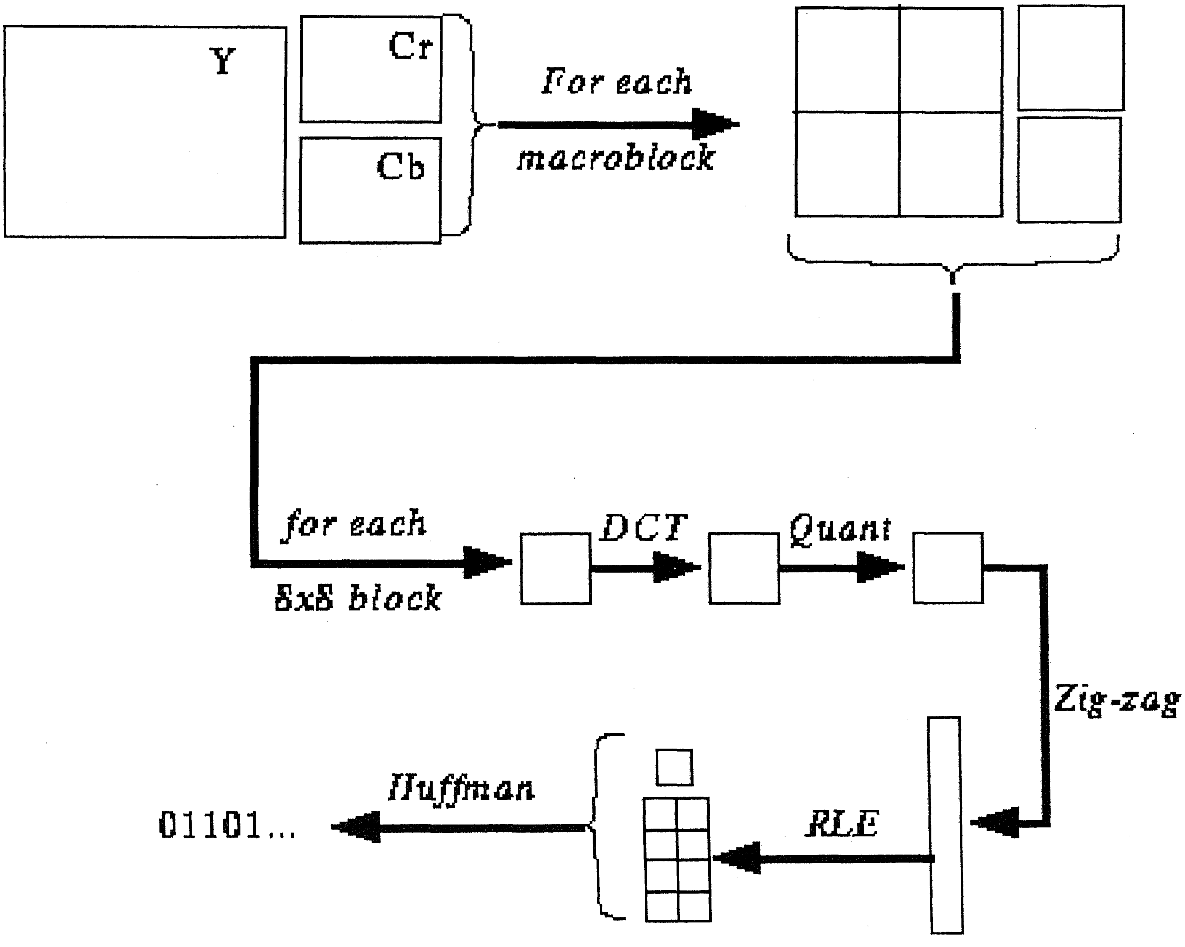

Figure A.1: Block diagram of the baseline JPEG compression scheme.

A.2 Transformation in color space

JPEG sets no restriction on the type of the input color space. Instead, it views each image as a collection of image components. The image is first transformed into a more suitable color space. For color images, the RGB data is transformed into luminance / chrominance color space. A widely accepted color scheme is the YCbCr. The components are defined by:

$Y = 0.299R + 0.587G + 0.114B$

$Cb = 0.1687R - 0.3313G + 0.5B$

$Cr = 0.5R - 0.4187G - 0.0813B$

Where, R, G and B represent the original Red, Green and Blue components respectively. The luminance component (Y) is the grayscale picture, which can be used directly as a black and white version of the image. The chrominance axes (Cb and Cr) contain all of the color information. Using our prior knowledge that the human visual system is more sensitive to changes in brightness, we can predict that an acceptable image can be reconstructed using fewer Cb and Cr samples than Y samples. Therefore, the three axes are processed separately, with the luminance axis at a much higher quality than the two-chrominance axes.

It is not essential to transform the color space to luminance / chrominance. The JPEG algorithm would work on the original RGB values, however the compression will be reduced, since all three components would have to be coded at the higher luminance quality.

A.3 Subsampling

Image with multiple components can be stored and processed either with or without data interleaving. This stage is also optional, and involves averaging together groups of pixels. Usually, the two color components are 'downsampled' at ratios of 2:1 that is every two adjacent pixels are averaged into one pixel value. The luminance component is left at full resolution. By simple calculations, each component (Y, Cb and Cr) contains 1/3rd of the data. If Cb and Cr are downsampled at 2:1, they are reduced by half to 1/6th of the original data. Thus the corresponding data volume becomes: 1/3 + 1/6 + 1/6 = 2/3 and hence is immediately reduced by 1/3rd with almost no decline in perceived picture quality.

These two stages mentioned above are optional and are used only as a form of preprocessing of the image and setting it up for the actual compression using JPEG.

A.4 Discrete Cosine Transform Coding

DCT is a lossless, reversible process, which can decorrelate the image signal and achieve energy compaction. It can therefore reduce the redundancy in the image signal before transmitting through a band-limited channel, or storing in a memory-limited media. Thus key to the compression process is the Discrete Cosine Transform (DCT). The basic operation performed by this transforms is to take a signal and transform it from one type of representation to another.

The pixel values of each component from the previous step are grouped into blocks, and the Discrete Cosine Transform (DCT) is used to transform the block into frequency domain coefficients. Generally, an 8 × 8 block of pixels is used, but this is purely arbitrary - it is mainly dependant upon the power of the software / hardware used to apply the DCT. The data points in each block are numbered from (0,0) in the upper left corner to (7,7) in the lower right corner. The DCT produces a new 8 × 8 block of spatial frequencies, F(u,v) using the formula:

$$F(u,v) = \frac{2}{8}c(u)c(v)[\sum_{m=0}^{7}\sum_{n=0}^{7} f(m,n) * cos(\frac{\pi(2m+1)u}{16})cos(\frac{\pi(2n+1)v}{16})] \tag{A.1}$$

where $c(w) = 2^{-1/2}$ for $w = 0; c(w) = 1$ for $w = 1, 2, ...7$.

After the transformation, the set of coefficients represent successively higher-frequency changes within the block in both the x and y directions. F(0,0) represents the rate of no change in either direction and is known as the DC coefficient. It is also the average of the

8×8 input values. This allows us to separate the much more noticeable low- frequency information from the higher frequencies - which contain the 'fine detail' and can be removed without too much picture degradation. After DCT, as the rows and columns move away from the origin, the coefficients in the transformed DCT matrix begin to represent higher frequencies, with the highest frequencies found in the lower right corner of the matrix. Recalling the fact that most images have their important signal energy at low frequencies and that the human eye has less sensitivity to representation errors in high frequencies we can now identify which part of the image can be discarded without much change in the quality of the image.

DCT is a lossless transformation that doesn't actually perform compression. It sets up the base for the "lossy" stage of the compression.

A.5 Quantization

The actual image compression is performed by quantization. Quantization is simply the process of reducing the number of bits needed to store an integer value by reducing the precision of the integer. The encoded image must include the 64 entries in the quantization-weighting matrix, which specify the stepsizes that were used to quantize the different DCT frequency components. A suggested quantization matrix was developed by subjective visual trials and is included in Annex K of the JPEG specification although it is not stored as a default in the decoder (it must be transmitted). The table is stored in the JPEG file header so that the encoder can use adjusted coefficients for particular images. Most commonly, there is one table for the Y data, and another one for the Cb and Cr components. Many encoders use this suggested QM and scale it up or down based on a user-supplied "quality factor" to increase or decrease the amount of compression.

Since JPEG is a lossy compression scheme, the reconstructed image differs from the original image, which results in some visible distortion. The key to successful JPEG compression, given a fixed encoded bit rate or file size, is the minimization of the amount of distortion that can be perceived by the human eye at that bit rate.

To compress a picture using JPEG, we must first divide it into 8 × 8 blocks, then perform a two-dimensional DCT on each block. The result is a set of 8 × 8 blocks of DCT coefficients, c_{ijk}, where i and j range from 0 to 7, and k ranges over the number of blocks. The c_{00} position in each block corresponds to the low frequencies (DC) of the original image block in both horizontal and vertical directions while the c_{77} coefficient contains the high frequency content of that block in the original image. The JPEG uses uniform midtread quantization to quantize the various coefficients. For lossy compression, each coefficient is divided by the corresponding quantization matrix entry and then round to the nearest integer: $u_{ijk} = round(c_{ijk}/q_{ij})$. (In JPEG, this quantized data is then losslessly compressed using Huffman or arithmetic coding.) The decoder reverses this process by multiplying the quantized coefficients by the quantization matrix and performing the inverse DCT.

Assuming the standard 8-bit quantization matrix, the least distortion and lowest compression are obtained with a matrix of all ones while the highest distortion and highest compression occur when using a QM filled with the maximum value 255. Each frequency component is divided by a separate quantization coefficient and rounded to the nearest integer. Each coefficient determines the extent to which a coefficient is weighted. A higher weighting means an increased loss of information. These values are the most varied component of the JPEG algorithm and the best results are hard to determine. CCITT standard recommendation lists the example of a luminance quantization table given in Table A.1.

This table is based upon "psychovisual thresholding", and has apparently been used with good results on 8-bit per sample luminance and chrominance images. Since many experiments in perception have shown that the human visual system has different sensitivities at different frequency bands, it is not surprising that subjective trials would result in this table. From this table it can be observed that as we move from the DC coefficient to the higher-order coefficients the step size increases. Because the quantization error is an increasing function of the step size, more quantization error will be introduced in the higher-frequency coefficients than in the lower-frequency coefficients. The lower

Table A.1: Standard quantization matrix for JPEG

16	12	10	16	24	40	51	61
11	12	14	19	26	58	60	55
14	13	16	24	40	57	69	56
14	17	22	29	51	87	80	62
18	22	37	56	68	109	103	77
24	35	55	64	81	104	113	92
49	64	78	87	103	121	120	103
72	92	95	98	112	100	101	99

Table A.2: Quantization matrix at quality factor of 10

80	60	50	80	120	200	255	255
55	60	70	95	130	255	255	255
70	65	80	120	200	255	255	255
70	85	110	145	255	255	255	255
90	110	185	255	255	255	255	255
120	175	255	255	255	255	255	255
245	255	255	255	255	255	255	255
255	255	255	255	255	255	255	255

weights at top and left also indicate our generally higher sensitivity to the low frequency components of images. In practical terms, this means that we should choose different weights for different frequency bands based on how well we are able to perceive distortion in that band (how our evaluation of image quality will be affected by loss of detail in that band).

Most existing coders use simple multiples of this example, but the values are not claimed to be optimal. The common JPEG encoding practice is the use of a "quality factor" from 1 to 100. For a quality factor of 50, the suggested QM is used; for $qf >$ 50 (higher rate, lower distortion), the suggested QM is multiplied by (100-qf)/50; for $qf <$ 50 (lower rate, higher distortion), the suggested QM is multiplied by 50/qf. The scaled matrices are rounded and clipped to the range [1, 255] before being used to encode images (because the QM is transmitted and used for decoding, while the quality factor

Table A.3: Quantization matrix at quality factor of 90

3	2	2	3	5	8	10	12
2	2	3	4	5	12	12	11
3	3	3	5	8	11	14	11
3	3	4	6	10	17	16	12
4	4	7	11	14	22	21	15
5	7	11	13	16	21	23	18
10	13	16	17	21	24	24	21
14	18	19	20	22	20	20	20

is not). For example, the matrices given in Table A.2 and Table A.3 are obtained for quality factors of 10 and 90, respectively:

The bit-rate (entropy encoded size/number of pixels) is a function of the exact image being encoded. If we have a target rate in mind, we must iteratively try different quality factors, although the process is made easier because the rate is a monotonic function of the quality factor. However, this method leaves much to be desired, since it does not calculate or optimize the amount of visible distortion at the desired rate.

A.6 DC Coding and ZigZag Sequence

After quantization, the DC coefficient is treated separately from the 63 AC coefficients. The DC coefficient is a measure of the average value of the 64 image samples. Because there is usually strong correlation between the DC coefficients of adjacent 8×8 blocks, the quantized DC coefficient is encoded as the difference from the DC term of the previous block in the encoding order. This special treatment is worthwhile as DC coefficients frequently contain a significant fraction of the total image energy. Re-ordering of non-zero coefficients is performed to better exploit the statistical occurrence of zero valued coefficients in an energy compacting transform. The most popular coefficient re-ordering is that of incremental zigzag scanning of DCT coefficients from its DC value up to its highest frequency components. This process will reduce the number of code words needed to code non-zero coefficients. Thus coefficients of the AC components are arranged in a "zigzag sequence" and then are encoded using two different methods. The first is run-length encoding of zero values. This method takes advantage of the large number of zeroes that exist in the bottom half of the matrix. The second is what JPEG calls "Entropy Coding". This involves sending out the coefficient codes using either Huffman codes or arithmetic coding depending on the choice of the implementer. However, baseline JPEG implementation uses Huffman coding only.

A.7 Entropy Coding

Entropy encoding is the last step of the sequential JPEG compression algorithm. An entropy encoder further compresses the quantized values losslessly to give better overall compression. It uses a model to accurately determine the probabilities for each quantized value and produces an appropriate code based on these probabilities so that the resultant output code stream will be smaller than the input stream. Two approaches are specified by the JPEG standard. The baseline system uses simple Huffman coding while the extended system uses arithmetic coding and is suitable for a wider range of applications.

The number of previous zeros and the bits needed for the current numbers amplitude form a pair. Each pair has its own code word, assigned through a variable length code (for example Huffman, Shannon-Fano or Arithmetic coding). In baseline JPEG, Huffman coding is also used for AC coefficients. JPEG outputs the code word of the pair, and then the code word for the coefficient's amplitude (also from a variable length code). After each block, JPEG writes a unique end-of-block sequence to the output stream, and moves to the next block. When finished with all blocks, JPEG writes the end-of-file marker.

A.8 File Construction

Finally, a header is added at the top of the file, containing all of the compression parameters needed to reverse the encoding process.

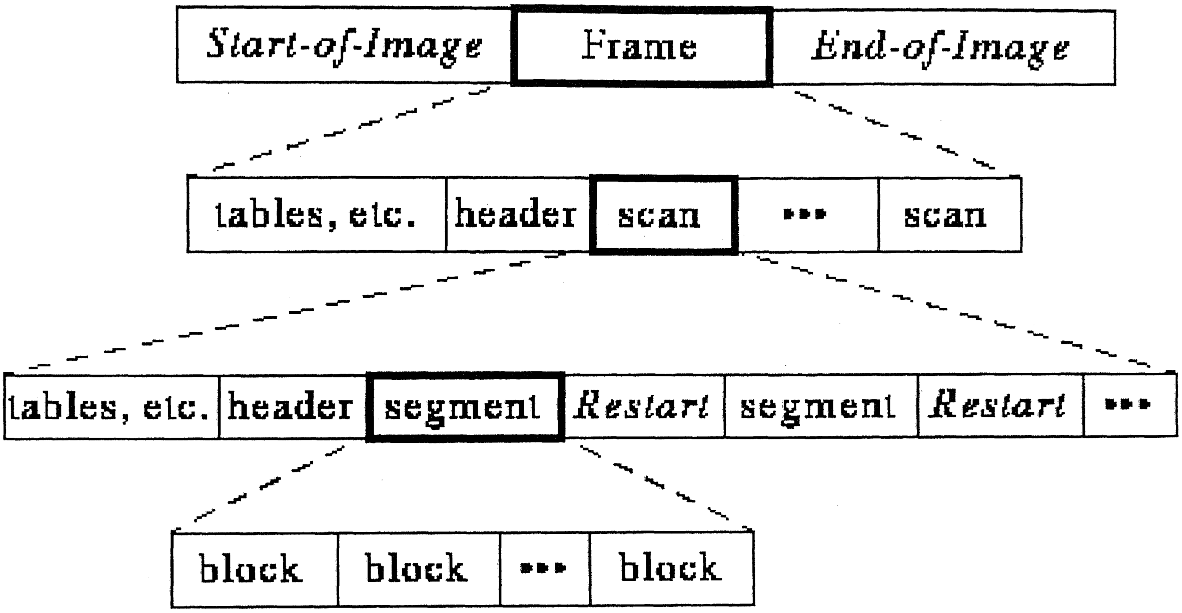

Figure A.2: Format of JPEG bit stream.

A.8.1 Overview of the JPEG bit stream

A "Frame" is a picture, a "scan" is a pass through the pixels (e.g., the red component), a "segment" is a group of blocks, a "block" is an 8×8 group of pixels. The format for the JPEG bit stream is shown in Fig. A.2. The frame header and the scan header contain the following information:

Frame header:

- sample precision
- (width, height) of image
- number of components
- unique ID (for each component)
- horizontal/vertical sampling factors (for each component)
- quantization table to use (for each component)

Scan header:

- Number of components in scan
- component ID (for each component)
- Huffman table for each component (for each component)

The following miscellaneous information can occur between headers: **Miscellaneous**

- Quantization tables
- Huffman Tables
- Arithmetic Coding Tables
- Comments
- Application Data

JPEGs are suitable for the compression of true color or grayscale images of photographs and realistic scenes. But the disadvantage with JPEG is that it is not suited for artwork with sharply defined lines, lettering and simple cartoons. This is because JPEG tends to blur the borders between one color and another.

Authors Publications

[1] **Srivastava**, V. K. and **Ray**, G. C., "Design of 2D-multiple notch filter and its application in reducing blocking artifact from DCT coded image," *Proc. IEEE Int. Conf. Engineering in Medicine and Biology, Chicago 2000 World Congress, 23-28 July*, vol. TH-G301-06, 2000.

[2] **Srivastava**, V. K. and **Ray**, G. C., "A hybrid scheme for the post-processing of DCT coded images," *Accepted for the presentation and publication in Int. Conf. on Biomedical Engineering, Jan. 24-26, 2001, Chennai, India.*

[3] **Srivastava**, V. K. and **Ray**, G. C., "A new scheme for postprocessing of DCT coded images in DCT domain," *Accepted for the presentation and publication in National Conference on Communications, Jan. 27-28, 2001, Kanpur, India.*

[4] **Srivastava**, V. K. and **Ray**, G. C., "A hybrid scheme for reducing blocking artifacts from DCT coded images," *Accepted for the presentation and publication in National Conference on Communications, Jan. 27-28, 2001, Kanpur, India.*

[5] **Srivastava**, V. K. and **Ray**, G. C., "Design of linear-phase 2D FIR multiple-notch filter and its application in reducing blocking artifact from DCT coded images," *communicated to IEE Proceedings - Vision, Image and Signal Processing.*

[6] **Srivastava**, V. K. and **Ray**, G. C., "Computationally efficient algorithms for reducing blocking artifacts from DCT coded images," *communicated to IEEE Trans. Circuits Syst. Video Technol.*

Bibliography

[1] **Ramamurthi**, B. and **Gersho**, A., “Non-linear space-variant post processing of block coded image,” *IEEE Trans. Acoustics, Speech and Signal Processing*, vol. ASSP-34, pp. 1258–1268, Oct. 1986.

[2] **Hsia**, S. C., **Yang**, J. F., and **Liu**, B. D., “Efficient postprocessor for blocky effect removal based on transform characteristics,” *IEEE Trans. Circuits Syst. Video Technol.*, vol. 7, pp. 924–929, Dec. 1997.

[3] **Park**, Hyun Wōok and **Lee**, Yung Lyul, “A postprocessing method for reducing quantization effects in low bit-rate moving picture coding,” *IEEE Trans. Circuits Syst. Video Technol.*, vol. 9, pp. 161–171, Feb. 1999.

[4] **Paek**, Hoon, **Kim**, Rin-Chul, and **Lee**, Sang-Uk, “A DCT-based spatially adaptive post-processing technique to reduce the blocking artifacts in transform coded images,” *IEEE Trans. Circuits Syst. Video Technol.*, vol. 10, pp. 36–41, Feb. 2000.

[5] **Jeon**, B. and **Jeong**, J., “Blocking artifacts reduction in image compression with block boundary discontinuity criterion,” *IEEE Trans. Circuits Syst. Video Technol.*, vol. 8, pp. 345–357, June 1998.

[6] **Pei**, Soo-Chang and **Tseng**, Chien-Cheng, “Two dimensional IIR digital notch filter design,” *IEEE Trans. on circuits and systems-II: Analog and digital signal processing*, vol. 41, pp. 227–231, March 1994.

[7] **Pei**, Soo-Chang and **Tseng**, Chien-Cheng, “IIR multiple notch filter design based on all pass filter,” *IEEE Trans. on circuits and systems-II: Analog and digital signal processing*, vol. 44, pp. 133–136, Feb. 1997.

[8] **Huang**, J., **Shi**, Y. Q., and **Dai**, X., “Blocking artifact removal based on frequency analysis,” *Electronics letters*, vol. 34, pp. 2323–2325, Nov. 1998.

[9] **Yu**, T. H., **Mitra**, S. K., and **Babic**, H., “Design of linear phase FIR filters,” *Sadhana*, vol. 15, pp. 133–155, Nov. 1990.

[10] **Xiong**, Z., **Ramchandran**, K., **Orehard**, M. T., and **Zhang**, Y. Q., “A comparative study of DCT and wavelet-based image coding,” *IEEE Trans. Circuits Syst. Video Technol.*, vol. 9, pp. 692–695, Aug. 1999.

[11] **Ahmed**, N., **Natarajan**, T., and **Rao**, K. R., "Discrete cosine transform," *IEEE Trans. on Computers*, vol. 23, Jan. 1974.

[12] **Rao**, K. R. and **Yip**, P., *Discrete Cosine Transform: Algorithms, Advantages, Applications.* San Diego: Academic Press,San Diego, California, 1990.

[13] **Ahmed**, N. and **Rao**, K. R., *Orthogonal transform for Digital Signal processing.* Berlin, Germany:Springer-Verlag,, 1975.

[14] **Elliot**, D. F. and **Rao**, K. R., *Fast Transforms: Algorithms, Analyisis, Applications.* New York: Academic Press, 1982.

[15] **Jain**, Anil Kumar, *Fundamentals of Digital Image Processing.* Englewood Cliffs, NJ: Prentice-Hall Int. ed., 1989.

[16] **Pratt**, W. K., *Digital Image Processing.* New York: welly, 1978.

[17] **Bhaskaran**, Vasudev and **Konstantinides**, Konstantinos, *Image and Video Compression Standards: Algorithms and Architectures.* Kluwer Academic publishers, Boston, 1995.

[18] **ISO/IEC/JTC1/SC1/WG8,** *Joint Photographic Expert Group.* JPEG Technical specification, Rivision 8, 1990.

[19] **Wallace**, G. K., "The JPEG still picture compression standard," *Commmun. ACM*, vol. 34, pp. 30–44, Apr. 1991.

[20] **Pennebakar**, W. B. and **Mitchell**, J. L., *JPEG Still Image Compression Standard.* New York: Van Nostrand Reinhold, 1993.

[21] **Liou**, M., "Overview of the p × p kbits/s video coding standard," *Commun. ACM*, vol. 34, pp. 46–56, Apr. 1991.

[22] **Reeves**, H. C. and **Lim**, J. S., "Reduction of blocking effect in image coding," *Jr. optical Engineering*, vol. 23, pp. 34–37, Jan/Feb. 1984.

[23] **Hsu**, Y. F. and **Chen**, Y. C., "A new adaptive separable median filter for removing blocking effect," *IEEE Trans. on Consumers Electronics*, vol. 39, pp. 510–513, Aug. 1993.

[24] **Kuo**, C. J. and **Hsieh**, R. J., "Adaptive postprocessor for block encoded images," *IEEE Trans. Circuits Syst. Video Technol.*, vol. 5, pp. 298–304, Aug. 1995.

[25] **Castagno**, R., **Marsi**, S., and **Ramponi**, G., "A simple algorithm for the reduction of blocking artifacts in image and its implementation," *IEEE Trans. on Consumers Electronics*, vol. 44, pp. 1062–1070, Aug. 1998.

[26] **Lee**, Y. L., **Kim**, H.C., and **Park**, H. W., "Blocking effect reduction of JPEG images by signal adaptive filtering," *IEEE Trans. on Image Processing*, vol. 7, pp. 229–234, Feb. 1998.

[27] **Kim**, Sung Deuk, **Yi**, Jaeyoun, **Kim**, Hyun Mun, and **Ra**, Jong Beom, "A deblocking filter with two separate modes in block based video coding," *IEEE Trans. Circuits Syst. Video Technol.*, vol. 9, pp. 156–160, Feb. 1999.

[28] **Apostolopoulos**, J. G. and **Jayant**, N. S., "Postprocessing for very low bit rate video compression," *IEEE Trans. on Image Processing*, vol. 8, pp. 1125–1129, Aug. 1999.

[29] **Comes**, S., **Macq**, B., and **Mattavelli**, M., "Postprocessing of images by filtering the unmasked coding noise," *IEEE Trans. on Image Processing*, vol. 8, pp. 1050–1061, Aug. 1999.

[30] **Zakhor**, Avideh, "Iterative procedures for reduction of blocking effect in transform coded image," *IEEE Trans. Circuits Syst. Video Technol.*, vol. 2, pp. 91–95, March 1992.

[31] **Reeves**, S. J. and **Eddins**, S. L., "Comments on iterative procedures for reduction of blocking artifacts in transform image coding," *IEEE Trans. Circuits Syst. Video Technol.*, vol. 3, pp. 439–440, Dec. 1993.

[32] **Yang**, Y., **Galatsanos**, N., and **Katsaggelos**, A. K., "Regularized reconstruction to reduce blocking artifacts of discrete cosine transform compressed image," *IEEE Trans. Circuits Syst. Video Technol.*, vol. 3, pp. 421–432, Dec. 1993.

[33] **Minami**, Shigenobu and **Zakhor**, Avideh, "An optimization approch for removing blocking effects in transform coding," *IEEE Trans. Circuits Syst. Video Technol.*, vol. 5, pp. 74–81, April 1995.

[34] **O'Rourke**, T. P. and **Stevenson**, R. L., "Improved image decompression for reduced transform coding artifacts," *IEEE Trans. Circuits Syst. Video Technol.*, vol. 5, pp. 490–499, Dec. 1995.

[35] **Ozcelik**, T., **Brailean**, J. C., and **Katsaggelos**, A. K., "Image and video compression algorithms based on recovery techniques using mean field annealing," *proc. of IEEE*, vol. 83, pp. 304–316, Feb. 1995.

[36] **Molina**, Rafael, **Katsaggelos**, Aggeloss K., and **Mateos**, Javier, "Bayesian and regularization methods for hyperparameters estimation in image retoration," *IEEE Trans. on Image Processing*, vol. 8, pp. 231–246, Feb 1999.

[37] **Mateos**, Javier, **Katsaggelos**, Aggeloss K., and **Molina**, Rafael, "A bayesian approach for the estimation and transmission of regularization parameters for reducing blocking artifact," *IEEE Trans. on Image Processing*, vol. 9, pp. 1200–1215, July 2000.

[38] **Kim**, T. K. and **Paik**, J. K., "Fast image restoration for reducing blocking artifacts based on adaptive constraint optimization," *Jr.of Visual Communication and Image Representation*, vol. 9, pp. 234–241, Sept. 1998.

[39] **Paek**, Hoon, **Kim**, Rin-Chul, and **Lee**, Sang-Uk, "On the POCS-based postprocessing techniques to reduce the blocking artifacts in transform coded images," *IEEE Trans. Circuits Syst. Video Technol.*, vol. 8, pp. 358–167, June. 1998.

[40] **Tien**, C. N. and **Hang**, H. M., "Transform domain post processing of DCT-coded images," *Proc. SPIE, Visual communication Image Processing*, vol. 2094, pp. 1627–1638, Nov. 1993.

[41] **Wang**, Y., **Zhu**, Q. F., and **Shaw**, L., "Maximally smooth image recovery in transform coding," *IEEE Trans. Communications*, vol. 41, pp. 1544–1551, Oct. 1993.

[42] **Choy**, Steven S.O., **Chan**, Yuk-Hee, and **Siu**, Wan-Chi, "Reduction of block-transform image coding artifacts by using local statics of transform coefficients," *IEEE Signal Processing Letter*, vol. 4, pp. 5–7, Jan. 1997.

[43] **Chan**, Yuk-Hee, **Hong**, Sung-Wai, and **Siu**, Wan-Chi, "A practical postprocessing technique for real-time block-based coding system," *IEEE Trans. Circuits Syst. Video Technol.*, vol. 8, pp. 4–8, Feb. 1998.

[44] **Xiong**, Z., **Orehard**, M. T., and **Zhang**, Y. Q., "A deblocking algorithm for JPEG images using overcomplete wavelet representation," *IEEE Trans. Circuits Syst. Video Technol.*, vol. 7, pp. 433–436, April 1997.

[45] **Kim**, Nam Chul, **Jang**, Ick Hoon, and **Hong**, Won Hak, "Reduction of blocking artifacts in block-based images using wavelet transform," *IEEE Trans. Circuits Syst. Video Technol.*, vol. 8, pp. 253–257, June 1998.

[46] **chiu Hsung**, Tai, **Lun**, Daniel Pak-Kong, and **Siu**, Wan-Chi, "A deblocking technique for block transform compressed image using wavelet transform modulus maxima," *IEEE Trans. on Image Processing*, vol. 7, pp. 1488–1496, Oct. 1998.

[47] **Choi**, Hyuk and **Kim**, Taejeong, "Blocking-artifact reduction in block-coded images using wavelet-based subband decomposition," *IEEE Trans. Circuits Syst. Video Technol.*, vol. 10, pp. 801–805, Aug. 2000.

[48] **Hirano**, K., **Nishimura**, S., and **Mitra**, S. K., "Design of digital notch filter," *IEEE Trans. on circuits and systems*, vol. CAS-21, pp. 540–546, July 1974.

[49] **Joshi**, Y. V. and **Roy**, S. C. Dutta, "Design of IIR multiple notch filter based on all-pass filter," *IEEE Trans. on circuits and systems-II: Analog and digital signal processing*, vol. 46, pp. 1–1, Feb. 1999.

[50] **Roy**, S. C. Dutta, **Jain**, S.B., and **Kumar**, B., "Design of digital FIR notch filters," *IEE Proc. - Vis. Image Signal Process.*, vol. 141, pp. 334–338, Oct. 1994.

[51] **Pei**, Soo-Chang and **Tseng**, Chien-Cheng, "Corrections on two dimensional IIR digital notch filter design," *IEEE Trans. on circuits and systems-II: Analog and digital signal processing*, vol. 41, p. 680, Sept. 1994.

[52] **Pei**, Soo-Chang, **Lu**, Wu-Sheng, and **Tseng**, Chien-Cheng, "Analytical two-dimensional IIR notch filter design using outer product expansion," *IEEE Trans. on circuits and systems-II: Analog and digital signal processing*, vol. 44, pp. 479–483, Sept. 1997.

[53] **Pei**, Soo-Chang, **Lu**, Wu-Sheng, and **Tseng**, Chien-Cheng, "Two-dimensional FIR notch filter design using singular value decomposition," *IEEE Trans. on circuits and systems-I: Fundamental theory and applications*, vol. 45, pp. –, March 1998.

[54] **Srivastava**, V. K. and **Ray**, G. C., "A hybrid scheme for the post-processing of DCT coded images," *Accepted for the presentation in International Conference on Biomedical Engineering, Jan. 24-26, 2001, Chennai, India.*

[55] **Srivastava**, V. K. and **Ray**, G. C., "A new scheme for postprocessing of DCT coded images in DCT domain," *Accepted for the presentation in National Conference on Communications, Jan. 27-28, 2001, Kanpur, India.*

[56] **Srivastava**, V. K. and **Ray**, G. C., "Design of 2D-multiple notch filter and its application in reducing blocking artifact from DCT coded image," *Proc. IEEE Int. Conf. Engineering in Medicine and Biology, Chicago 2000 World Congress, 23-28 July*, vol. TH-G301-06, 2000.

[57] **Chen**, W.H. and **Fralick**, S. C., "Image inhancement using cosine transform filtering," *in proc. Image Science and Mathematics Symp.*, vol. Monterey, CA, Nov. 1976.

[58] **Ngan**, K. N. and **Clarke**, R. J., "Low pass filtering in the cosine transform domain," *in proc. Int. Conf. Communications*, vol. Seattle, WA, June 1980.

[59] **Chitprasert**, B. and **Rao**, K. R., "Discrete cosine transform filtering," *Signal processing, Elsevier Sc.Pub.*, vol. 19, pp. 233–245, March 1990.

[60] **Martucci**, S. A., "Symmetric convolution and discrete sine and cosine transforms," *IEEE Trans. on Signal Processing*, vol. 42, pp. 1038–1051, May 1994.

[61] **Martucci**, S. A., "Digital filtering of images using the discrete sine anf cosine using transforms," *Optical Engineering*, vol. 35, pp. 119–127, Jan 1996.

[62] **Kresch**, Renato and **Merhav**, Neri, "Fast DCT domain filtering using the DCT and the DST," *IEEE Trans. on Image Processing*, vol. 8, pp. 821–832, June 1999.

[63] **Srivastava**, V. K. and **Ray**, G. C., "Design of linear-phase 2D FIR multiple-notch filter and its application in reducing blocking artifact from DCT coded images," *communicated to IEE Proceedings - Vision, Image and Signal Processing.*

[64] **Huang**, T. S., **burnett**, J. W., and **Deczky**, A. G., "The importance of phase in image processing filters," *IEEE Trans. Acoustics, Speech and Signal Processing*, vol. ASSP-23, pp. 529–542, Dec. 1975.

[65] **Rabiner**, Lawrence R. and **Gold**, Bernard, *Theory and Application of Digital Signal Processing.* Englewood Cliffs, NJ: Prentice-Hall Int. ed., 1975.

[66] **McClellan**, J. H., **Parks**, T. W., and **Rabiner**, L. R., "A computer program for designing optimum FIR linear phase digital filters," *IEEE trans. Audio Electracoust.*, vol. AU-21, pp. 506–526, Dec. 1973.

[67] **Rabiner**, L. R., **McClellan**, J. H., and **Parks**, T. W., "FIR digital filter design techniques using weighted Chebyshev approximation," *proc. of IEEE*, vol. 63, no. 4, pp. 595–610, 1975.

[68] **Mitra**, S. K. and **Yu**, T. H., "Complementary two-dimensional digital filters," *proc. of IEEE*, vol. 74, pp. 299–300, Jan. 1986.

[69] **Andrews**, H. C. and **Patterson**, C. L., "Singular value decompositions and digital image processing," *IEEE Trans. Acoustics, Speech and Signal Processing*, vol. ASSP-24, pp. 26–53, Feb 1976.

[70] **Natarajan**, B. K., "Filtering random noise from deterministic signals via data compression," *IEEE Trans. on Signal Processing*, vol. 43, pp. 2595–2605, Nov. 1995.

[71] **Konstantinides**, Konstantinos, **Natarajan**, Balas, and **Yovanof**, Gregory S., "Noise estimation and filtering using block-based singular value decomposition," *IEEE Trans. on Image Processing*, vol. 6, pp. 26–53, Mar. 1997.

[72] **Avril**, C. and **Nguyen-Trong**, T., "Linear filterig for reducing blocking effects in orthogonal transform image coding," *J. Electron. Imaging*, vol. 1, pp. 183–191, Apr. 1992.

[73] **Meier**, T., **Ngan**, K. N., and **Crebbin**, G., "Reduction of blocking artifacts in image and video coding," *IEEE Trans. Circuits Syst. Video Technol.*, vol. 9, pp. 490–500, April 1999.

[74] **Egger**, O., **Fleury**, P., **Ebrahimi**, T., and **Kunt**, M., "High-performance compression of visual information- A tutorial review. I. still pictures," *proc. of IEEE*, vol. 87, pp. 976–1013, June 1999.

[75] **Ebrahimi**, T. and **Kunt**, M., "Visual data compression for multimedia applications," *proc. of IEEE*, vol. 86, pp. 1109–1125, June 1998.

[76] **Yang**, Y., **Galatsanos**, N., and **Katsaggelos**, A. K., "Projection-based spatially adaptive reconstruction of block- transform compressed images," *IEEE Trans. on Image Processing*, vol. 4, pp. 896–908, July 1995.

[77] **Corte-Real**, L. and **Alves**, A. P., "Vector quantization of image sequences using variable size and variable shape blocks," *Electronics Letter*, vol. 26, pp. 1483–1484, Aug. 1990.

[78] **Corte-Real**, L. and **Alves**, A. P., "A very low bit rate video coder based on vector quantization," *IEEE Trans. on Image Processing*, vol. 5, pp. 263–273, Feb. 1996.

[79] **Shapiro**, J. M., "Embedded image coding using zerotrees of wavelet coefficients," *IEEE Trans. on Signal Processing*, vol. 41, pp. 3445–3462, Dec. 1993.

[80] **Xiong**, Z., **Guleryuz**, O. G., and **Orchard**, M. T., "A DCT based embedded image coder," *IEEE Signal Processing Letter*, vol. 3, pp. 289–290, Nov. 1996.

[81] **Jeong**, Y. A. and **Cheong**, C. K., "A DCT based embedded image coder using wavelet structure of DCT for very low bit rate video codec," *IEEE Trans. on Consumer Electronics*, vol. 44, pp. 500–508, Aug. 1998.

[82] **Aghdasi**, Farzin and **Ward**, Rabab K., "Reduction of boundary artifacts in image restoration," *IEEE Trans. on Image Processing*, vol. 5, pp. 611–618, April 1996.

[83] **Srivastava**, V. K. and **Ray**, G. C., "A hybrid scheme for reducing blocking artifacts from DCT coded images," *Accepted for the presentation in National Conference on Communications, Jan. 27-28, 2001, Kanpur, India.*

[84] **Srivastava**, V. K. and **Ray**, G. C., "Computationally efficient algorithms for reducing blocking artifacts from DCT coded images," *communicated to IEEE Trans. Circuits Syst. Video Technol.*

[85] **Mersereau**, Russell M. and **Dudgeon**, Dan E., "Two dimensional digital filtering," *proc. of IEEE*, vol. 63, no. 4, pp. 610–623, 1975.

[86] **Netravali**, A. N. and **Limb**, J. O., "Picture coding: A review," *proc. of IEEE*, vol. 68, pp. 366–406, June 1980.

[87] **Karunasekhera**, S. A. and **Kingsbury**, N. G., "A distortion measure for blocking artifacts in images based on human visual sensitivity," *IEEE Trans. on Image Processing*, vol. 4, pp. 713–724, June 1995.

[88] **Gall**, D. L., "MPEG: A video compression standard for multimedia applications," *Commmun. ACM*, vol. 34, pp. 46–58, Apr. 1991.

[89] **Zhang**, Y. Q., **Pickholtz**, R. L., and **Loew**, M. H., "A new approach to reduce the blocking effect of transform coding," *IEEE Trans. on Commun.*, vol. 41, pp. 299–302, Feb. 1993.

[90] **Er**, M. H., "Designing notch filter with controlled null width," *Signal Process.*, vol. 24, no. 3, pp. 319–329, 1991.

[91] **Luo**, J. B., **Chen**, C. W., **Parker**, K. J., and **Huang**, T. S., "Artifact reduction in low bit-rate DCT-based image compression," *IEEE Trans. on Image Processing*, vol. 5, pp. 1363–1368, Sept. 1996.

[92] **Lakhani**, G. and **Zhang**, N., "Derivation of prediction equations for blocking artifact reduction," *IEEE Trans. Circuits Syst. Video Technol.*, vol. 9, pp. 415–418, Apr. 1999.

[93] **Park**, S. H. and **Kim**, D. S., "Theory of projection onto the narrow quantization constraint set and its application," *IEEE Trans. on Image Processing*, vol. 8, pp. 1361–1373, Oct. 1999.

[94] **Karunasekera**, S. A. and **Kingsbury**, N. G., "A distortion measure for blocking artifacts in images based on human visual sensitivity," *IEEE Trans. on Image Processing*, vol. 4, pp. 713–724, June 1995.

[95] **Liu**, T. S. and **Jayant**, N. S., "Adaptive postprocessing algorithms for low bit rate video signals," *IEEE Trans. on Image Processing*, vol. 4, pp. 1032–1035, July 1995.

[96] **Stevenson**, R. L., "Reduction of coding artifacts in transform image coding," *in Proc. IEEE Int. Conf. Acoust., Speech, Signal Processing, Minneapolis, MN*, pp. 401–404, Mar. 1993.

[97] **Jarske**, T., **Haavisto**, P., and **Defe'e**, I., "Post-filterig methods reducing blocking effects from coded images," *IEEE Trans. on Consumers Electronics*, vol. 40, no. 3, pp. 521–526, 1994.

[98] **Papoulis**, A., *Probability, Random Variables, and Stochastic processes.* New York: McGraw-Hill,, 1984.

[99] **Lim**, J. S., *Two-Dimensional Signal and Image Processing.* Englewood Cliffs, NJ: Prentice-Hall Int. ed., 1990.

[100] **Jayant**, N. S. and **Noll**, P., *Digital Coding of Waveform, Principles and Applications to Speech and Video.* Englewood Cliffs, NJ: Prentice-Hall Int. ed., 1984.

[101] **Gersho**, A. and **Gray**, R. M., *Vector Quantization and Signal Compression.* Kluwer Academic publishers, Boston, 1992.

[102] **Sayood**, Khalid, *Introduction to data Compression.* Morgan Kaufmann publishers,Inc., 1996.